Evolutionary basis of intermale sexual behavior by multiple pheromone switches in *Drosophila*

Youcef Ouadah [1], Thomas H. Naragon [2], Hayley Smihula [2], Emily L. Behrman [3,†], Mohammed A. Khallaf [4,‡], Yun Ding [5], David L. Stern [3,§], Joseph Parker [2], and David J. Anderson [1,*]

[1] Division of Biology and Biological Engineering, Tianqiao and Chrissy Chen Institute for Neuroscience, and Howard Hughes Medical Institute, Caltech; Pasadena, CA, USA

[2] Division of Biology and Biological Engineering, Caltech; Pasadena, CA, USA

[3] Janelia Research Campus, Howard Hughes Medical Institute; Ashburn, VA, USA

[4] Department of Evolutionary Neuroethology, Max Planck Institute for Chemical Ecology; Jena, Germany

[5] Department of Biology, University of Pennsylvania; Philadelphia, PA, USA

[†] Present address: Department of Biological Sciences, Dartmouth College; Hanover, NH, USA

[‡] Present address: Molecular Physiology of Somatic Sensation Laboratory, Max Delbrück Center for Molecular Medicine; Berlin, Germany and Department of Zoology and Entomology, Faculty of Science, Assiut University; Assiut, Egypt

[§] Present address: Stowers Institute for Medical Research and Howard Hughes Medical Institute; Kansas City, MO, USA

[*] Correspondence: wuwei@caltech.edu

Abstract

We have identified a *Drosophila* species which exhibits spontaneous and robust intermale sexual behavior. *D. santomea* males distinguish conspecific sexes but court both vigorously and seldom attack. Elevated intermale courtship stems from at least three evolutionarily derived pheromonal changes. In males, the sexually monomorphic cuticular pheromone 7-tricosene promotes rather than inhibits courtship and the courtship-inhibiting olfactory pheromone cVA is reduced 84-92% compared to close relatives. The third switch is in *D. santomea* females, where cVA suppresses rather than promotes sexual receptivity. Female cVA aversion and male cVA reduction may have co-evolved to maintain efficient intraspecific mating but prevent hybridization with the sympatric sibling species D. *yakuba*. High intermale courtship and low cVA also co-occur and appear selectively derived in a distant monomorphic species *D. persimilis*, implying pheromonal and social behavioral convergence. Changes in pheromone valence and levels may therefore explain the recent evolutionary emergence of intermale sexual behavior in *Drosophila*.

Introduction

Social behaviors, including aggregation, aggression, courtship, mating, parenting, and cooperation, are remarkably diverse in the animal kingdom (*1*), and can vary between closely related sibling species (*2*) or even entire orders (*3*). The ultimate causes of social behaviors (in terms of natural and sexual selection) have received considerable theoretical attention (*4*, *5*) and proximate causes (including genetic loci, hormones, neural circuits, pheromones, and sensory releasers) identified (*6–15*). The ~2,000 species of the genus *Drosophila* (*16*) have historically excelled in this regard as models for intersexual social behaviors (*17–22*), providing notably an unparalleled genetic, neural, and pheromonal understanding of the iconic courtship dance of *D. melanogaster* males (*23–25*). Comparisons of male courtship in other members of the genus have revealed flexible substrates, in genomes (*26–29*) and nervous systems (*30–33*), of its rapid evolution and revealed general principles of reproductive function and isolation (*34*, *35*). However, comparative investigations of intrasexual social behaviors between *Drosophila* males or females have relatively lagged.

Interactions between same-sex conspecifics can vary greatly across species, strains, individuals, and time (*36*, *37*), and can be as opposed as altruistic cooperation (*38*) or lethal aggression (*39*). Such flexibility implies that intrasexual social behaviors can evolve quickly under varying selection pressures or neutral drift, but the underlying changes in pheromone systems, neural circuits, and genomes are often difficult to pinpoint. We sought to identify phylogenetic patterns of variation in intermale social behavior in *Drosophila* and, by leveraging experimental strengths of the genus, reveal proximate and ultimate evolutionary causes. We identified a species, *D. santomea*, in which males show vigorous sexual behavior toward other males that includes multiple species-typical motor and acoustic features of the female-directed courtship dance, and is accompanied only rarely by overt aggression. Three distinct changes in pheromone levels or behavioral valence compared to *D. melanogaster* have occurred during *D. santomea* evolution, both before and after divergence from the sibling species *D. yakuba*. Together these changes have highly and selectively amplified intermale courtship without eliminating sex discrimination or the latent potential for intense attack, which can be revealed by optogenetic activation of conserved aggression-promoting neural circuits. The results, together with information from natural history and phylogenetic inference, provide insight into the pheromonal mechanism and evolutionary logic of recent social evolution in *Drosophila* that may apply broadly to other taxa.

Results

Evolutionary variation in male-male social behavior within the genus *Drosophila*

In the presence of food or a female, pairs of single-housed *D. melanogaster* males will fight (*40–48*), employing a stereotyped set of contact- and non-contact-mediated motor actions including lunging, tussling, and wing threat (*49*, *50*). We assessed aggression (and other intermale social behaviors) comparatively in 15 *Drosophila* species using food as the stimulating resource (*51*), screening for qualitative and quantitative variation in male social engagement, frequency, and motor pattern. We sampled species densely within the *melanogaster* subgroup (7 tested of 9 assigned) (*52*) to monitor potential behavior variation at close phylogenetic distances to *D. melanogaster* with high resolution. At larger evolutionary distances we sampled sparsely (typically one species per subgenus group or subgroup) to broadly survey genus social evolution, apart from including both members of the *D. pseudoobscura* / *D. persimilis* sibling species pair from the *obscura* group (*53*). We standardized assay conditions but occasionally varied the food source over which flies competed to account for host specializations (*54*). Fly behavior was measured in dyadic male-male interactions by combining saturated manual scoring of 11 social actions on a subset of representative recordings (Fig. 1A,B, fig. S1A) with automated behavior classifications for the remainder (fig. S2A,B) (*55–57*). Separate behavior classifiers detected either lunge, a major consummatory attack action in males (*43*, *49*, *50*), or unilateral wing extension (UWE), a cross-genus indicator of male sexual behavior (*20*), as proxies for aggression and courtship, respectively.

Aggression among *D. melanogaster* males was the most prominent and intense of any *melanogaster* subgroup species tested (Fig. 1A-C, fig. S2C,E). Species in the neighboring *simulans* clade (*D. simulans*, *D. mauritiana*, and *D. sechellia*) also fought, though less frequently, using a similar set of actions (Fig. 1A-C, fig. S2C,E). Varying foods usually had little effect on the behavior of specialists, with the notable exception of *D. sechellia* which fought significantly more over *Morinda* than the standard apple juice (fig. S3A), consistent with its specialization (*54*). Male-male interactions in *D. melanogaster* and *simulans* clade species all included very little recognizable courtship, and the few bouts we observed never progressed to attempted copulations (Fig. 1A,B). Thus, intermale aggressive actions in the subgroup branch that includes *D. melanogaster* are almost entirely distinct from the courtship that males perform toward females (Fig. 1E,F, fig. S4).

The other branch of the *melanogaster* subgroup, which includes *D. erecta*, *D. yakuba*, and *D. santomea*, exhibited dramatically different male-male dynamics. *D. erecta* males hardly interacted or locomoted, even on a *Pandanus* substrate (Fig. 1A,B, fig. S1B, fig. S3) (*58*). *D. yakuba* and *D. santomea,* by contrast, exhibited low levels of aggression and multiple distinct, clearly recognizable courtship actions (Fig. 1A,B). Male-male courtship in both species was visually similar as toward females (Fig.

1G,H, fig. S4), but the two sibling species differed markedly from each other in penetrance and expressivity. Courtship and attack between *D. yakuba* males were both infrequent, whereas *D. santomea* males courted other males considerably more than they fought them and far more than did *D. yakuba* or any other subgroup species (Fig. 1B,D, fig. S2D,F). High levels of male-directed courtship and low aggression were conserved in three additional *D. santomea* strains (fig. S2C-F), were not limited to the initial moments of an encounter when sex identification might be incomplete (Fig. 1D) (*51*, *59*), and sometimes culminated in copulation attempts (Fig. 1A). Audio recordings (*60*) confirmed that *D. santomea* males sang to males as they did to females, emitting both "pulse" and "clack" song (*61–63*) with similar (though not identical) acoustic features (Fig. 1I,J, fig. S5).

Thus, under our conditions we find a striking difference in intermale social behavior between *D. melanogaster* and *D. santomea*. *D. melanogaster* and *simulans* clade relatives attack males with varying frequencies using a conserved set of actions, whereas *D. santomea* courts both males and females with nearly indistinguishable motor and acoustic features. While widely described in other taxa (*64*) and various *D. melanogaster* mutants (*24*), the frequent courtship among wildtype adult males shown by *D. santomea* in naturalistic settings is, to the best of our knowledge, novel in the *Drosophila* genus. Importantly, *D. santomea* male-directed courtship is not due to sex misidentification, because individual flies that courted and sometimes also attacked males immediately switched to exclusive courtship with significantly increased vigor when encountering a female (Fig. 1K-M). In a trio assay for target sex preference, *D. santomea* males also exhibited a slight preference for courting females over males (Fig. 1N).

The abundant and monomorphic cuticular pheromone 7-tricosene is sexually attractive to *D. santomea* males

Five of the nine *melanogaster* subgroup species (*D. simulans*, *D. santomea*, *D. yakuba*, *D. teissieri*, and *D. orena*) are considered pheromonally monomorphic because the same cuticular hydrocarbon (CHC) is the most abundant compound on the cuticles of females and males (*65–67*). For all five the defining monomorphism is of (Z)-7-tricosene (7-T) (Fig. 2A, fig. S6), a nonvolatile compound detected via contact chemosensation (*68*, *69*). *D. santomea* courts in the dark (although copulation rate is reduced) (Fig. 2B) (*70*), and removing CHCs in bulk from either females or males strongly diminishes their attractiveness (Fig. 2C), implying the existence of courtship-promoting pheromone(s) shared between sexes. That 7-T is an aphrodisiac signal for *D. santomea* males is supported by monomolecular add-back following bulk CHC removal from *D. santomea* females (Fig. 2D), ectopic addition to intact females of species lacking endogenous 7-T (*D. melanogaster* and others) (Fig. 2E, fig. S7), and positive correlation between 7-T presence and courtship elicited from *D. santomea* males in a variety of

113 heterospecific male-male pairings (Fig. 2F). Thus, 7-T appears necessary and is sufficient to evoke sexual
114 attraction in *D. santomea* males. The inversion from 7-T suppressing courtship in *D. melanogaster* (where
115 it is male-specific) (*71–74*) to promoting courtship in *D. santomea* is shared with *D. yakuba* (*32*),
116 suggesting that the 7-T valence switch arose in tandem with or soon after monomorphism in the *D.*
117 *santomea / D. yakuba* common ancestor on mainland Africa (Fig. 2G) (*75*).
118

119 **Selectively low cVA abundance on *D. santomea* males amplifies intermale courtship**

120 If *D. santomea* sexual attraction uses an abundant and monomorphic signal (7-T), then it would
121 seem unsurprising that male-directed courtship is a corollary outcome of this relatively simple pheromone
122 arrangement. However, intermale courtship in *D. yakuba* and other 7-T monomorphic species is rare (Fig.
123 2G) (*30*, *32*, *76*), hinting that *D. santomea* males have either gained an additional courtship-promoting
124 signal absent in the other species or lost a courtship-inhibiting signal otherwise present. Consistent with
125 the latter, we found that *D. santomea* males produce significantly less (Z)-11-octadecenyl acetate (cVA)
126 than other subgroup members (84-92% reduction, 89% less than *D. yakuba*) (Fig. 3A, fig. S8). cVA is a
127 semi-volatile olfactory pheromone produced in the ejaculatory bulb of male drosophilids (*67*, *77*, *78*) and
128 has pleiotropic social roles including promoting aggregation (*79–81*) and aggression (*82–85*) and
129 suppressing courtship (*86–90*), either natively on males or after transfer to females during copulation.
130 Behavioral dose-response curves with cVA applied onto a piece of filter paper indicated that cVA indeed
131 suppresses courtship in *D. santomea* (Fig. 3B-D), with the primary effect being to increase latency to
132 initiation (Fig. 3C). In trios, *D. santomea* tester males showed nearly universal preference for courting
133 solvent control treated males or females over flies directly coated with cVA (Fig. 3E). Triggering fictive
134 cVA sensation in *D. santomea* males by phasic optogenetic activation of Or67d-expressing olfactory
135 sensory neurons (OSNs) (*89*, *91–95*) was sufficient to interrupt natural courtship towards conspecific
136 partners of both sexes (Fig. 3F-I, fig. S9), as also observed in *D. melanogaster* (*96*). Interestingly, the
137 photostimulation light intensity needed to pause ongoing courtship was lower with male targets than with
138 females (Fig. 3J), consistent with some courtship suppression even by the low endogenous amount of cVA
139 present on *D. santomea* males.

140 Unlike its courtship-inhibiting function, cVA's aggression-promoting function in *D. melanogaster*
141 (*82*, *83*) does not appear to be conserved in *D. santomea* males. cVA addition experiments, either onto
142 filter paper or directly onto live target males, showed no effect of inducing aggression (Fig. 3K,L) nor did
143 strong and direct photoactivation of Or67d OSNs (Fig. 3M). Pairings with unmanipulated heterospecific
144 male partners presenting high endogenous cVA levels also failed to significantly increase attack behavior
145 by *D. santomea* males (fig. S10). The ineffectiveness of cVA to promote aggression in *D. santomea* males

146 may be due to the 7-T valence switch described above (Fig. 3N-P) or could reflect a reduced behavioral
147 sensitivity to the pheromone relative to *D. melanogaster*.
148 The sexual attraction promoted by monomorphic 7-T and low levels of the male-specific anti-
149 aphrodisiac cVA thus provide a pheromonal basis for selectively elevated courtship among *D. santomea*
150 males. One curious additional effect was observed, presumably also due at least in part to the low cVA
151 abundance on *D. santomea* males. When paired with males of other *melanogaster* subgroup species that
152 find cVA sexually aversive (*32*, *67*, *89*) and show minimal sexual behavior in conspecific male-male pairs
153 (*D. melanogaster*, *D. simulans*, *D. yakuba*), *D. santomea* males elicited 200-580% higher levels of
154 courtship and 53-91% reduced levels of aggression from the heterospecific males relative to the amount
155 those species showed in conspecific settings (fig. S11). Thus, *D. santomea* male attractiveness extends
156 even across species boundaries to multiple other drosophilids.
157
158 **Central aggression circuits in *D. santomea* can evoke intense attack when photoactivated**
159 *D. santomea* intermale sexual behavior is frequent but does not fully saturate the time that two
160 males interact (Fig. 1B). Even so very little attack occurs outside of courtship periods. This observation,
161 in addition to the ineffectiveness of cVA to promote aggression, prompts the question of whether *D.*
162 *santomea* aggression circuitry is conserved and functional.
163 Multiple aggression-promoting neurons have been identified in *D. melanogaster* males (*97*, *98*),
164 among which are P1/pC1 (and subsets therein) (*57*, *85*, *96*, *99–105*) and AIP (also called CL062) (*106–*
165 *108*). We generated transgenic reagents necessary to access P1/pC1 (referred to here as $P1^{dsx}$ to reflect the
166 $71G01^{DBD};dsx^{AD}$ split driver combination used) and AIP in *D. santomea* by combination CRISPR-Cas9
167 knock-in (*109*, *110*) and phiC31 recombination into existing landing site lines (*111*, *112*), and tested
168 photoactivation effects in single or paired flies using CsChrimson as the opsin effector (*113*). In
169 comparison to *D. melanogaster* (*106*), AIP neurons had the expected position and morphology in *D.*
170 *santomea* males (Fig. 4A), and photoactivation in solitary flies elicited bilateral wing elevation (i.e. threat
171 display, the major non-contact-mediated form of aggression in *Drosophila*) (*41*, *49*, *50*) time-locked to the
172 onset and offset of photostimulation (Fig. 4B-D, fig. S12). $P1^{dsx}$ neurons were similarly present with a
173 morphology resembling that in *D. melanogaster* (Fig. 4E) (*114*, *115*) and photostimulation evoked reliable
174 time-locked courtship measured by unilateral wing extension in solitary *D. santomea* males (Fig. 4F, fig.
175 S13).
176 In same-genotype pairs of *D. santomea* males both experiencing titrated photoactivation, $P1^{dsx}$
177 stimulation induced a mix of aggressive and courtship actions similar to the effects seen in *D.*
178 *melanogaster* (Fig. 4G-J, fig. S14) (*57*). Lunge attacks were detected during low frequency stimulations
179 (significantly at 2 Hz) and escalated in intensity as the stimulus frequency increased (Fig. 4H,I, fig. S14A-

C). Fighting remained persistently elevated following the final photostimulation period for the duration of the recording. Thirty-second high frequency stimulations (>10 Hz) at one-minute intervals interrupted the otherwise monotonic increase in attack intensity with temporary phases of courtship and locomotor arrest time-locked to photostimulation (Fig. 4H,J, fig. S14D,E). Mixed-genotype pairs (in which one of the two photoactivated males was replaced with a wildtype male prepared to be passive during the assay by group-housing) confirmed that stimulated aggression was fly-autonomous and not exclusively caused by social feedback (fig. S15). However, these experiments also revealed some contextual flexibility in the expression of optogenetically evoked attack. $P1^{dsx}$ photoactivated flies in mixed pairs required slightly higher stimulation frequency to initiate attack (5 instead of 2 Hz, fig. S15A vs. Fig. 4I) and their attack intensity remained ~50-60% lower than in same-genotype pairs throughout the trials (fig. S15B). Interestingly, increased attack latency by $P1^{dsx}$ photoactivated males in mixed pairs did not also obtain for courtship (fig. S15C), resulting in a shift from nearly equal balance between flies exhibiting attack or courtship first in same-genotype pairs to a majority of cases where courtship preceded attack in mixed pairs (fig. S15E). This suggests that passive male opponents can, to a limited degree, favor expression of courtship instead of attack by *D. santomea* males.

Major nodes within at least two distinct aggression-promoting circuits ($P1^{dsx}$ and AIP) are therefore conserved in *D. santomea* and both contact- and non-contact-mediated agonistic behaviors can be efficiently evoked by their photoactivation. This rules out that the paucity of spontaneous attack in *D. santomea* male pairs under naturalistic conditions derives from an evolved loss of function of (at least these) aggression circuits. $P1^{dsx}$ experiments reveal that *D. santomea* aggression can be elevated to supernormal intensity and exhibit persistence under optimal photoactivation conditions (~23-fold higher lunge rate observed after the final photostimulation compared to the average during spontaneous interactions, Fig. 4I vs. Fig. 1C), but the direct effect of courtship dominates and strongly suppresses attack during $P1^{dsx}$ photostimulation, as also in *D. melanogaster* (*57*). An opponent whose pheromone bouquet activates *D. santomea* $P1^{dsx}$, especially a non-aggressive one, would therefore be expected to elicit courtship instead of attack as long as the activation perdures.

A switch from cVA sexual attraction to aversion in *D. santomea* females

D. santomea has an interesting natural history (Fig. 5A-C) (*116–118*). They are endemic to the equatorial West African island of São Tomé, located 280 km from Gabon in the Gulf of Guinea. *D. yakuba* also inhabits São Tomé, and the two sibling species largely segregate along the elevation gradient from the volcanic island's warm, dry, and open perimeter (*D. yakuba's* range) to its cool, humid, forested summit (*D. santomea's*). A sympatric zone is formed at their mid-elevation boundary, where both species and rare F1 hybrids can be collected that adhere to Haldane's rule for sterility in the heterogametic sex

(i.e., males) (*119*). Since *D. santomea* and *D. yakuba* males court females of both species promiscuously (*120*, *121*), male offspring sterility strongly pressures females to discriminate against heterospecific matings and maintain reproductive isolation (*122*). In flies this challenge would normally be expected to be met by females detecting species-specific acoustic features of male courtship song (*123*), but although *D. santomea* and *D. yakuba* songs are distinct (*61*, *63*), *D. santomea* females are still able to distinguish males of each species even if they are muted by wing amputation (*62*). These observations implicate additional species-identifying cues.

The cVA addition experiments above demonstrated that *D. santomea* males show increased copulation latency and reduced copulation rates in the presence of high cVA (Fig. 3C,D), but we noticed that the effects may not derive exclusively from alterations in the males' behavior. *D. santomea* females exhibited reduced innate attraction to cVA in a place preference assay compared to *D. melanogaster* (fig. S16), and cVA exposure with courting males dramatically increased expression of ovipositor extrusion (Fig. 5D, fig. S17), a sexual rejection behavior typically seen in recently mated, unreceptive *Drosophila* females (*124–127*). Significant rejection occurred at a lower cVA dose than was required to reduce male courtship (1 vs. 2 mg, Fig. 5D vs. Fig. 3B) even after normalization to the amount of male courtship observed (Fig. 5E). Incorporating observations of wing spreading, a distinct female behavior signaling sexual acceptance (*128*), into a combined index of *D. santomea* receptivity also captured the cVA-dependent rejection response (Fig. 5F). Strikingly, Or67d OSN silencing via ectopic expression of the inward rectifying potassium channel Kir2.1 (*129*) in *D. santomea* females paired with wildtype conspecific males resulted in ~2-fold increased copulation rates compared to controls (Fig. 5G). Sensation of endogenous cVA on *D. santomea* males therefore normally limits *D. santomea* female sexual responses.

Thus, the effect of cVA to promote sexual receptivity in *D. melanogaster* females (*89*, *130*, *131*) is reversed in *D. santomea*. This unexpected switch represents a third pheromonal change accrued in *D. santomea*, along with attraction to 7-T and reduced cVA abundance in males, relative to *D. melanogaster* and other *melanogaster* subgroup species. We hypothesize that the cVA valence reversal may help *D. santomea* females identify and avoid unwanted hybridization with high cVA-expressing *D. yakuba* males, thereby maintaining reproductive isolation in São Tomé (Fig. 5H). A question arises then of whether the increased intermale courtship that results from cVA reduction is simply a costly but necessary accommodation by *D. santomea* males to the changing olfactory preferences of conspecific females. According to this view, same-sex sexual behavior (SSB) is inherently "non-reproductive" and may be detrimental to fitness or, at best, a waste of energy (*64*). We next explored whether male-male courtship might have any adaptive value in *D. santomea.*

248 **P1^{dsx} activation or natural male-directed courtship induces a competitive mating advantage in *D.***
249 ***santomea* males**

250 In the original comparative screen and multiple experiments conducted thereafter, paired *D.*
251 *santomea* males were derived from the same stock and prepared for dyadic behavior assays identically,
252 but nevertheless exhibited a surprising degree of courtship bias between members of the pair (Fig. 6A,
253 fig. S18). That is, it was usually the case that just one male performed most of the total courtship
254 observed, similar to biases observed during intermale aggression in *D. melanogaster* (*43*, *46*, *132*). In
255 pairs where fighting also took place the two actions were most often attributable to the same fly (Fig. 6B),
256 hinting that biased courtship and attack might both contribute to agonistic social dominance in *D.*
257 *santomea.*

258 *D. santomea* males do not appear to be territorial in the laboratory (fig. S19), but we reasoned that
259 the dominant courting male in dyadic male pairs might be afforded a courtship advantage in subsequent
260 female encounters, due to persistent social arousal. Given that activity in homologous P1^{dsx} neurons is
261 required for both female- and male-directed courtship in *D. santomea* (Fig. 6C), we first confirmed that
262 the long-lasting, behaviorally latent internal state that is evoked by transient activation of P1/pC1 neurons
263 in *D. melanogaster* (*57*, *97*, *100*) is also obtained in *D. santomea* (fig. S20A). Persistent effects of
264 transient P1^{dsx} photoactivation on later social behavior were assessed using a "sliding door" assay as
265 described previously (*57*). *D. santomea* P1^{dsx} tester or genetic control males were loaded into behavior
266 chambers on the opposite side of a removable barrier from a wildtype target conspecific female or male
267 prepared to be passive by group-housing. A one-minute P1^{dsx} photostimulation was performed during the
268 initial isolation phase, during which time tester males exhibited stimulus-locked unilateral wing extension
269 (fig. S20B-E). Barriers were removed ten minutes following stimulation offset, after which tester and
270 target flies were allowed to interact for an additional ten minutes (Fig. 6D). P1^{dsx} tester males showed
271 vigorous courtship, but not aggression, upon encountering target females, exceeding that observed in
272 genetic controls and with greatly reduced latency to initiation (Fig. 6E-I, fig. S20F). When encountering a
273 target male, P1^{dsx} tester males exhibited a mixture of courtship and aggression at levels that both also
274 exceeded genetic controls (Fig. 6J-N, fig. S20G). Thus, brief P1^{dsx} photoactivation induces a persistent
275 internal state that can enhance subsequent social interactions for at least a period of multiple minutes in *D.*
276 *santomea*, resulting in courtship to both sexes but aggression exclusively to males. *D. santomea* males
277 can therefore discriminate conspecific sexes and adjust social behaviors accordingly even when highly
278 aroused.

279 Next, we investigated whether a naturalistic male-male social interaction, rather than P1^{dsx}
280 photoactivation, would induce a persistent arousal state transferrable to subsequent male-female
281 interactions. Wildtype tester males were exposed to two consecutive social encounters: first in a pair with

another male, during which asymmetric courtship was displayed by one of the males, and second in a trio with the same two males and a newly added female (Fig. 6O-Q). Courtship bouts by both males were tracked in both periods (accounting for target sex in trios), to assess whether dominance in male-directed courtship during the first encounter would translate to dominance in female-directed courtship in the second. *D. santomea* males that dominated courtship in the paired male setting exhibited a significant courtship advantage toward females in the trio phase of the experiment, compared to their sub-dominant male partners (Fig. 6R,S). Copulations were rare (3/9 trios), but two of the three observed were by the previously dominant male (Fig. 6T) (in the third case, the male pair exhibited very weak dominance). Thus, an episode of male-directed courtship in *D. santomea* increases the likelihood of courtship with a subsequently encountered female, suggesting a carry-over effect of a state of $P1^{dsx}$-evoked social arousal that generalizes to mating behavior with both sexes.

Convergent social behaviors and pheromones in *D. persimilis* males

Our behavioral screen also uncovered a second species highly prone to male-directed courtship, *D. persimilis* (Fig. 1B, fig. S1A). *D. santomea* and *D. persimilis* last shared a common ancestor ~50 million years ago and intermale courtship appears to be selectively derived in each species (Fig. 7A). *D. persimilis* and *D. santomea* both inhabit cool, high elevation, montane regions, *D. santomea* in West Africa and *D. persimilis* in North America, and both are members of a sibling species pair with which they geographically overlap (*53*). Importantly, males of *D. persimilis* and *D. pseudoobscura* (the sibling species) both court females interspecifically but females show strong discrimination against hybridization (*133–135*). Like *D. santomea, D. persimilis* male-directed courtship shares visual resemblance with the female-directed form and is most often biased to just one male within each pair (Fig. 7B-D, fig. S21A,C,D). *D. pseudoobscura* males instead show the more genus-typical social patterns of male-directed aggression and female-directed courtship (Fig. 7E-G, fig. S21B-D) (*136*). Finally, *D. persimilis* males have also converged on the two key pheromonal features of CHC monomorphism and low cVA expected to reduce or eliminate major chemical barriers to male-male courtship (Fig. 7H,I) (*67*, *137*). Similar phylogenies and natural histories therefore correlate with convergent pheromones and male-male sexual behaviors shared between these two distantly related and geographically separated *Drosophila* species.

Discussion

Evolutionary changes in the expression and central processing of cuticular hydrocarbons (CHCs) have been shown to underlie phylogenetic variation in pheromonal control of male-female courtship in *Drosophila* (*22*, *67*, *138*). For example, changes in the sex-specificity of pheromone production can switch species from dimorphic to monomorphic CHC patterns (*28*, *139*), as is inferred to have occurred at least twice in the *melanogaster* subgroup (*30*, *32*). Reversal in the behavioral valence of certain CHCs can also alter patterns of sexual attraction and aversion, as for 7-tricosene (7-T), which inhibits male courtship in dimorphic *D. melanogaster* (*71–74*) but promotes courtship in monomorphic *D. yakuba* (*32*) and, to a lesser extent, *D. simulans* (*27*, *30*, *71*).

Here we have identified a set of three evolutionary changes to pheromone signaling in *D. santomea*: a switch to monomorphism and sexual attraction to 7-T in males, a roughly ten-fold reduction of the olfactory signal cVA relative to other *melanogaster* subgroup species also in males, and a behavioral valence switch to cVA in females from promoting (*89*, *130*, *131*) to inhibiting sexual receptivity. Together these changes can explain the striking and selective amplification of *D. santomea* intermale courtship and illustrate how multiple changes in the behavioral valence or abundance of pheromones in both sexes can collectively drive evolutionary variation in intrasexual social behaviors. Though definitive evolutionary causes for the three changes are difficult to resolve retrospectively, strong selection pressure on *D. santomea* to maintain reproductive isolation from *D. yakuba* in their overlapping habitat in São Tomé (West Africa) offers a unifying and plausible explanation for the emergence and fixation of these changes. A similar pattern of pheromonal and intermale behavioral changes is shown by *D. persimilis* in North America, whose females also need to maintain reproductive isolation from the sympatric sibling species *D. pseudoobscura* (*53*), implying generality and convergent evolution of responses to similar selection pressures in these two drosophilid species.

A layered evolutionary path to elevated intermale courtship in *D. santomea*

D. melanogaster males (*50*, *97*) and males of most *Drosophila* species surveyed here exhibit primarily female-directed courtship and male-directed aggressive behavior. The sex-specificity of these social behaviors in dimorphic *D. melanogaster* is controlled in part by male-specific 7-T and cVA, which function similarly to suppress intermale courtship and promote aggression (*69*, *72*, *82*, *83*). However, *D. santomea* and *D. yakuba* are monomorphic for 7-T (*65–67*) and males show 7-T sexual attraction rather than aversion (*32*). This permits these species to pursue females and mate in the dark like dimorphic species can, but shifts the function of sex discrimination to other pheromones or sensory modalities. Despite high 7-T abundance and monomorphism, intermale sexual behaviors in these species are usually minimal. The rare evolutionary occurrence (within our screen, at least) of elevated intermale courtship in

D. santomea parallels a selective reduction in the abundance of cVA, an olfactory signal which in *D. melanogaster* suppresses male courtship (*71*, *86–90*) and is otherwise present at high levels on males of *melanogaster* subgroup species. That this correlation reflects causation is demonstrated by the fact that *D. santomea* male courtship behavior can be suppressed either by addition of exogenous cVA or by direct photoactivation of olfactory sensory neurons (OSNs) expressing the cVA receptor Or67d (*89*, *91–95*). Thus, the high level of sexual behavior among *D. santomea* males can be explained by two evolutionary changes in distinct cuticular and olfactory pheromone signaling pathways: a switch in the behavioral valence of 7-T (shared with *D. yakuba*) and a reduction in the abundance of cVA (specific to *D. santomea*).

A potential evolutionary explanation for the derived male cVA reduction in *D. santomea* was lacking until our unexpected discovery of a second sexual valence switch (and third pheromonal change in total), this time in the behavioral response to cVA by females. cVA promotes mating receptivity in *D. melanogaster* females (*89*, *130*, *131*) but has the opposite effect in *D. santomea*. The switch may be related to interspecific sexual dynamics between *D. santomea* and *D. yakuba* at their geographic boundary in São Tomé. *D. yakuba* males court *D. santomea* females vigorously (*120*, *121*) and rare (sterile) F1 hybrid males can be collected within the sympatric zone (*116–118*). Thus, we speculate that the *D. santomea* female cVA valence switch arose due to ongoing selection pressure to maintain reproductive isolation from *D. yakuba* (*122*). If this explanation is correct, it would imply that *D. santomea* females use the high level of cVA on *D. yakuba* males as a sex- and species-identifying cue to ward off unwanted advances from heterospecific suitors (though we cannot exclude that *D. yakuba* courtship song is also used by *D. santomea* females for species discrimination) (*61–63*). This female aversion to cVA may have led in turn to reduced cVA production by *D. santomea* males under sexual selection pressure (*140*).

However, two other evolutionary scenarios are also possible. *D. santomea* males may have initially reduced cVA abundance due to neutral drift or to pheromonally distinguish themselves from *D. yakuba* males (*141*), which in turn may have pressured *D. santomea* females to develop cVA aversion by sexual selection operating in the reverse direction. Alternatively, *D. santomea* female cVA aversion and male cVA reduction may have evolved simultaneously, potentially in genetic linkage (*142*). In any of these scenarios, the ultimate outcome would still be an elegant pheromonal mechanism which maintains efficient intraspecific mating in *D. santomea* while minimizing unfit hybridization with *D. yakuba*. Interestingly, a similar sexual reversal from cVA promoting to inhibiting female receptivity has been reported in one other drosophilid, the agricultural pest *D. suzukii* (*143*), whose males show fully eliminated cVA production (*144*). The evolutionary circumstances and selection pressures leading to *D. suzukii* cVA changes are unclear, however, as are potential consequences for intermale social behaviors.

Mechanistic explanations for the changes to cVA signaling in *D. santomea* females remain to be elucidated. In *D. suzukii*, female cVA valence reversal correlates with dramatic size reduction of the olfactory glomerulus targeted by Or67d OSNs (DA1) (*144*), but this mechanism does not seem to be shared with *D. santomea* where DA1 size and position appear similar to closely related species (*145*). In *D. melanogaster*, cVA promotes female receptivity through activation of DA1-lvPN (*84*) and pCd neurons (*100*, *146*) in the central brain. Whether behavioral valence inversion in *D. santomea* females is reflected in a physiological inversion of the effect of cVA on these neurons, from excitatory to inhibitory, is an interesting possibility. A challenge also remains in resolving the genetic and biochemical nature of reduced cVA abundance in males and determining whether the divergent *D. santomea* and *D. persimilis* lineages achieved reductions by similar means. A biosynthetic logic for cVA production in the ejaculatory bulb has been proposed (*147*) and one elongase identified (*148*), but additional enzymes necessary to generate cVA from fatty acid precursors have not yet been identified. *Cyp6a20* has been identified as a potential degradative enzyme for cVA which is expressed by non-neuronal cells in Or67d-expressing sensillae (at1) (*44*, *47*), and may be another target of selection.

Mechanisms for suppressing aggression in *D. santomea* males

D. santomea males show little spontaneous attack. However, photoactivation of aggression-promoting neural circuits in the central brain is sufficient to elicit multiple contact- or non-contact-mediated agonistic actions (e.g., threat displays, lunging, tussling) with supernormal intensity, ruling out a lack of vigor or selective atrophy of aggression circuits as explanations for the low level of spontaneous aggressive behavior. Because *D. santomea* males can discriminate conspecific sexes they must be able to detect male- and/or female-specific cues. Evidently, male-specific cues are either insufficient to activate aggression circuits, or their action is overridden by coincident male-derived courtship-promoting cues (e.g., 7-T) (*97*). Notably, as in *D. melanogaster* (*57*), *D. santomea* males only attack each other during the light-off periods of phasic $P1^{dsx}$ photoactivation experiments. This OFF-activation pattern of aggression may reflect a post-inhibitory rebound mechanism following stimulation-locked courtship, perhaps resulting from reciprocal inhibition between courtship and aggression circuits (*97*, *99*). Apparently the effects of this rebound are long lasting, since propensity for male-directed attack remains elevated even ten minutes after $P1^{dsx}$ neurons have been stimulated in the sliding door assay, as initially demonstrated in *D. melanogaster* (*57*). One key difference from *D. melanogaster* is apparent, however: *D. santomea* males also court the conspecific males they subsequently encounter, consistent with the high 7-T, low cVA, or other sexually attractive male features occasionally overriding rebound aggression by promoting courtship. This interpretation is supported by the fact that no aggression and instead exclusive courtship is performed towards females following barrier removal.

412 In addition to inhibiting male courtship, cVA and Or67d signaling can promote aggression among
413 *D. melanogaster* males (*82–85*). If this were also the case in *D. santomea*, then cVA reduction alone could
414 have parsimoniously explained both the elevated courtship and reduced fighting observed in *D. santomea*
415 intermale social interactions. However we have so far been unable to verify this prediction, because
416 various experimental efforts to elevate cVA including strong and direct photoactivation of Or67d OSNs
417 have been ineffective at increasing *D. santomea* aggression (although effective at suppressing intermale
418 courtship). A possible explanation for these negative results is suggested by the established hierarchical
419 control of male-male social behavior by 7-T and cVA in *D. melanogaster* (*72*). There, cVA can promote
420 fighting but only if 7-T signaling remains intact. In flies lacking 7-T or its receptor Gr32a (*69*), cVA has
421 no effect to promote aggression or to inhibit the extensive male-male courtship unmasked by genetic
422 disruption of 7-T signaling. Thus, suppression of intermale courtship by 7-T is apparently a prerequisite
423 for the aggression-promoting effect of cVA in *D. melanogaster*. By extension, since in *D. santomea* 7-T
424 no longer suppresses courtship, then according to this hierarchical model increasing cVA experimentally
425 should be unable to promote fighting, as is observed. This hypothesis does not exclude the possibility that
426 thus-far undetected evolutionary changes in aggression-promoting components of cVA central processing
427 circuitry (*84*, *100*) may also prevent this pheromone from promoting aggression in *D. santomea* males.
428

429 **Recent speciation and intermale sexual behavior**

430 It seems unlikely to be a coincidence that the two cases of highly expressive and penetrant male
431 same-sex sexual behavior (SSB) discovered here in *Drosophila* are each observed in members of
432 sympatric sibling species pairs susceptible to unfit hybridization. This correlation suggests that recent
433 speciation may promote elevated SSB expression (or alternatively that high SSB may promote
434 speciation), especially in the species inferred to be derived due to its more restricted geographic range.
435 Interestingly, such a correlation was also found in a phylogenetic analysis of SSB incidence across all
436 mammals, including the Hominidae (*149*). Our findings provide a general model that may explain at least
437 some of these cases. Namely, where sympatry necessitates enforcement of reproductive isolation between
438 interfertile species that produce unfit hybrid offspring (such as sterile F1 males) (*122*), mechanisms that
439 evolve to prevent interspecific mating may draw upon sensory cues that, once altered, also modify
440 intraspecific social behaviors in such a way as to release SSB. If the condition of sympatry is removed, or
441 additional species-identifying cues are enlisted, or compensatory mechanisms evolve to alter the resulting
442 pattern of intrasexual social interactions, then SSB may eventually disappear, unless it provides adaptive
443 value.

444 Such an adaptive value for SSB may have accrued in *D. santomea* for either of two reasons, not
445 mutually exclusive. Males performing natural courtship during male-male encounters (or courtship

446 evoked by P1^{dsx} photostimulation) initiate courtship more quickly and sustain it more vigorously toward a
447 female if she appears within a few minutes. Males could therefore benefit from this persistent social
448 arousal or "priming" effect. Alternatively, the strong courtship bias observed in dyadic male-male
449 interactions, and the fact that the same male that courts is also the one more likely to attack, suggests that
450 intermale courtship could have an adaptive function in mediating social dominance (*64*). Interestingly,
451 evidence in laboratory mice suggests that most episodes of male SSB reflect dominance mounting, a low-
452 intensity form of aggressive behavior, rather than affiliative sexual behavior (*150*). SSB as a dominance
453 behavior has also been proposed in other taxa (*151*, *152*).
454 The general relationship between SSB and aggression across species appears more complex. The
455 survey study in mammals (*149*) found a positive correlation between SSB and lethal male violence,
456 motivating the hypothesis that SSB may evolve to ease escalating intermale aggression. If this alternative
457 model also pertains to *Drosophila*, then the sequence and causal role of evolutionary events identified
458 here should be reinterpreted: rather than the key benefit of pheromonal (especially cVA) changes being to
459 avoid cross-species hybridization, it may instead have been to effectively replace intermale aggression
460 with courtship, a form of social interaction carrying reduced risk of harm to individuals (*64*). In other
461 words, *D. santomea* males may have evolved a social strategy in which the ultimate functions of
462 aggression that improve fitness (e.g., securing resources, mates, etc.) can be achieved by asymmetric
463 intermale courtship instead, avoiding aggression's injurious costs but maintaining its agonistic or
464 competitive function (*153*). Resolving or harmonizing these alternatives, potentially by modeling or
465 controlled selection experiments, should help to clarify the evolutionary origins of social behavior across
466 the animal kingdom, perhaps including in *Homo sapiens*.
467
468 **Caveats**
469 Our data implicating 7-T as a male aphrodisiac involves addition of exogenous pheromone to
470 dead females. Therefore, we cannot exclude that other components of the CHC bouquet and/or non-CHC
471 pheromones contribute to *D. santomea* male sexual attraction to live conspecific females or males, or that
472 non-chemosensory signals also play a role (*30*). We have also so far been unable to demonstrate that 7-T
473 sensation or physical or olfactory contact with unaltered conspecific females or males is sufficient to
474 induce physiological activation of P1^{dsx} somata or neuropil in restrained *D. santomea* males using two-
475 photon calcium imaging. We believe these negative imaging results likely reflect technical issues rather
476 than biology, since both 7-T and conspecific females carrying endogenously high levels of 7-T can
477 activate P1^{dsx} neuropil in the sibling species *D. yakuba* (*32*). Finally, our evidence that cVA inhibits *D.*
478 *santomea* male courtship derives from gain-of-function experiments involving exogenous cVA addition or
479 optogenetic activation of Or67d OSNs, all of which are vulnerable to behavioral outcomes resulting from

480 supraphysiological pheromone exposure (whether chemical or fictive). It is therefore possible that cVA
481 pheromonal signaling can have distinct effects on courtship or other social behaviors at lower
482 concentrations or under weaker activation conditions.
483

Acknowledgments

We thank the Anderson lab (Caltech) for help throughout the project, including experimental suggestions and conceptual advice. Liliana Chavarria, Gina Mancuso, Celine Chiu (Caltech) for administrative help. Arnold Sanchez (Caltech) for fly stock maintenance. Heather Dionne, Jeremy Hasseman, Elizabeth Kim, Katie Schretter, and Hiroshi Shiozaki (Janelia Research Campus) for constructs, reagents, and fly stocks. Rory Coleman (NYU) and Vanessa Ruta (Rockefeller) for constructs, fly stocks, information regarding unpublished results, and comments on the manuscript. Hong Yu and Garrett Kuiken (Rainbow Transgenic Flies) for embryo injections. Kathy Musial, Gary Roberson (Huntington Botanical Gardens), and David Orr (Waimea Botanical Garden) for access to fruits for host specialization experiments. Ryan York (Arcadia Science) for help with behavioral and evolutionary analyses. Peter Andolfatto (Columbia) for access to an assembled and annotated *D. santomea* reference genome. Markus Knaden (MPI Chemical Ecology) for permission to reanalyze published TD-GC-MS data.

Funding

NIH NIDA 5R37DA031389 (DJA)

Howard Hughes Medical Institute (DJA)

Caltech Center for Evolutionary Science (YO, DJA)

Jane Coffin Childs Memorial Fund Postdoctoral Fellowship (YO)

Della Martin Foundation Postdoctoral Fellowship (YO)

Author Contributions

Conceptualization: YO, DJA

Formal Analysis: YO, DJA

Funding Acquisition: YO, DJA

Investigation: YO, THN, HS, ELB

Methodology: ELB, YD, DLS

Resources: HS, MAK, YD, DLS, JP

Software: THN, HS

Visualization: YO, DJA

Writing – Original Draft Preparation: YO

Writing – Review & Editing: YO, THN, HS, ELB, MAK, YD, DLS, JP, DJA

Competing Interests

The authors declare no competing interests.

Data and Materials Availability

All data are available in the main manuscript or the supplementary materials. Raw source data, analytical code, constructs and associated maps, and fly stocks will be made publicly available in adherence with current Caltech and HHMI policies.

524 **Main Figure Legends**

525

526 **Figure 1. Evolutionary variation in male-male social behavior within the genus *Drosophila***

527 **(A)** Ethograms from twenty-minute male-male interactions over food depicting aggressive and courtship
528 actions scored in three representative conspecific pairs per species across the melanogaster subgroup.
529 Nodes are bout counts of a given action type, with sizes representing frequency normalized to summed
530 bouts scored across all actions (expert annotation). Edges indicate action transitions, with weights
531 representing the fraction of bouts of a given action (arrow origin) for which a second action (arrow
532 destination) occurred within one second. Eleven total actions in each ethogram are arranged in four rows:
533 first, three aggressive threat actions (threat, pump, charge) (*106*); second, three aggressive contact-
534 mediated actions (lunge, hold, tussle) (*49*); third, three courtship actions utilizing the wings and typically
535 directed toward females (UWE, BWE, row) (*20*); fourth, two courtship actions involving locomotory
536 maneuvers (circle, copulation attempt). Nodes indicating aggressive actions are filled with blue shades
537 and courtship actions with reds. Species arrangement and divergence times according to compilation of
538 available phylogenies (*75*, *154*, *155*). Note emergence of male-directed courtship and reduction of
539 aggression in *D. santomea* (orange) and, to a lesser extent, its sympatric sister species *D. yakuba* (green).
540 *D. erecta* ethogram gray coloration indicates that very few social actions of any kind were observed.
541 Abbreviations: UWE, unilateral wing extension; BWE, bilateral wing extension; Cop. att., copulation
542 attempt. See table S2 for wildtype strains used in figures throughout.

543 **(B)** Stacked barplots showing cumulative time spent by paired males in any aggressive (blue) or courtship
544 action (red) as a fraction of the twenty-minute total interaction. Additional Sophophora subgenus species
545 for which male-male interactions were scored for the same action set are included. Note unusually high
546 time dedication to male-directed courtship by *D. santomea. D. serrata* aggression scoring is inflated due
547 to unusually long holds.

548 **(C,D)** Expressivity and temporal dynamics of male-male aggression (C) and courtship (D) in *D.*
549 *melanogaster* (black), *D. simulans* (gray), *D. santomea* (orange), and *D. yakuba* (green). Bold traces
550 indicate the mean fraction of frames annotated as lunge (for aggression, C) or UWE (for courtship, D) by
551 automated classifiers in a 10-second sliding window. Envelopes represent standard error of the mean
552 (s.e.m.). Note high aggression in *D. melanogaster* male-male pairs and high courtship in *D. santomea*
553 throughout twenty-minute interactions (significance by Kolmogorov-Smirnov tests). See table S4 for
554 statistics related to figures throughout.

555 **(E-H)** Video stills of *D. melanogaster* (E,F) and *D. santomea* males (G,H) interacting with conspecific
556 female (E,G) or male targets (F,H). *D. melanogaster* court females (E, male shown in UWE) and attack

557 males (F, shown mid-lunge). *D. santomea* court both sexes using a similar set of motor patterns (G,H,
558 males shown in UWE for both) and rarely attack. Scale bars, 1 mm.
559 **(I,J)** Representative *D. santomea* courtship song traces showing "pulse" and "clack" emitted toward both
560 females (I) and males (J).
561 **(K)** Scheme for assessing social behavioral differences by *D. santomea* male tester flies paired
562 consecutively with a male then female conspecific target for twenty minutes each.
563 **(L.M)** Aggression (L, measured as lunges per minute) and courtship (M, fraction of total interaction time
564 performing UWE) exhibited by *D. santomea* male testers towards male then female targets in sequential
565 pairings. Data points derived from the same tester are paired and distribution means shown as paired
566 black dots. Note aggression towards males is never also observed to females and significantly increased
567 courtship rates to females (paired Mann-Whitney *U* tests).
568 **(N)** Courtship preference index exhibited by *D. santomea* male testers towards conspecific female and
569 male targets presented simultaneously in ten-minute trio assays. Index calculated as the difference in time
570 spent courting each sex normalized by the sum. Significance compared to a null median of zero
571 (indicating no preference) determined by one-sample Mann-Whitney *U* test. Note slight but significant
572 preference for courting females.
573

Figure 2. The abundant and monomorphic cuticular pheromone 7-tricosene is sexually attractive to *D. santomea* males

(A) Mirrored gas chromatograms representing male (purple, top) and female (pink, bottom) *D. santomea* cuticular hydrocarbon (CHC) profiles. Individual measurements made on hexane extracts from ten pooled, age-matched adult flies (3 male, 2 female replicates). Peaks representing the internal standard (C18, 1), male-specific (Z)-11-octadecenyl acetate (cVA, 2), and monomorphic (Z)-7-tricosene (7-T, 3) are indicated.

(B) Fraction of time *D. santomea* males spend courting conspecific females or males in ambient light vs. dark during ten-minute interactions. Boxplots show full distribution range within whiskers (excluding statistically identified outliers) and second and third quartiles within boxes, with medians in bold. Individual data points (including outliers) overlayed as gray or, for males courting females that successfully copulated, red dots. Outliers retained in all summary metrics and statistical comparisons here and throughout. Note slight but non-significant decreases in courtship toward both sexes in the dark (Mann-Whitney *U* tests), although a significantly reduced copulation rate with females is observed (binomial test).

(C) Fraction of time *D. santomea* males spend courting conspecific dead females or males with or without endogenous CHCs (removed by hexane washes) during ten-minute interactions. Significantly reduced courtship without CHCs for both target sexes (Mann-Whitney *U* tests).

(D) Similar to (C), with 10% 7-T add-back (20 µg/fly) or hexane solvent control to conspecific dead females after CHC removal. 7-T treatment partially restores attractiveness to *D. santomea* male testers (lettered statistical groupings assigned by post-hoc Dunn's tests following significant Kruskal-Wallis). Cohen's *d* effect size for 10% 7-T addition (fourth) vs. no addition after CHC wash (second), 0.692 (95% CI -0.379-0.821, p=0.401). Cohen's *d* effect size for solvent addition (third) vs. no addition after CHC wash (second), 0.221 (95% CI 0.076-1.31, p=0.042). Cohen's *d* effect size for 10% 7-T addition (fourth) vs. solvent addition (third), 0.617 (95% CI 0.069-1.17, p=0.039).

(E) Fraction of time *D. santomea* males spend courting dead *D. melanogaster* females (endogenous 7-T low) perfumed with 10% 7-T or solvent control (hexane). 7-T addition elicits courtship from *D. santomea* males. Significance by Dunn's tests.

(F) Fraction of time *D. santomea* males spend courting conspecific (orange) or heterospecific males (*D. yakuba* green, all others black) during twenty-minute interactions. 7-T presence in each species from GC-MS and phylogeny shown below, statistical groupings by Dunn's tests above. Note correlation between 7-T presence and elevated *D. santomea* courtship.

(G) Summarized indications of 7-T monomorphism (*65*, *66*), evidence for 7-T as a sexual attractant (*32*, *71*, *72*), and binarized male-male courtship expression in *melanogaster* subgroup species arranged by

608 phylogeny. “(–)” indicates dimorphic species for which 7-T is not expected to be sexually attractive but
609 has not yet been tested. Pheromone status of common ancestors at phylogeny branchpoints inferred by
610 parsimony.
611

612 **Figure 3. Selectively low cVA abundance on *D. santomea* males amplifies intermale courtship**
613 **(A)** cVA abundance on males of the *melanogaster* subgroup measured in single flies (5-8 per species) by
614 TD-GC-MS. Statistical groupings by Dunn's tests; "a.u." arbitrary units. Note low cVA level selectively
615 in *D. santomea* males. Data derived from (*67*) with permission from the authors.
616 **(B-D)** *D. santomea* sexual behavior during twenty-minute interactions with females in the presence of
617 increasing cVA on a piece of filter paper nearby (0, 1, or 2 mg). (B) Fraction of time spent courting. (C)
618 Latency to first courtship bout. (D) Latency to copulation. Pairwise statistical significance by Dunn's
619 tests, binomial tests for copulation rates. Note decreased courtship, increased latency, and decreased
620 copulation rate at the highest cVA abundance (2 mg).
621 **(E)** Preference index for *D. santomea* courtship towards 10% cVA (20 µg/fly) vs. solvent control
622 (acetone) perfumed live target female or male conspecific flies during twenty-minute trio interactions.
623 Index calculated as the difference in time spent courting each target normalized by the sum. Significance
624 between distributions and between each distribution and a null median of zero (indicating no preference)
625 determined by two- and one-sample Mann-Whitney *U* tests, respectively. Note that *D. santomea* male
626 testers exhibit clear aversion to cVA-perfurmed targets of either sex. All three observed copulations
627 occurred with the solvent control female.
628 **(F)** Photomicrograph showing labeling pattern of $Or67d^{Gal4}$ in the antennal lobes (AL) of a *D. santomea*
629 male. Immunostaining for Gal4-dependent cytoplasmic tdTomato pseudocolored green with Bruchpilot
630 synaptic counterstain (using nc82 monoclonal antibody) in magenta. Uniglomerular labeling pattern in
631 each AL matches the expected size and position of cVA-sensitive DA1 (*145*). Scale bar, 25 µm. See table
632 S3 for genotypes of transgenic strains used in figures throughout.
633 **(G)** Courtship rasters (red) for a single-housed *D. santomea* male carrying $Or67d^{Gal4}$ and Gal4-dependent
634 CsChrimson paired with a group-housed wildtype conspecific male target. Two representative sham trials
635 (above dash) and two photostimulation (PS) trials (below dash) are shown. Two-second PS blocks repeat
636 every ten seconds for a total of six activations after a one-minute baseline. PS frequencies increase in
637 pairs from 10 to 40 Hz within each trial and increase in intensity across trials. Note that PS immediately
638 interrupts spontaneous courtship by tester males in experimental but not sham trials.
639 **(H,I)** Quantification of (G) showing fraction of $Or67d^{Gal4}$ tester males courting males (H) or females (I)
640 during six-second windows surrounding PS blocks (H, purple; I, pink) or sham controls (black). Data
641 filtered for blocks where tester males showed spontaneous courtship within a half second of PS onset.
642 Data from all three frequencies were grouped since they gave similar results but separated by intensity:
643 120 (H) or 260 $\mu W/mm^2$ (I). Most tester males cease courtship by PS offset in experimental trials
644 (significant for both target sexes by Kolmogorov-Smirnov tests).

645 **(J)** Summary of courtship suppression effects in *Or67d*^{Gal4} tester males as a function of PS intensity with
646 male (purple) and female (pink) targets. Baselines (horizontal dashed lines) calculated as the fraction of
647 spontaneous courtship bouts in sham trials lasting more than two seconds. Note strong effects with male
648 targets at low intensities but only at the strongest intensity with females.
649 **(K)** *D. santomea* male aggression during twenty-minute interactions between single-housed males in the
650 presence of increasing cVA on filter paper. Not significant by Kruskal-Wallis test.
651 **(L)** *D. santomea* male aggression towards males directly perfumed with 10% cVA or solvent control
652 (acetone) during twenty-minute trio interactions. Not significant by Mann-Whitney *U* test.
653 **(M)** Aggression in *D. santomea* males carrying *Or67d*^{Gal4} and Gal4-dependent CsChrimson or genetic
654 controls during twelve-minute photoactivation trials. Pairs of group-housed males are exposed to six
655 thirty-second photostimulation (PS) blocks with fixed intensity and monotonically increasing frequency
656 (1-40 Hz), with a two-minute baseline and one-minute inter-block intervals. Measurements represent
657 cumulative lunge counts from all six PS blocks. Note insufficiency of *Or67d*^{Gal4} activation to induce
658 attack (no significance between genotypes by Kruskal-Wallis test).
659 **(N-P)** Logic models for control of male social behaviors by 7-T and cVA in *D. melanogaster* (7-T
660 dimorphic, N), *D. yakuba* (7-T monomorphic, O), and *D. santomea* (7-T monomorphic with reduced cVA,
661 P). In *D. melanogaster* where 7-T inhibits intermale courtship, 7-T also gates the effect of cVA to promote
662 aggression (*72*). A switch in 7-T function from suppressing to stimulating courtship in monomorphic
663 species is predicted to reduce or eliminate the aggression-promoting effect of cVA without impacting its
664 courtship-suppressing effect, as evident in *D. santomea.* Intermale courtship promoted by 7-T in *D.*
665 *santomea* is further amplified due to reduced inhibition by cVA. Edge terminating in white box indicates a
666 permissive "gating" effect by 7-T on cVA-induced aggression, in addition to its direct effect.
667

668 **Figure 4. Central aggression circuits in *D. santomea* can evoke intense attack when photoactivated**
669 **(A)** Photomicrograph showing labeling pattern of *20E08*^{Gal4} in the central brain of a *D. santomea* male.
670 Immunostaining for Gal4-dependent cytoplasmic tdTomato (green) with synaptic counterstain (nc82,
671 magenta). Close-up (A') shows AIP somata and axons (arrowhead) from boxed region. Scale bars, 50 µm
672 (A), 10 µm (A').
673 **(B)** Video still of bilateral wing elevation (threat) elicited by PS in a solitary *D. santomea* male carrying
674 *20E08*^{Gal4} and Gal4-dependent CsChrimson. Scale bar, 1 mm.
675 **(C,D)** Quantification of PS effects in solitary *20E08*^{Gal4} tester males (purple) and genetic controls (black)
676 exposed to two fifteen-second PS blocks with thirty-second baseline and inter-block interval. (C) Fraction
677 of flies showing threat (penetrance). (D) Mean fraction of frames with flies showing threat in a five-
678 second sliding window with s.e.m. envelopes (expressivity). Significant induction of threat during PS in
679 *20E08*^{Gal4} by Mann-Whitney *U* tests.
680 **(E)** Photomicrograph showing *P1*^{dsx} split-Gal4 (*71G01*^{DBD}*;dsx*^{AD}) labeling in the central brain of a *D.*
681 *santomea* male. Immunostaining for Gal4-dependent cytoplasmic tdTomato (green) with synaptic
682 counterstain (nc82, magenta). Close-ups show a characteristic region of *P1*^{dsx} neuropil (lateral junction,
683 E') and somata and axons (E'') from boxed regions. Scale bars, 50 µm (F), 10 µm (F',F'').
684 **(F,G)** Courtship elicited in solitary (F) and aggression in paired (G) *D. santomea* males carrying *P1*^{dsx}
685 split-Gal4 and Gal4-dependent CsChrimson or a genetic control during twelve-minute photoactivation
686 trials. In both cases group-housed males are exposed to six thirty-second PS blocks with fixed intensity
687 and monotonically increasing frequency (1-40 Hz), with a two-minute baseline and one-minute inter-
688 block intervals (as in H). "PS–" represents the two-minute baseline period prior to first PS. "PS+"
689 cumulatively represents all six PS blocks (for courtship, G) or all five inter-block intervals (IBIs) and
690 period following final PS (for aggression, F). See behavior dynamics in (H) for justification of aggression
691 quantification during IBIs. Note significant PS induction for both actions (Dunn's tests).
692 **(H)** Fraction of flies showing attack (lunge, blue) and courtship (UWE, red) in same-genotype pairs of
693 *P1*^{dsx} males during six PS blocks with fixed intensity and increasing frequencies. Note highly penetrant
694 attack mostly during light-off periods punctuated by time-locked courtship during high frequency PS
695 blocks. Video stills at right show aggressive tussling following 2 Hz PS (1) and simultaneous courtship by
696 both tester males during 10 Hz PS (2). Scale bars, 1 mm.
697 **(I,J)** Expressivity and temporal dynamics of attack (I) and courtship (J) elicited by PS in *P1*^{dsx} male pairs
698 (I, blue; J, red) or a genetic control (black). Significant attack induction during inter-block intervals and
699 after final PS (I) or courtship during PS compared to control (J) by Mann-Whitney *U* tests.
700

701 **Figure 5. A switch from cVA sexual attraction to aversion in *D. santomea* females**
702 **(A)** Elevation map of equatorial Central and West Africa with the volcanic island of São Tomé in the Gulf
703 of Guinea boxed. Data from (*156*) and Terrain Tiles (Mapzen, accessed Aug. 24, 2025).
704 **(B)** Elevation map of São Tomé. Note the central summit of Pico de São Tomé.
705 **(C)** Latitudinal elevation profile of Pico de São Tomé showing *D. santomea* (orange) and *D. yakuba*
706 zones (green) separated by a hybrid zone where both pure species and F1 hybrid males are found (*118*).
707 **(D,E)** Behavioral dose-response curves of *D. santomea* female ovipositor extrusion (OE) to increasing
708 cVA on filter paper during conspecific male courtship. (D) Female OE as fraction of total observation
709 time. (E) Female OE normalized to male courtship (difference divided by sum of time spent by female in
710 OE and time spent by male in UWE). Red dots, females that copulated. The lowest cVA dose induces an
711 intermediate effect while both higher doses induce significant increases in OE expression (Dunn's tests).
712 **(F)** *D. santomea* female "receptivity index" as function of increasing cVA. For each female an index
713 value of 1, 0, or -1 is possible. Observations of female wing spreading (WS, an acceptance behavior) and
714 courtship-normalized OE (rejection, from E) were each binarized as present or absent (WS>0,
715 OE(norm)>-0.25) and overall index per dose is calculated as the difference between the two binary values
716 (WS-OE) normalized by the number of females scored. Note significantly decreased sexual acceptance
717 again at the two higher cVA doses (Dunn's tests).
718 **(G)** Cumulative copulation latencies and rates by *D. santomea* tester females carrying $Or67d^{Gal4}$ and
719 Gal4-dependent Kir2.1 (black) or genetic controls (grays) grouped with an equal number of wildtype
720 conspecific males for 45 minutes in large chambers. "BDP" refers to a Gal4 driver without labeling
721 evident in the central brain. 24 total females tested of each genotype (two trials each of 12 single-housed
722 males x 12 group-housed females), significance by Kolmogorov-Smirnov tests comparing latencies or
723 binomial tests comparing rates.
724 **(H)** Evolutionary model for the emergence of high intermale courtship and low intermale aggression in *D.*
725 *santomea,* incorporating three key pheromone changes inferred to occur prior to or following *D. santomea*
726 speciation in São Tomé. A common sexual attractant for *D. santomea* and *D. yakuba* males (7-T)
727 generates the behavioral potential for unfit hybridization in sympatry due to F1 hybrid male sterility
728 (*116*). *D. santomea* females evolve sexual aversion to cVA and *D. santomea* males reduce cVA, thereby
729 maintaining efficient intraspecific mating while also maintaining reproductive isolation from *D. yakuba*
730 (the two events cannot be definitively ordered). Reduced male cVA, together with monomorphic 7-T,
731 releases high intermale courtship. Reduced efficacy of cVA to promote aggression further suppresses
732 fighting. Placement of *D. yakuba* secondary colonization after allopatric *D. santomea* speciation (instead
733 of speciation in sympatry) from (*117*).
734

735 **Figure 6. P1^{dsx} activation or natural male-directed courtship induces a competitive mating**
736 **advantage in *D. santomea* males**
737 **(A)** Spontaneous bias observed between flies in male-male *D. santomea* and *D. melanogaster* pairs for
738 attack and courtship. Indices derived from the same fly pair are connected as lines and distribution means
739 shown as paired orange (*D. santomea)* or black dots (*D. melanogaster*). Note high courtship bias in *D.*
740 *santomea.*
741 **(B)** Fraction of *D. santomea* male-male pairs with high attack bias where the same fly also showed
742 majority of courtship (left), or with high courtship bias where the same fly also showed majority of attack
743 (right). Significance compared to random chance (50%) by binomial tests.
744 **(C)** Courtship in the dark by single-housed *D. santomea* males carrying *P1^{dsx}* split-Gal4 and Gal4-
745 dependent Kir2.1 or a genetic control paired with group-housed wildtype conspecific female (left) or male
746 targets (right). Red dots, males that copulated (only observed in controls). Significant courtship reduction
747 in *P1^{dsx}* tester males toward both sexes by Mann-Whitney *U* tests.
748 **(D)** Scheme for assessing persistent behavioral effects of *D. santomea P1^{dsx}* split-Gal4 activation. After a
749 one-minute baseline, isolated *P1^{dsx}* tester males or genetic (non-activated) controls experience one-minute
750 PS and a ten-minute delay. Dividers ("sliding doors") are then removed to allow paired flies to interact
751 spontaneously for an additional ten minutes. Pairings are between a *P1^{dsx}* or control tester male and either
752 a wildtype conspecific female (E-I) or male group-housed partner (J-N).
753 **(E)** Behavior rasters for *P1^{dsx}* tester males paired with wildtype conspecific females during the ten-minute
754 interaction phase. Red, courtship (UWE); blue, attack (lunge, none observed).
755 **(F-I)** Expressivity and temporal dynamics of female-directed courtship (F,H,I) and aggression (G) by
756 *P1^{dsx}* tester males compared to genetic controls during the interaction phase. Note increased courtship
757 expression (F,H) and decreased courtship latency (I) without any coincidence of attack. Significance by
758 Kolmogorov-Smirnov (F,G) or Mann-Whitney *U* tests (H,I).
759 **(J-N)** Behavior rasters (J), temporal dynamics (K,L), and expressivity of male-directed courtship (M) and
760 aggression (N) by *P1^{dsx}* tester males compared to genetic controls during the interaction phase. Note
761 significant increases for both social actions.
762 **(O)** Scheme for determining a sexual priming effect of male-directed courtship. Two single-housed
763 wildtype *D. santomea* males are paired for ten minutes before a wildtype female is added for an additional
764 ten minutes (trio period). Male-directed courtship dominance is measured and identity of the dominant
765 courter ascertained in the paired period then compared to female-directed courtship dominance in the trio.
766 **(P,Q)** Video stills of a male courting another male first in the paired period (P) then courting a female in
767 the trio (Q). Scale bars, 1 mm.

(R) Quantification of the sexual priming effect (O-Q). Female-directed courtship dominance in trios (y-axis) plotted as a function of male-directed courtship dominance in pairs (x-axis). Points above the x-axis represent cases where the same male exhibited male-directed courtship dominance in pairs and female-directed courtship dominance in trios. Dot size (scale on right) represents total amount of male-directed courtship in pairs and data are filtered for pairs with at least twenty seconds of courtship during this phase, no matter the bias. Red dots, males that copulated. Gray box, region reflecting cases where males exhibited with high levels of courtship dominance during the paired period. Note enrichment of points above the x-axis in cases of high male-male courtship dominance.

(S,T) Categorization of effects on female-directed courtship dominance (S) and copulation advantage (T) from (R). (S) All but one male exhibiting male-directed courtship dominance in pairs (89%) also exhibited female-directed courtship dominance in trios (significant by binomial test). (T) Two out of three copulations observed were by the male exhibiting male-directed courtship dominance in pairs (circled red dots in R). The exception was from a “submissive” male in which courtship bias was very weak (uncircled red dot at bottom left in R).

783 **Figure 7. Convergent social behaviors and pheromones in *D. persimilis* males**
784 **(A)** Summarized indications of male-male courtship presence/absence in *Drosophila* species arranged by
785 phylogeny. Note sibling species *D. persimilis* (purple) and *D. pseudoobscura* (blue) in the obscura group.
786 **(B,C)** Video stills of *D. persimilis* males courting conspecific female (B) and male targets (C). Images
787 selected to represent species-typical action selection. Scale bars, 1 mm.
788 **(D)** Action biases in *D. persimilis* male-male pairs. Male-directed courtship (red dots) is more common
789 than attack (blue dots) and often shows strong bias to one fly (boxed region). Attack and courtship
790 measurements from the same pair connected by thin lines. Circled "X" indicates mean value for the
791 corresponding action.
792 **(E-G)** Video stills (E,F) and action biases (G) for *D. pseudoobscura* as for *D. per*. Note female-directed
793 courtship (E) and biased male-directed attack (F,G). Scale bars, 1 mm.
794 **(H)** cVA abundance on males of the *melanogaster* subgroup and *D. persimilis* / *D. pseudoobscura* by TD-
795 GC-MS (*67*). Statistical groupings by Dunn's tests; "a.u." arbitrary units. Note low cVA levels in *D.*
796 *persimilis* and high in *D. pseudoobscura* as in *D. santomea* / *D. yakuba*.
797 **(I)** Summary of relevant pheromones (*67*, *76*, *137*) and social behaviors for the *melanogaster* subgroup
798 (excluding *D. teissieri* and *D. orena*) and the *D. persimilis* / *D. pseudoobscura* sibling species pair. CHC
799 monomorphism is common to multiple species but low cVA abundance and high male-male courtship are
800 shared only between *D. santomea* (orange) and *D. persimilis* (purple). Information compiled from the
801 current study and prior sources.
802

803 **Supplemental Figure Legends**

804

805 **Figure S1. Additional behavior ethograms and locomotor analyses of *Drosophila* intermale social**
806 **interactions**

807 **(A)** Ethograms from twenty-minute interactions depicting aggressive and courtship actions scored in three
808 representative conspecific male-male pairs per species across various *Sophophora* and *Drosophila*. Nodes
809 are bout counts of a given action type, with sizes representing frequency normalized to summed bouts
810 scored across all actions (expert annotation). Edges indicate action transitions, with weights representing
811 the fraction of bouts of a given action (arrow origin) for which a second action (arrow destination)
812 occurred within one second. Nine total actions in each ethogram are arranged in five rows: first, two
813 aggressive threat actions (threat, pump) (*106*); second, two aggressive contact-mediated actions (lunge,
814 hold) (*49*); third, two additional contact-mediated aggressive actions (headbutt, barrage) (*157*); fourth,
815 two courtship actions utilizing the wings and typically directed toward females (UWE, BWE) (*20*); fifth,
816 copulation attempt. Nodes indicating aggressive actions are filled with blue shades and courtship actions
817 with reds, except for headbutt (white) and barrage (black). Species arrangement and divergence times
818 according to compilation of available phylogenies (*75*, *154*, *155*). Gray coloration indicates that very few
819 social actions of any kind were observed. Abbreviations: UWE, unilateral wing extension; BWE, bilateral
820 wing extension; Cop. att., copulation attempt. Barrage described previously in *D. pseudoobscura*
821 (*136*) but named here.

822 **(B-E)** Locomotor summaries for all fifteen species included in the behavioral screen. Per-frame
823 calculations of each fly's forward velocity (B), angular velocity (C), facing angle relative to the partner
824 (D), and inter-fly distance (E) are derived from automated tracking of both flies (*56*) in all recorded male-
825 male pairs. Distributions shown as violin plots with dotted means. *D. santomea,* orange; *D. yakuba*,
826 green.

827

828 **Figure S2. Performance and usage of automated behavior classifiers for intermale social**
829 **interactions within the *melanogaster* subgroup and additional *D. santomea* strains**
830 **(A,B)** Automated behavior classifier performance for lunge (A) and unilateral wing extension (B). Three
831 twenty-minute representative recordings of male-male pairs for each species were manually scored for
832 both actions (expert annotation, same pairs as in Fig. 1A) and exposed to automated behavior classifiers
833 trained previously for *D. melanogaster* (*57*), implemented in JAABA (*55*). Manual (x-axis) vs. classifier-
834 generated annotations (y-axis) are compared in $\log_{10}$ scale, using either the number of bouts (lunge) or
835 their cumulative time duration (UWE). Solid lines, diagonals; dashed lines, linear fits. Adjusted R^2,
836 significance by F-tests for fits, and Pearson correlations (r) indicated at bottom right. *D. melanogaster*,
837 black; *D. santomea,* orange; *D. yakuba*, green; *D. simulans*, *D. mauritiana*, *D. sechellia*, *D. erecta*, gray.
838 Note near-perfect overlap with the diagonal for lunge and strong correlation for UWE despite classifier
839 false positives in cases with few manual annotations (all subgroup species except *D. santomea* show very
840 little male-male courtship).
841 **(C,D)** Aggression (lunge, C) and courtship (UWE, D) measurements from automated classifiers in all
842 recorded male-male pairs for *melanogaster* subgroup species and additional *D. santomea* strains. *D.*
843 *santomea* 00 (also called STO.4) is the strain included in the behavioral screen and used throughout as
844 "wildtype" (National Drosophila Species Stock Center 14021.0271.00). Strains 146 (STO-CAGO 1482),
845 148 (STO.7), and 151 (STO.6) also derive from São Tomé from females collected between 1100 and 1500
846 m elevation (*117*). Boxplots show full distribution range within whiskers (excluding statistically identified
847 outliers) and second and third quartiles within boxes, with medians in bold. Individual data points
848 (including outliers) overlayed as gray dots. Outliers retained in all summary metrics and statistical
849 comparisons here and throughout. Lettered statistical groupings assigned by post-hoc Dunn's tests
850 following significant Kruskal-Wallis. Note low aggression and high courtship conserved in *D. santomea*
851 strains (orange), low aggression and courtship in the sibling species *D. yakuba* (green), and high
852 aggression and low courtship in *D. melanogaster* (black).
853 **(E,F)** Summaries of penetrance (x-axes) and expressivity (y-axes) for aggression (E) and courtship (F)
854 across subgroup species and *D. santomea* strains. Metrics derived from data in (C,D).
855

Figure S3. Intermale aggression and courtship in *melanogaster* subgroup species with fruit host specializations

(A,B) Aggression (A) and courtship (B) in *D. melanogaster*, *D. sechellia*, *D. santomea* (orange), and *D. erecta* male-male pairs competing over the standard apple juice substrate and other fruits based on reported specializations (*54*). Significance for each fruit/species combination by pairwise Mann-Whitney *U* tests to apple. Removing the food source significantly reduces aggression in *D. melanogaster* (*51*). *Morinda* (also called noni) significantly increases aggression but not courtship among *D. sechellia* males. *D. santomea* aggression and courtship depend only weakly if at all on food presence and source. *Morinda* and fig juices obtained commercially, *Marula* (*Sclerocarya birrea*) and *Pandanus* (*Pandanus furcatus*) obtained from botanical gardens (table S1).

867 **Figure S4. Male- and female-directed social behaviors by *D. melanogaster*, *D. simulans*, *D.***
868 ***santomea,* and *D. yakuba* males**
869 **(A,B)** Ethograms representing male-male (A) and male-female (B) social behaviors for *melanogaster*
870 subgroup species of interest. Phylogeny also includes *D. mauritiana* and *D. sechellia* from the *simulans*
871 clade, *D. teissieri* from the *yakuba* clade, and *D. erecta* without associated ethograms. Female-directed
872 ethograms represent expert annotation for three recordings of male-female pairs per species, with male
873 flies similarly prepared by single-housing and interactions taking place under identical conditions. Male-
874 directed ethograms reproduced from Fig. 1A for visual comparison to female-directed counterparts. Note
875 nearly exclusive male-directed aggressive actions (blue nodes) by *D. melanogaster* and *D. simulans* males
876 but prevalence of male-directed courtship actions (red nodes) by *D. santomea* and *D. yakuba* (though in
877 *D. yakuba* total male-direcetd actions are many fewer on average than *D. santomea)*, matching the actions
878 taken when paired with females.
879

Figure S5. Acoustic features of female- and male-directed courtship song by *D. santomea* males

(A,B) Representative courtship song traces by *D. santomea* males toward a female (A, pink) or male conspecific target fly (B, purple). Key acoustic features are indicated including pulse, pulse train, inter-pulse interval (IPI), clack, clack train, and inter-clack interval (ICI) (*63*). Traces reproduced and enlarged from Fig. 1I,J.

(C,D) Video stills of song recording chambers (*60*) containing *D. santomea* males courting either a female (C) or male (D). Isolated waveforms of single clacks and pulse trios shown below, with asterisks indicating event peaks. Scale bars, 1 mm.

(E-J) Quantitative acoustic analyses of female- (pink) and male-directed *D. santomea* courtship songs (purple). Clacks (E-G) and pulses (H-J) were identified by expert annotation from three recordings with each sex (clack, 32-103 events per recording; pulse, 140-346 events per recording). Data shown as "hemiviolin" plots in which female- and male-directed distributions are vertically mirrored. Distribution means are semicircles on the appropriate side. Note general similarity between female- and male-directed song features (significant differences based on Mann-Whitney *U* tests despite small difference magnitudes are often because so many data points make up the underlying distributions). Analyses of absolute event abundances were omitted since annotations captured only a fraction of events in each recording.

898 **Figure S6. GC-MS profiling of *D. santomea* male and female cuticular hydrocarbons (CHCs)**
899 **(A,B)** Absolute (A) and relative abundances (B) of 41 compounds identifiable as peaks in *D. santomea*
900 male (purple) and female hexane extracts (pink). Individual measurements are made on ten pooled, age-
901 matched adult flies (3 male, 2 female replicates). Calculation of absolute abundance uses known
902 concentration of the internal standard (octadecane/C18, not shown) and normalizes for number of flies
903 included in the extract. Relative abundances normalize to the summed absolute abundance of all
904 compounds excluding the standard. Male-specific (Z)-11-octadecenyl acetate (cVA, purple) and
905 monomorphic (Z)-7-tricosene (7-T, black) are indicated. Question marks in compound names indicate
906 uncertainty in chemical assignment. See table S5 for retention times and diagnostic ions used to identify
907 and assign CHCs.
908

909 **Figure S7. 7-tricosene (7-T) abundance in males and females of various *Drosophila* species and**
910 **additional 7-T add-back experiments**
911 **(A)** Absolute 7-T abundances on males (purple) and females (pink) *Drosophila* measured by GC-MS on
912 hexane extracts from ten pooled, age-matched adult flies (2-8 replicates each). Monomorphic species (*D.*
913 *santomea, D. yakuba*, *D. simulans*) show similar 7-T abundance between sexes while dimorphic species
914 show large differences (*D. erecta*, *D. melanogaster*). nd, not detected in either sex (*D. serrata*, *D.*
915 *ananassae*, *D. willistoni*).
916 **(B-D)** Fraction of time *D. santomea* males spend courting conspecific (B) or heterospecific dead females
917 (C,D) perfumed with 10% 7-T (20 μg/fly) or solvent control (hexane). Heterospecific female targets
918 selected for having either low (*D. erecta*) or undetectable (*D. ana*) endogenous 7-T levels (from GC-MS,
919 A). *D. santomea* female targets as positive controls. 7-T addition elicits courtship from *D. santomea*
920 males in both heterospecific cases. Significance by Dunn's tests.
921

Figure S8. Reduced cVA on *D. santomea* males compared to *D. yakuba* and *D. erecta*

(A-C) Mirrored gas chromatograms representing male (purple, top) and female (pink, bottom) cuticular hydrocarbon (CHC) profiles of *D. santomea* (A), *D. yakuba* (B), and *D. erecta* (C). Individual measurements made on hexane extracts from ten pooled, age-matched adult flies (2-3 replicates each). Peaks representing male-specific (Z)-11-octadecenyl acetate (cVA) indicated. *D. santomea* chromatograms reproduced from Fig. 2A for visual comparison.

(D,E) Absolute (D) and relative abundances (E) of cVA on *D. santomea* (orange), *D. yakuba* (green), and *D. erecta* males. Calculation of absolute abundance uses known concentration of the internal standard (C18) and normalizes for number of flies included in the extract. Relative abundances normalize to the summed absolute abundance of all compounds detected excluding the standard. *D. santomea* males show 63% and 75% reduced cVA comparing absolute abundance means or 64% and 65% reductions comparing relative abundance means to *D. yakuba* and *D. erecta*, respectively.

935 **Figure S9. CRISPR-Cas9 HDR knock-in strategy used to generate *D. santomea Or67d*^{Gal4}**
936 **(A)** Schematic diagrams of the Gal4 transgene and selection marker assembled into an Atalanta vector
937 (pJAT32, addgene #204297) (*158*) and *Or67d* genomic target locus shown with upstream and downstream
938 sgRNA cleavage sites. Transgene (above) contains two cassettes: *T2A-Gal4-stop(hsp70)* oriented natively
939 to the genomic target, and downstream *ie1-mCherry-stop(p10)* fluorescent marker for successful
940 integration (*32*) with inverted orientation. One kilobase homology arms flank both ends. *Or67d* genomic
941 locus (below) is targeted using sgRNAs directing double-strand breaks to immediately (15 bp)
942 downstream of the translational start codon and 348 bp downstream of the stop, resulting in removal of
943 1152 of 1167 protein coding base pairs (99%). Co-injection of the assembled Atalanta vector and nls-
944 Cas9-nls protein into wildtype *D. santomea* eggs gives mosaic *ie1-mCherry*^{pos} G0 progeny carrying *T2A-*
945 *Gal4* inserted in-frame with the five residual residues of *Or67d*. G1 progeny resulting from G0 crosses to
946 wildtype are re-screened for abdominal *ie1-mCherry* expression to ensure germline transmission. In this
947 strategy spatiotemporal patterns and magnitude of Gal4 expression are controlled entirely by *Or67d*
948 endogenous genomic regulation.
949 **(B,C)** Photomicrographs showing labeling patterns of *Or67d*^{Gal4} in the whole brain of a *D. santomea* male
950 (B, same fly from which close-up of antennal lobes (ALs) is shown in Fig. 3F) and female (C).
951 Immunostaining for Gal4-dependent cytoplasmic tdTomato pseudocolored green with Bruchpilot synaptic
952 counterstain (using nc82 monoclonal antibody) in magenta. Uniglomerular labeling pattern in each AL
953 (arrowheads) matches the expected size and position of cVA-sensitive DA1 targeted by Or67d OSNs
954 (*145*). Bifurcating OSN commissures (axon bundles) from the antennae leading into ALs can also be seen.
955 Scale bars, 50 µm.
956

957 **Figure S10. Ineffectiveness of naturally varying cVA levels on various species to promote aggression**
958 **by *D. santomea* males**
959 **(A)** Absolute cVA abundance on *Drosophila* males measured by GC-MS on hexane extracts from ten
960 pooled, age-matched adult flies (2-8 replicates each). Calculation uses known concentration of the
961 internal standard (C18) and normalizes for number of flies included in the extract. *D. santomea* (orange),
962 *D. yakuba* (green), and *D. erecta* measurements reproduced from fig. S8 for visual comparison to
963 additional species. Means indicated above and phylogeny below.
964 **(B)** Spontaneous aggression (lunges per minute) exhibited by *D. santomea* males toward conspecific
965 (orange) or heterospecific males (*D. yakuba* green, all others black) in single-housed pairs during twenty-
966 minute interactions. Statistical groupings by Dunn's tests shown above and phylogeny below. Note
967 similarly low or even decreased attack levels toward males of all species.
968 **(C)** Correlation between cVA abundance measured by GC-MS and aggression elicited from *D. santomea*
969 males. Dashed line, linear fit. Adjusted R^2, significance by F-test for fit, and Pearson correlation (r)
970 indicated at bottom right. Note marginally significant correlation driven mostly by low attack rates toward
971 distant species (*D. serrata*, *D. ananassae*, *D. willistoni*) with many other pheromone changes in addition
972 to low cVA. Three of four species with higher cVA abundance than *D. santomea* elicit less attack than
973 observed among *D. santomea* males (*D. simulans* is the exception but the slight increase is non-
974 significant). Data derived from (A,B).
975

Figure S11. Social behavior changes by *melanogaster* subgroup males toward *D. santomea* males

(A) Relative fraction of time *D. melanogaster*, *D. simulans*, and *D. yakuba* (green) males court conspecific males (first distribution of each pair) vs. *D. santomea* males (second distribution, orange). All measurements within each species normalized to the conspecific median and $\log_{10}$ transformed. Males of all three *melanogaster* subgroup species show significantly increased courtship toward *D. santomea* males by Mann-Whitney *U* tests, including *D. melanogaster* where 7-T (abundant on *D. santomea* males) is male-specific and sexually aversive (*71–74*).

(B) Similar to (A) but showing paired relative distributions for aggression within and between males of the three subgroup species. Note decreases in male-directed aggression by all three toward *D. santomea* (significant for *D. melanogaster* and *D. yakuba* by Mann-Whitney *U* tests).

(C) Heatmap showing median fraction time spent courting by males in conspecific (diagonal) and heterospecific male-male pairs (off-diagonal) among the four subgroup species. Rows ("courters") are males whose courtship is measured (UWE). Columns ("courtees") are males targeted by courtship. Gray entry where data not collected. Data derived from (A) and additional pairings. Horizontal dashed arrows identify relevant comparisons between conspecific male- and *D. santomea* male-directed courtship for visual aid.

(D) Similar heatmap showing median aggression (lunge rate) by male "attackers" (rows) and "attackees" (columns). Data derived from (B) and additional pairings. Note consistently decreased aggression toward *D. santomea* males.

(E) Summarized changes in courtship (first row) and aggression rates (second row) by heterospecific males toward *D. santomea* compared to conspecific rates for each, derived from data in (A,B). Percent increases in first row (courtship) and percent decreases in second (aggression).

999 **Figure S12. Induction of time-locked wing threat by photoactivation of AIP neurons in solitary *D.***
1000 ***santomea* males**
1001 **(A)** Optogenetic photoactivation scheme for solitary *D. santomea* males carrying $20E08^{Gal4}$ and Gal4-
1002 dependent CsChrimson. Group-housed $20E08^{Gal4}$ tester males or genetic controls are exposed to two
1003 fifteen-second photostimulation (PS) blocks with a thirty-second baseline and inter-block interval.
1004 **(B)** Manually scored wing threat rasters (purple) for solitary $20E08^{Gal4}$ males during the two-minute trial.
1005 Note threat induction time-locked to PS in most flies. Genetic controls showed no threat.
1006

1007 **Figure S13. Induction of time-locked courtship by photoactivation of P1^{dsx} neurons in solitary *D.***
1008 ***santomea* males**
1009 **(A)** Optogenetic photoactivation scheme for solitary group-housed *D. santomea* males carrying *P1^{dsx}*
1010 split-Gal4 (*71G01^{DBD};dsx^{AD}*) and Gal4-dependent CsChrimson. *P1^{dsx}* tester males or a genetic control are
1011 exposed to six thirty-second photostimulation (PS) blocks with fixed intensity and monotonically
1012 increasing frequency as indicated, with a two-minute baseline and one-minute inter-block intervals.
1013 **(B)** Courtship rasters (red) for *P1^{dsx}* tester males during the twelve-minute trial. Note early but sporadic
1014 courtship bouts that time-lock to PS blocks and increase in penetrance starting at 5 and 10 Hz.
1015 **(C,D)** Penetrance (C) and expressivity (D) of courtship (UWE) elicited by *P1^{dsx}* PS. Significant courtship
1016 expression during PS blocks compared to the genetic control in (D) by Mann-Whitney *U* tests.
1017

1018 **Figure S14. Induction of courtship and attack by photoactivation of P1^{dsx} neurons in same-genotype**
1019 **pairs of *D. santomea* males**
1020 **(A)** Optogenetic photoactivation scheme for same-genotype pairs of group-housed *D. santomea* males
1021 carrying *P1^{dsx}* split-Gal4 and Gal4-dependent CsChrimson. *P1^{dsx}* tester males or a genetic control are
1022 exposed to six thirty-second photostimulation (PS) blocks with fixed intensity and monotonically
1023 increasing frequency as indicated, with a two-minute baseline and one-minute inter-block intervals.
1024 **(B,C)** Behavior rasters for *P1^{dsx}* male pairs (B) and genetic controls (C) during the twelve-minute trial.
1025 Blue, attack (lunge); red, courtship (UWE). Note early induction of attack which increases in penetrance
1026 and expressivity as the trial continues. Attacks interrupted by time-locked courtship during later PS blocks
1027 (>5 Hz). Genetic controls show little courtship or attack.
1028 **(D,E)** Locomotor dynamics in *P1^{dsx}* males (browns) and genetic controls (black). Per-frame calculations
1029 of each fly's forward velocity (D) and angular velocity (E) derived from automated tracking (*56*). Data
1030 smoothed by averaging within a ten-second sliding window. Envelopes represent s.e.m. PS time-locked
1031 locomotor arrest similar to observed previously in *D. melanogaster* (*57*).
1032

1033 **Figure S15. Photoactivation effects of *D. santomea* P1^{dsx} neurons in mixed-genotype male pairs**
1034 **(A)** Expressivity and temporal dynamics of attack (lunge) elicited by PS in mixed-genotype pairs between
1035 a *P1*^{dsx} split-Gal4 tester male carrying Gal4-dependent CsChrimson (or genetic control) and group-housed
1036 wildtype *D. santomea* target male. Traces show the mean fraction of frames containing lunge in a ten-
1037 second sliding window with s.e.m. envelopes for *P1*^{dsx} (blue) and control (black). PS block frequency,
1038 intensity, and timing indicated above for the twelve-minute trial. Note significant attack induction (Mann-
1039 Whitney *U* tests) in *P1*^{dsx} starting after 5 Hz.
1040 **(B)** Attack elicited during inter-bout intervals and after final PS in same-genotype *P1*^{dsx} male pairs (blue,
1041 data from Fig. 4I) vs. mixed-genotype pairs between a *P1*^{dsx} tester and group-housed wildtype male
1042 (orange, from A). Period means connected with solid lines and data from individual flies shown as thin
1043 lines. Note significant right shift in mixed pairs (Mann-Whitney *U* tests) indicating higher PS frequencies
1044 required to induce intense attack.
1045 **(C)** Action latencies for courtship and attack exhibited by *P1*^{dsx} tester males in same- and mixed-genotype
1046 pairs under identical PS trial structures. Data points derived from the same fly pair (or tester fly for mixed
1047 pairs) are connected as lines and distribution means shown as paired dots. Attack and courtship latencies
1048 are similar on average in same-genotype pairs whereas attack is significantly delayed in mixed pairs.
1049 Significance by paired or unpaired Mann-Whitney *U* tests (for within- or between-genotype group
1050 comparisons, respectively).
1051 **(D)** Fraction of flies showing attack (lunge, blue) and courtship (UWE, red) in *P1*^{dsx} mixed-genotype
1052 pairs.
1053 **(E)** Relative frequencies of *P1*^{dsx} same- and mixed-genotype pairs showing courtship (red) or attack (blue)
1054 first. Significance between distributions and between each distribution and a null probability of 50%
1055 (random chance) determined by binomial tests. Note courtship precedence in mixed pairs.
1056

1057 **Figure S16. Unconditioned place preference tests with cVA in *D. melanogaster* and *D. santomea***
1058 **(A)** Video still illustrating the y-maze arena. Four group-housed *D. melanogaster* males are introduced
1059 into the central bowl at the bottom and odors (10% cVA in acetone or acetone control) into ports at the
1060 head of each arm. Vacuum pressure continuously pulls air down the arms through an outlet. Flies can
1061 walk freely within the bowl and arms during ten-minute trials and odors are replaced into the same port
1062 (to avoid contamination) before each trial. Scale bar, 10 mm.
1063 **(B)** Cumulative position trace representing movement of all four flies throughout the duration of the trial.
1064 Position density in each of multiple trials is used to calculate the odor preference index.
1065 **(C-H)** Video stills and cumulative position traces as in (A,B) for *D. santomea* males (C,D), *D.*
1066 *melanogaster* females (E,F), and *D. santomea* females (G,H). Scale bars, 10 mm.
1067 **(I)** Odor preference indices by species and sex. Index calculated as the difference in fly occupancy
1068 between the two arms normalized by the sum. Small gray dots represent single trials with 2-4 flies each
1069 (8-14 trials and 26-44 flies per species/sex). Distributions represented as violins with means shown as
1070 large black dots. Note significantly reduced attraction (or increased aversion) to 10% cVA in both *D.*
1071 *santomea* males and females (orange) compared to *D. melanogaster* (black). Significance by Mann-
1072 Whitney *U* tests.
1073

1074 **Figure S17. cVA promotes *D. santomea* female sexual rejection during courtship by conspecific**
1075 **males**
1076 **(A)** Rasters of *D. santomea* female and male sexual behaviors during dyadic courtship interactions with
1077 increasing cVA on a nearby piece of filter paper. For each pair, male courtship (UWE, red) is shown
1078 above and female rejection (ovipositor extrusion, orange) or acceptance (wing spreading, cyan) below.
1079 Timing of copulations indicated with asterisks. cVA doses indicated at top. Note increased rejection and
1080 decreased copulation rates at 1 and 2 mg cVA.
1081

1082 **Figure S18. Aggression and courtship biases in *melanogaster* subgroup male-male pairs**
1083 **(A-D)** Behavior rasters for three twenty-minute conspecific male-male pairs each of wildtype *D.*
1084 *melanogaster* (A), *D. simulans* (B), *D. yakuba* (C), and *D. santomea* (D) (same pairs as in Fig. 1A).
1085 Annotations of six aggressive interactions by manual scoring (blues) are shown above the horizontal
1086 dashed lines and five courtship actions (reds) beneath. Actions split by identity of the male to which they
1087 are attributed with the one exhibiting the greater total number of actions assigned as "Male 1." *D.*
1088 *melanogaster* and *D. simulans* males fight with some characteristic bias between flies, *D. yakuba* males
1089 are mostly passive but can either fight or court, and *D. santomea* males show frequent and elaborate
1090 courtship often with strong bias.
1091 **(E)** Spontaneous action biases observed between flies in male-male pairs. Male-directed courtship (red
1092 dots) and attack (blue) are plotted as a function of their bout abundance (x-axis) and bias indices (y-axis).
1093 Measurements from the same pair connected by thin lines. Cases where the same fly is dominant for both
1094 actions show connections confined to the sector above the x-axis. Circled "X" indicates mean value for
1095 the corresponding action by color. Boxed regions indicate pairs with high attack expression and wide
1096 range of biases in *D. melanogaster* or high courtship expression and consistently strong bias in *D.*
1097 *santomea,* for visual aid.
1098

1099 **Figure S19. Weak supporting evidence for territoriality in paired *D. santomea* males**
1100 **(A)** Video still of a pair of single-housed, wildtype *D. santomea* males in a large behavior chamber (40
1101 mm wide x 50 mm long x 60 mm tall) containing an apple juice-based "food patch" (25 mm diameter)
1102 and neutral surround used to test territoriality. (A') Close-up of intermale courtship from boxed region.
1103 Scale bars, 10 mm (A), 1 mm (A').
1104 **(B-D)** Heatmaps representing cumulative spatial patterns of all fly positions (B), attack (lunge) positions
1105 (C), and courtship (UWE) positions (D) for 17 *D. santomea* male-male pairs recorded during ten-minute
1106 interactions. Normalization in (B) to all frames, in (C) to attack frames only, and in (D) to courtship
1107 frames only. Note little sign of increased density on or around the food patch in any case, unlike
1108 previously observed for *D. melanogaster* aggression in similar assays (*51*).
1109 **(E)** Quantification of (B-D) showing the fraction of time spent on the food patch in total, during attack,
1110 and during courtship for each individual *D. santomea* male. Normalizations as in heatmaps above. None
1111 are significantly different from having a null median of 25% (random chance, calculated as surface area
1112 of the food patch relative to the full arena) by one-sample Mann-Whitney *U* tests. Attack frames show
1113 near-significant deviation from chance, but in the opposite direction from that expected for territoriality
1114 (enrichment off the food patch).
1115 **(F)** "Territoriality index" for *D. santomea* males calculated as the difference in time spent on the food
1116 patch between flies normalized by the sum. First distribution represents all pairs, second filtered for pairs
1117 where one of the flies showed attack dominance, and third filtered for pairs where one of the flies showed
1118 courtship dominance. None are significantly different from having a null median of zero (no territorial
1119 advantage) by one-sample Mann-Whitney *U* tests.
1120

1121 **Figure S20. Additional behavior characterizations for the sliding door assay**
1122 **(A)** Summary of immediate and delayed behavioral outcomes in *D. santomea* males following brief $P1^{dsx}$
1123 PS in the sliding door assay, with evidence below. $P1^{dsx}$ PS evokes immediate, time-locked courtship
1124 during the early isolation phase and in parallel generates a persistent internal state of social arousal.
1125 Subsequent encounters with conspecific females or males during the interaction phase elicit pure
1126 courtship or mixed courtship and aggression, respectively. Panels containing relevant data for each
1127 behavioral outcome are indicated. Figure modified from (*100*).
1128 **(B)** Optogenetic photoactivation scheme for isolated *D. santomea* males carrying $P1^{dsx}$ split-Gal4
1129 ($71G01^{DBD};dsx^{AD}$) and Gal4-dependent CsChrimson during the first phase of the delayed encounter
1130 ("sliding door") assay. After a one-minute baseline, two group-housed $P1^{dsx}$ tester males on either side of
1131 a removable divider are exposed to a one-minute photostimulation (PS) block. PS is followed by a ten-
1132 minute delay before doors are opened and flies allowed to interact. Delay phase shown as split into one-
1133 and nine-minute subphases to reflect cessation of detailed courtship annotations one minute after PS
1134 offset.
1135 **(C)** Manually scored courtship rasters (UWE, red) for isolated $P1^{dsx}$ tester males during the first three
1136 minutes of the trial.
1137 **(D,E)** Expressivity (C) and penetrance (D) of courtship elicited by PS. (C) Traces show the mean fraction
1138 of frames containing UWE in a ten-second sliding window with s.e.m. envelopes for $P1^{dsx}$ (red) and a
1139 genetic control (black, no courtship observed). (D) Fraction of flies showing courtship. Note extremely
1140 high penetrance and expressivity of induced courtship time-locked to PS in $P1^{dsx}$ testers.
1141 **(F,G)** Fraction of $P1^{dsx}$ tester males showing courtship (red) and attack (blue) toward wildtype conspecific
1142 females (E) or males (F) during the ten-minute interaction phase after doors open. Exclusive courtship is
1143 observed toward females and a mix of courtship and attack toward males.
1144

1145 **Figure S21. Aggression and courtship by *D. persimilis* and *D. pseudoobscura* males**
1146 **(A,B)** Behavior rasters for three twenty-minute conspecific male-male pairs each of wildtype *D.*
1147 *persimilis* (A) and *D. pseudoobscura* (B). Annotations of seven aggressive interactions by manual scoring
1148 (blues and black) are shown above the horizontal dashed lines and five courtship actions (reds) beneath.
1149 Actions split by identity of the male to which they are attributed with the one exhibiting the greater total
1150 number of actions assigned as "Male 1." *D. persimilis* males court frequently including making
1151 copulation attempts (e.g., Pair 3). *D. pseudoobscura* also show some courtship but attack more intensely
1152 and often.
1153 **(C,D)** Ethograms representing male- (C) and female-directed social behaviors (D) by *D. persimilis* and *D.*
1154 *pseudoobscura* males. Male-female ethograms represent expert annotation for three recordings of male-
1155 female pairs per species, with male flies similarly prepared by single-housing and interactions taking
1156 place under identical conditions. Male-directed ethograms reproduced from fig. S1A for visual
1157 comparison to female-directed counterparts. Note similarity between interactions with males and females
1158 in *D. per*.
1159 **(E)** Spontaneous bias observed between flies in male-male *D. persimilis* and *D. pseudoobscura* pairs for
1160 attack and courtship. Indices derived from the same fly pair are connected as lines and distribution means
1161 shown as paired purple (*D. per*) or blue dots (*D. pse*). Both species show strong behavioral biases.
1162

1163 **Materials and Methods**

1164

1165 **Fly stocks**

1166 All species, stocks, and crosses were reared at 24-25C and 50% humidity on a 12hr:12hr light
1167 cycle with standard Caltech fly media. Details about the flies used in each experiment (species, strain,
1168 sex, genetic background, and experimental and control genotypes) are listed in table S2 and table S3.
1169 Table S2 provides identifiers for the 18 wildtype strains and lists their usage by figure. Table S3 provides
1170 similar information for *D. santomea* transgenic lines. All wildtype strains were obtained from the
1171 National Drosophila Species Stock Center (Cornell College of Agriculture and Life Science, Ithaca, NY)
1172 except *D. melanogaster* Canton-S (Anderson lab, Caltech) and three additional *D. santomea* strains
1173 (David Stern lab, Janelia Research Campus).

1174

1175 **Generation of transgenic and knock-in alleles in *D. santomea***

1176 Transgenic *D. santomea* driver and hemidriver lines using enhancer fragments to regulate Gal4
1177 expression were made using phiC31 recombination (*111*) into existing attP landing sites (*112*). White-
1178 mutant *D. santomea* attP sites 2251 (2R) and 2253 (3R) (*112*) were targeted using Gal4 (pBPGUw),
1179 Gal4DBD (pBPZpGAL4DBDUw), or p65AD (pBPp65ADZpUw) vectors carrying an attB recognition
1180 site and mini-white selection marker (*159*, *160*). When available, ready-made constructs with desired
1181 enhancer sequences were obtained from Janelia. Otherwise enhancer sequences were obtained from (*159*),
1182 synthesized by Twist Bioscience (South San Francisco, CA) with flanking attL1/L2 recognition sites, and
1183 cloned upstream of transcriptional control cassettes in the backbone vectors using Gateway LR reactions
1184 (Thermo Fisher Scientific, Waltham, MA). Assembled constructs were verified by sequencing and
1185 restriction digest, maxi-prepped using endotoxin-free kits, and cleaned using ethanol precipitation before
1186 sending for injection. Rainbow Transgenic Flies, Inc. (Camarillo, CA) generated injection mixes
1187 containing the construct and phiC31 integrase mRNA (and sometimes also integrase plasmid to increase
1188 efficiency) and performed injections into *D. santomea* eggs in batches of 200-250 per desired
1189 transformant. Viable G0 (injected) flies were collected and crossed to a white-mutant strain (*2041/w-*
1190 *[3.2]*) (*112*) before screening for yellow-eyed (transgene heterozygous) flies in the G1 progeny to confirm
1191 germline transmission. Heterozygotes were crossed together to generate transgene homozygotes as stable
1192 lines used for experiments.

1193 Knock-in driver lines were generated using CRISPR/Cas9-mediated homology-directed repair
1194 (HDR) (*109*). Donor construct assembly and sgRNA selection for *D. santomea dsx-p65AD* were
1195 performed previously (*110*) but transformants positive for the selection marker (*MHC-DsRed*) had not
1196 been obtained. The same reagents were re-injected into *D. santomea 146/STO-CAGO 1482* (David Stern,

1197 Janelia) in a mixture with nls-Cas9-nls protein (PNA Bio, Thousand Oaks, CA) and one transformant with
1198 germline transmission of abdominal mCherry was successfully recovered. Crosses among G1 progeny
1199 yielded sporadic G2 flies with the expected *dsx* genital phenotype, verifying the genomic insertion.
1200 *D. santomea Or67d*^{Gal4} was generated using the Atalanta strategy (*158*). A backbone vector with
1201 two U6 promoters (for expression of two sgRNAs) and an "empty payload" (pJAT32) was selected as the
1202 Gateway acceptor. Two donor sequences were synthesized by Twist Bioscience and cloned into the
1203 acceptor in a simultaneous double-Gateway reaction. The first (flanked by attL3/L4) is a *T2A-Gal4-*
1204 *stop(hsp70)* cassette (*Gal4-stop(hsp70)* from pBPGUw) designed to be inserted downstream from but as
1205 close as possible to the *D. santomea Or67d (3L:LOC120447699)* translational start codon. Placement of
1206 the adjacent homology arm ensures that insertion occurs in-frame with the residual 15 coding base pairs
1207 so that Gal4 is properly translated. The second (flanked by attL5/L6) is an *ie1-mCherry-stop(p10)*
1208 selection marker (*32*) with inverted orientation relative to Gal4. Both donors also contain a 1 kb
1209 homology arm and U6-tRNA-sgRNA-tRNA array which, following LR recombination, is positioned
1210 downstream of U6. Candidate sgRNAs were designed in Geneious Prime (Auckland, NZ) and a pair was
1211 selected which excises 99% of *Or67d* coding sequence, resulting in a null allele (upstream
1212 *AATGGCAAAAGTTGAGCCCG*, downstream *ACTGCTGGTTTCCAAAGGAG*). Successful Gateway
1213 products were verified by restriction digest and tiled sequencing. Injection into *D. santomea 146/STO-*
1214 *CAGO 1482* was performed by Rainbow Transgenic Flies using nls-Cas9-nls protein as the enzyme
1215 source and G1 progeny were screened for germline-transmitting abdominal mCherry. Multiple
1216 independent insertion lines were recovered and homozygosed, one of which was used throughout after
1217 anatomical verification of uniglomerular labeling in the antennal lobes of the size and position expected
1218 for Or67d OSNs (*145*). Note that in this strategy Gal4 expression is controlled exclusively by the *Or67d*
1219 native genomic regulatory context rather than an exogenous promoter.
1220

1221 **Spontaneous behavior experiments with video recording**

1222 Experimental crosses were seeded with 10-12 virgin females and 5-6 males and flipped every 3-4
1223 days. Experimental flies were collected mostly as virgins on the day of eclosion and reared either in
1224 isolation (single-housed, 1 individual per vial) or in same-sex groups (group-housed, 10-20 individuals
1225 per vial) for 5-6 days until testing. Group-housed (but not single-housed) flies were flipped into fresh
1226 vials 1-2 days before testing. For experiments requiring unambiguous determination of individual identity
1227 (e.g., in mixed-genotype or mixed-species male-male pairs), a small distal portion of one fly's wing was
1228 clipped using a razor blade under light anesthesia. Whenever possible, the "target" fly (individual whose
1229 behavior was not being measured) was selected for wing clipping. Otherwise clips were balanced between
1230 the two interacting species or genotypes. Females were collected and group-housed as were males (mostly

1231 as virgins on the day of eclosion, 10-20 individuals per vial) and age-matched to the males they were
1232 tested with as courtship targets. As this was usually a period of 5-6 days, it is likely that even the few
1233 females that were not virgins upon collection had by the time of the experiment shed residual male
1234 pheromones potentially transferred during prior copulation (e.g., cVA). Group-housed females were also
1235 flipped 1-2 days before testing. Housing for each experiment arranged by figure can be found in table S2
1236 and table S3 ("single" or "group" under the "Housing" heading).

1237 Behavior experiments took place in the morning between 9:00AM (ZT0) and 1:00PM (ZT4) in a
1238 temperature and humidity-controlled room (24C, 50% humidity) with ambient white lighting. Single,
1239 pairs, or trios of flies interacted in 8-well acrylic circular chambers (~2.0 cm^2 surface area, ~2.4 cm^3
1240 volume) designed and described previously (*57*, *161*). Walls of the chambers were coated with Fluon (Tar
1241 Heel Ants, Raleigh, NC) and lids with a siliconizing fluid (Thermo Fisher) to discourage flies from
1242 climbing. Chamber floors were covered with a thin layer of freshly prepared "food" (2.5% (w/v) sucrose,
1243 2.25% (w/v) agarose in Tropicana apple juice) and illuminated with an 855 nm backlight (Smart Vision
1244 Lights, Muskegon, MI). Experiments testing alternative foods replaced the apple with other juices
1245 acquired commercially (*Morinda*, fig) or from botanical gardens (*Marula*, *Pandanus*), or with water as a
1246 "no food" condition (sucrose was also omitted in this case). Flies were introduced one at a time into
1247 chambers by gentle aspiration through a small hole in the lid. Interactions were video recorded from
1248 above using a Point Grey Flea3 camera running at 30 Hz with a 780 nm long pass IR filter (Midwest
1249 Optical Systems, Palatine, IL). Experiments performed in 8-well chambers are listed as "small" under the
1250 "Chamber" heading in table S2 and table S3.

1251 For copulation tests of Or67d OSN-silenced *D. santomea* females and territoriality assays of
1252 wildtype *D. santomea* males, "large" chambers consisting of a central food patch (apple juice agarose)
1253 and a neutral surround (bare acrylic) were used. Chambers measure 20 cm^2 surface area and 120 cm^3
1254 volume, and the circular food patch ~4.9 cm^2 (25% surface area). Flies (12 females and 12 males for
1255 copulation tests, 2 males for territoriality tests) were gently aspirated into chambers and video recorded
1256 using identical lighting and camera settings as for small chambers described above.

1257

1258 **Optogenetic photoactivation experiments**

1259 Flies were collected on the day of eclosion into vials containing food supplemented with 400 μM
1260 all *trans*-Retinal (Millipore Sigma, Burlington, MA) and reared in the dark for 5-6 days, with one flip into
1261 fresh supplemented vials 1-2 days before testing. Photoactivated flies were usually group-housed (10-20
1262 males per vial), except in male Or67d OSN courtship suppression experiments which were single-housed
1263 to encourage spontaneous courtship prior to stimulation. Group-housed males paired together during
1264 behavior assays came from different vials.

1265 Experiments took place in the small chambers using an 8-LED array setup reported previously
1266 (*57*, *161*). LEDs delivered flashing 685 nm red light in photostimulation (PS) blocks with 10 ms pulse
1267 width, frequencies ranging from 1-40 Hz, and intensities 10-260 $\mu W/mm^2$, calibrated with a photodiode
1268 power sensor (S130VC, Thorlabs, Newton, NJ) placed at the location of the behavior chambers. Exact PS
1269 conditions (timing, frequency, intensity) for each experiment are shown in Figures and described in
1270 Figure Legends.
1271 "Sliding door" experiments testing persistent behavioral responses after PS were performed in 8-
1272 well chambers fitted with vertical slits to allow metal barriers to divide each chamber in half. Barriers
1273 remained in place during the isolation/PS phase of the experiment, which upon completion of the delay
1274 were manually removed during a ~30 second period while video recordings were paused. Once the
1275 barriers were removed recordings resumed for the interaction phase.
1276

1277 **Behavior annotations and analysis**

1278 Annotations of aggressive (A) and courtship behaviors (C) in male-male pairs from each species
1279 for the primary screen were performed manually using action definitions from (*56*) (threat (A), charge
1280 (A), lunge (A), hold (A), tussle (A), unilateral wing extension (C), circle (C), copulation attempt (C)),
1281 (*106*) (pump (A)), (*20*) (bilateral wing extension (C), row (C)), and (*157*) (headbutt (A)). One additional
1282 action observed exclusively in *D. pseudoobscura* males, "barrage," is defined as follows: *the attacking fly*
1283 *pushes into and quickly chases the opponent while both wings are fully extended and vibrating rapidly as*
1284 *if in flight.* This action appears to have been described once before without being named (*136*). Ethograms
1285 were constructed from calculations of action frequencies and transition matrices using a 1-second cutoff.
1286 For most experiments, video recordings were analyzed in an automated fashion by first tracking
1287 the absolute and relative positions of flies in the chamber at every frame (Caltech FlyTracker,
1288 https://kristinbranson.github.io/FlyTracker/) (*56*) and using the tracking information as input to automated
1289 behavior classifiers developed previously for *D. melanogaster* social interactions (*57*), implemented in
1290 JAABA (https://jaaba.sourceforge.net/) (*55*). Two classifiers were used extensively after satisfactory
1291 performance evaluation for species within the melanogaster subgroup: "lunge" for consummatory,
1292 contact-mediated male aggression, and "unilateral wing extension" for male courtship. Recordings
1293 analyzed in this way are listed as "automated" under the "Behavioral analysis" heading in table S2 and
1294 table S3. Manually annotated recordings, including ones analyzed for the female sexual behaviors
1295 ovipositor extrusion (*126*, *127*) and wing spreading (*128*), are instead labeled "manual." For experiments
1296 involving a male-female pair, analysis ended at the point of copulation (if it occurred) and the latency to
1297 copulation was used for normalization procedures rather than total interaction time.
1298

1299 **Courtship song recordings and analysis**

1300 Flies (*D. santomea* wildtype strain 14021-0271.00) were raised in standard laboratory conditions
1301 at 23C and 12:12 light cycle. Sexually naïve individuals were isolated within 3 hours of eclosion and
1302 single-housed for 5-7 days prior to behavioral analysis. Synchronized audio and video song recordings
1303 were made within 4 hours of lights-on in the morning using the Song Torrent system (*60*). Individual flies
1304 arranged in male-male or male-female pairs were loaded onto opposite sides of a divider in recording
1305 chambers and introduced to each other simultaneously at the beginning of 30-minute recordings.

1306 Videos of 16 male-male and 16 male-female pairs of *D. santomea* flies were visually scanned and
1307 3 pairs of each type with ample courtship were selected for audio analysis. Song traces were visualized
1308 and annotated in Tempo (*63*) until dozens to hundreds of both "pulse" and "clack" events had been
1309 recorded for each courting male (instead of to saturation). The exact amplitude and position of each
1310 event's peak was determined by obtaining the maximum signal intensity within a 20 ms time window
1311 centered on the annotation point. Events were assigned to being part of a "train" when their separation
1312 from another event of the same type was less than 200 ms for pulse and 400 ms for clack.

1313

1314 **Pheromone applications**

1315 (Z)-11-octadecenyl acetate (cVA) and (Z)-7-tricosene (7-T) were acquired commercially from Pherobank
1316 B.V. (Wijk bij Duurstede, NL) as neat liquid formulations (i.e., without a solvent). For behavioral
1317 experiments with cVA on filter paper, 0.5-2 µl neat formulation was applied just prior to introduction of
1318 flies into the chamber. For direct treatment of live flies, cVA neat formulation was diluted to a 10%
1319 working solution in acetone (179124, Millipore Sigma), from which 0.2 µl was pipetted onto the
1320 abdomen of target flies under anesthesia 1-2 hours prior to behavioral testing, as previously (*89*). Flies
1321 that did not rouse were discarded. For direct treatment of dead flies, 0.2 µl of 10% cVA (acetone) or 7-T
1322 (hexane) working solutions was directly pipetted onto the abdomen of flies freshly killed by freezing at -
1323 80C and glued to the chamber floor using melted agarose of the same "food" composition.

1324

1325 **Odor place preference tests**

1326 The olfactory "y-maze" was constructed by laser cutting multiple layers of 1/8th inch 3143
1327 infrared (IR)-transmitting acrylic (ACRY31430.125PM, ePlastics, San Diego, CA) to shape. The bottom
1328 floor layer was finely wet sanded for texture. Chambers at the end of each arm meant for odor reservoirs
1329 and a center port for the vacuum line were blocked off with fine mesh. Top layers consisted of a ceiling of
1330 static dissipating acrylic (8774K11, McMaster-Carr, Santa Fe Springs, CA) with a rim of IR acrylic to
1331 block ambient light, and a final roof layer with small holes above the chambers to allow air to be drawn
1332 into and down the arena by the vacuum line. The layers were supported and sealed with three threaded

rods and bolts. Acrylic layers were periodically cleaned with 1% SDS, water, and isopropanol. The arena was illuminated from below using a custom-built IR 810 nm LED lighting board and diffused with semi-opaque white acrylic. Videos were collected with a machine vision camera (BFS-U3-04S2M-C: 0.4 MP, Teledyne FLIR) running at 45 Hz and a Pentax 12mm 1:1.2 TV lens (FL-HC1212B-VG, Ricoh).

Flies were collected on the day of eclosion, separated by sex, and single- or group-housed for one week until testing. For each trial, 5 µl odor (10% cVA in acetone or acetone control) was first loaded at the top of each arm of the y-maze then 2-4 cold anesthetized males or females were aspirated into the central bowl and the lid quickly fastened. Ten-minute recordings initiated once the flies had roused. Cumulative position traces were obtained by first median filtering on a subset of frames to construct a background image. OpenCV (4.6.0) was used to perform thresholding on background-subtracted frames. The resulting "blob detection" indicated animal position per frame, and positions across the entire trial were plotted using Matplotlib (3.4.3). Normalized occupancy in the left vs. right arm was calculated from cumulative position traces using cutoffs including the two arms but excluding the central bowl.

Gas chromatography – mass spectrometry (GC-MS)

Flies were collected on the day of eclosion, separated by sex, and group-housed in sets of 10 for one week until analysis. Flies were anesthetized and transferred to 2 ml glass screw top vials (Thermo Fisher) containing 100 µl hexane (139386, Millipore Sigma) with 10 ng/µl octadecane (C18) internal standard (O652, Millipore Sigma). Hexane extraction was allowed to proceed for 15 minutes at room temperature, after which extracts were transferred to glass inserts (Ibis Scientific, Clark County, NV) positioned in new screw top vials for either immediate analysis or storage at -80C.

An AOC-2i autoinjector (Shimadzu, Kyoto, Japan) was used to inject 2 µl of each sample into a Shimadzu QP-2020 GC-MS system (Shimadzu, Kyoto, Japan) equipped with a ZB-5MS fused silica capillary column (30 m x 0.25 mmID, df=0.25) (Phenomenex, Torrance, CA) and helium as the carrier gas. The injection port was maintained at a temperature of 310C and was operated in splitless mode, with a column flow rate of 2.15 ml/min. The temperature program consisted of a 40C hold for 1 minute, followed by a 20C/min ramp to 250C, a 5C/min ramp to 320C, and a 320C hold for 7.5 minutes. The transfer line to the mass spectrometer was held at 320C and the ion source temperature at 230C. Electron ionization was performed at 70 eV and MS scans were collected at 2 Hz, spanning 40-650 m/z. Identification of cuticular hydrocarbon (CHC) and ester compounds was determined by retention index, diagnostic ions, and comparison to previous GC-MS results from *Drosophila* (*65*, *66*, *162*, *163*). GC-MS spectra were integrated in python using the pyteomics package (v4.4.0).

Immunostaining and imaging

1367 Whole brains were dissected in ice-cold phosphate-buffered saline (PBS) and fixed in 4%
1368 paraformaldehyde for 20 minutes at room temperature (RT). Samples were washed three times in 0.5%
1369 PBST (PBS containing 0.5% (v/v) Triton X-100) for 10 minutes at RT, then permeabilized in 2% PBST
1370 for 30 minutes at RT. Samples were blocked in 0.5% PBST with 5% normal goat serum (NGS) for 1 hour
1371 at RT or overnight at 4C. Samples were incubated with primary antibodies in blocking solution for 48-72
1372 hours at 4C (rabbit anti-DsRed 1:1000, mouse anti-Bruchpilot 1:50) followed by three 10-minute washes
1373 in 0.5% PBST. Samples were incubated in secondary antibodies (anti-rabbit IgG AF568 and anti-mouse
1374 IgG AF633, 1:1000) in blocking solution for 36-48 hours at 4C, then again washed three times in 0.5%
1375 PBST for 10 minutes at RT before mounting.
1376 Samples were mounted in VectaShield antifade medium (Vector Laboratories, Newark, CA) and
1377 imaged on an Olympus Fluoview FV3000 confocal microscope (Tokyo, JP) with inverted 30X/1.05 or
1378 60X/1.30 oil immersion objectives. Image stacks were acquired at 1024 x 1024 px^2 spatial resolution with
1379 1.0-1.5 µm z-step intervals. Images (referred to as "photomicrographs") are maximum intensity
1380 projections (MIPs) of image stacks generated in Fiji. Fiji was also used to pseudocolor, overlay, adjust
1381 brightness and contrast, and add scale bars to images.
1382
1383 **Quantification and statistical analysis**
1384 Fly positional tracking, automated social behavior annotations, and song analyses were performed
1385 using software implemented in MATLAB (MathWorks, Natick, MA). Odor place preference and GC-MS
1386 experiments were analyzed in python using Jupyter Notebooks (https://jupyter.org/). The tabulated
1387 outputs of these analyses were saved and exported as text files for final analyses in R (R Project for
1388 Statistical Computing) using RStudio (Posit PBC, Boston, MA). Custom scripts in R were used to
1389 calculate raw data derivations reported in figures, produce plots visualizing them, and perform statistical
1390 tests. Illustrator 2025 (Adobe, San Jose, CA) was used to adjust aesthetic features of plots and assemble
1391 figures.
1392 Measurement distributions are often shown as boxplots highlighting the median and overlayed
1393 data points. Outliers are identified in the standard way (if > Q3+1.5*QR or if < Q1-1.5*QR) and visually
1394 excluded from box whiskers, but are retained in all quantifications (including statistical tests) and still
1395 shown as overlayed dots. Violin plots show full distribution ranges as vertically mirrored kernel density
1396 plots with mean highlighted. Statistical tests consisted mostly of non-parametric comparisons between
1397 pairs of or multiple distributions and were implemented in R. Mann-Whitney *U* tests (R base *stats*
1398 package: *wilcox.test* function) were used to compare pairs of distributions (two-sample) or an empirical
1399 distribution to a null median (one-sample), and could be paired or unpaired depending on whether the
1400 comparison involved the same individual or interacting pair. Two-sample Kolmogorov–Smirnov tests

(*stats: ks.test*) were used to compare pairs of time-evolving distributions or cumulative distributions. Kruskal-Wallis tests (*stats: kruskal.test*) and post-hoc Dunn's tests (*FSA: dunnTest*) were used to compare multiple distributions and assign lettered groupings. Binomial tests (*stats: binom.test*) were used to compare pairs of frequencies for binary outcomes (two-sample) or an empirical frequency to a null probability (one-sample). Linear fits and Pearson correlations were calculated using the *lm* and *cor* functions (*stats*), respectively. Benjamini-Hochberg multiple test correction was used to adjust p-values whenever appropriate (*stats: p.adjust: method='BH'*). Standardized effect sizes were calculated using Cohen's *d* (*effsize: cohen.d*). Tests shown in each figure can be referenced in table S4 for details including sample sizes, sample units, test used, whether correction was applied, adjusted p-value, and effect size. Significance levels are reported in Figures as *<0.05, **<0.01, and ***<0.001.

References

1. T. Clutton-Brock, Social evolution in mammals. *Science* **373**, eabc9699 (2021).

2. C. B. Stanford, The Social Behavior of Chimpanzees and Bonobos: Empirical Evidence and Shifting Assumptions. *Curr Anthropol* **39**, 399–420 (1998).

3. E. O. Wilson, The Sociogenesis of Insect Colonies. *Science* **228**, 1489–1495 (1985).

4. R. D. Alexander, The Evolution of Social Behavior. *Annu Rev Ecol Syst* **5**, 325–383 (1974).

5. S. A. West, G. A. Cooper, M. B. Ghoul, A. S. Griffin, Ten recent insights for our understanding of cooperation. *Nat Ecol Evol* **5**, 419–430 (2021).

6. N. Tinbergen, A. C. Perdeck, On the Stimulus Situation Releasing the Begging Response in the Newly Hatched Herring Gull Chick (Larus Argentatus Argentatus Pont.). *Behaviour* **3**, 1–39 (1951).

7. A. Butenandt, R. Beckmann, E. Hecker, Über den Sexuallockstoff des Seidenspinners, I. Der biologische Test und die Isolierung des reinen Sexuallockstoffes Bombykol. *Hoppe-Seylers Z für Physiol Chem* **324**, 71–83 (1961).

8. D. W. Pfaff, Luteinizing Hormone-Releasing Factor Potentiates Lordosis Behavior in Hypophysectomized Ovariectomized Female Rats. *Science* **182**, 1148–1149 (1973).

9. M. de Bono, C. I. Bargmann, Natural Variation in a Neuropeptide Y Receptor Homolog Modifies Social Behavior and Food Response in C. elegans. *Cell* **94**, 679–689 (1998).

10. L. Keller, K. G. Ross, Selfish genes: a green beard in the red fire ant. *Nature* **394**, 573–575 (1998).

11. C. F. Yang, M. C. Chiang, D. C. Gray, M. Prabhakaran, M. Alvarado, S. A. Juntti, E. K. Unger, J. A. Wells, N. M. Shah, Sexually Dimorphic Neurons in the Ventromedial Hypothalamus Govern Mating in Both Sexes and Aggression in Males. *Cell* **153**, 896–909 (2013).

12. H. Lee, D.-W. Kim, R. Remedios, T. E. Anthony, A. Chang, L. Madisen, H. Zeng, D. J. Anderson, Scalable control of mounting and attack by Esr1+ neurons in the ventromedial hypothalamus. *Nature* **509**, 627–632 (2014).

13. Z. Wu, A. E. Autry, J. F. Bergan, M. Watabe-Uchida, C. G. Dulac, Galanin neurons in the medial preoptic area govern parental behaviour. *Nature* **509**, 325–330 (2014).

14. H. Chang, S. Cassau, J. Krieger, X. Guo, M. Knaden, L. Kang, B. S. Hansson, A chemical defense deters cannibalism in migratory locusts. *Science* **380**, 537–543 (2023).

15. N. Niepoth, J. R. Merritt, M. Uminski, E. Lei, V. S. Esquibies, I. B. Bando, K. Hernandez, C. Gebhardt, S. A. Wacker, S. Lutzu, A. Poudel, K. K. Soma, S. Rudolph, A. Bendesky, Evolution of a novel adrenal cell type that promotes parental care. *Nature* **629**, 1082–1090 (2024).

16. P. M. O'Grady, R. DeSalle, Phylogeny of the Genus Drosophila. *Genetics* **209**, 1–25 (2018).

17. A. H. Sturtevant, Experiments on sex recognition and the problem of sexual selection in Drosophila. *J Anim Behav* **5**, 351–366 (1915).

18. H. T. Spieth, Courtship Behavior in Drosophila. *Annu Rev Entomol* **19**, 385–405 (1974).

19. A. W. Ewing, Functional Aspects of Drosophila Courtship. *Biol Rev* **58**, 275–292 (1983).

20. M. Cobb, K. Connolly, B. Burnet, Courtship Behaviour in the Melanogaster Species Sub-Group of Drosophila. *Behaviour* **95**, 203–230 (1985).

21. R. J. Greenspan, J.-F. Ferveur, Courtship in Drosophila. *Annu Rev Genet* **34**, 205–232 (2000).

22. R. R. H. Anholt, P. O'Grady, M. F. Wolfner, S. T. Harbison, Evolution of Reproductive Behavior. *Genetics* **214**, 49–73 (2020).

23. M. Bastock, A. Manning, The Courtship of Drosophila melanogaster. *Behaviour* **8**, 85–110 (1955).

24. J. C. Hall, The Mating of a Fly. *Science* **264**, 1702–1714 (1994).

25. D. Yamamoto, M. Koganezawa, Genes and circuits of courtship behaviour in Drosophila males. *Nat Rev Neurosci* **14**, 681–692 (2013).

26. D. A. Wheeler, C. P. Kyriacou, M. L. Greenacre, Q. Yu, J. E. Rutila, M. Rosbash, J. C. Hall, Molecular Transfer of a Species-specific Behavior from Drosophila simulans to Drosophila melanogaster. *Science* **251**, 1082–1085 (1991).

27. J. Coyne, A. Crittenden, K. Mah, Genetics of a pheromonal difference contributing to reproductive isolation in Drosophila. *Science* **265**, 1461–1464 (1994).

28. T. R. Shirangi, H. D. Dufour, T. M. Williams, S. B. Carroll, Rapid Evolution of Sex Pheromone-Producing Enzyme Expression in Drosophila. *PLOS Biol* **7**, e1000168 (2009).

29. Y. Ding, A. Berrocal, T. Morita, K. D. Longden, D. L. Stern, Natural courtship song variation caused by an intronic retroelement in an ion channel gene. *Nature* **536**, 329–332 (2016).

30. L. F. Seeholzer, M. Seppo, D. L. Stern, V. Ruta, Evolution of a central neural circuit underlies Drosophila mate preferences. *Nature* **559**, 564–569 (2018).

31. O. M. Ahmed, A. Avila-Herrera, K. M. Tun, P. H. Serpa, J. Peng, S. Parthasarathy, J.-M. Knapp, D. L. Stern, G. W. Davis, K. S. Pollard, N. M. Shah, Evolution of Mechanisms that Control Mating in Drosophila Males. *Cell Rep* **27**, 2527-2536.e4 (2019).

32. R. T. Coleman, I. Morantte, G. T. Koreman, M. L. Cheng, Y. Ding, V. Ruta, A modular circuit coordinates the diversification of courtship strategies. *Nature* **635**, 142–150 (2024).

33. R. Tanaka, Y. Hara, K. Sato, S. Kohatsu, H. Murakami, T. Higuchi, T. Awasaki, S. Kondo, A. Toyoda, A. Kamikouchi, D. Yamamoto, Cross-species implementation of an innate courtship behavior by manipulation of the sex-determinant gene. *Science* **389**, 747–752 (2025).

34. T. Dobzhansky, Species of Drosophila. *Science* **177**, 664–669 (1972).

35. J. A. Coyne, H. A. Orr, Patterns of Speciation in Drosophila. *Evolution* **43**, 362–381 (1989).

36. N. Jourjine, H. E. Hoekstra, Expanding evolutionary neuroscience: insights from comparing variation in behavior. *Neuron* **109**, 1084–1099 (2021).

37. C. T. Miller, D. Gire, K. Hoke, A. C. Huk, D. Kelley, D. A. Leopold, M. C. Smear, F. Theunissen, M. Yartsev, C. M. Niell, Natural behavior is the language of the brain. *Curr Biol* **32**, R482–R493 (2022).

38. G. L. Hunt, M. W. Hunt, Female-Female Pairing in Western Gulls (Larus occidentalis) in Southern California. *Science* **196**, 1466–1467 (1977).

39. D. W. Mock, Siblicidal Aggression and Resource Monopolization in Birds. *Science* **225**, 731–733 (1984).

40. M. E. Jacobs, Influence of Light on Mating of Drosophila Melanogaster. *Ecology* **41**, 182–188 (1960).

41. M. A. Dow, F. von Schilcher, Aggression and mating success in Drosophila melanogaster. *Nature* **254**, 511–512 (1975).

42. K. H. Skrzipek, B. Kröner, H. Hager, Aggression bei Drosophila melanogaster— Laboruntersuchungen. *Z für Tierpsychol* **49**, 87–103 (1979).

43. A. A. Hoffmann, A laboratory study of male territoriality in the sibling species Drosophila melanogaster and D. simulans. *Anim Behav* **35**, 807–818 (1987).

44. H. A. Dierick, R. J. Greenspan, Molecular analysis of flies selected for aggressive behavior. *Nat Genet* **38**, 1023–1031 (2006).

45. A. C. Edwards, S. M. Rollmann, T. J. Morgan, T. F. C. Mackay, Quantitative Genomics of Aggressive Behavior in Drosophila melanogaster. *PLOS Genet* **2**, e154 (2006).

46. S. C. Hoyer, A. Eckart, A. Herrel, T. Zars, S. A. Fischer, S. L. Hardie, M. Heisenberg, Octopamine in Male Aggression of Drosophila. *Curr Biol* **18**, 159–167 (2008).

47. L. Wang, H. Dankert, P. Perona, D. J. Anderson, A common genetic target for environmental and heritable influences on aggressiveness in Drosophila. *PNAS* **105**, 5657–5663 (2008).

48. Q. Yuan, Y. Song, C.-H. Yang, L. Y. Jan, Y. N. Jan, Female contact modulates male aggression via a sexually dimorphic GABAergic circuit in Drosophila. *Nat Neurosci* **17**, 81–88 (2014).

49. S. Chen, A. Y. Lee, N. M. Bowens, R. Huber, E. A. Kravitz, Fighting fruit flies: A model system for the study of aggression. *PNAS* **99**, 5664–5668 (2002).

50. H. Dankert, L. Wang, E. D. Hoopfer, D. J. Anderson, P. Perona, Automated monitoring and analysis of social behavior in Drosophila. *Nat Methods* **6**, 297–303 (2009).

51. R. S. Lim, E. Eyjólfsdóttir, E. Shin, P. Perona, D. J. Anderson, How Food Controls Aggression in Drosophila. *PLOS One* **9**, e105626 (2014).

52. J. R. David, F. Lemeunier, L. Tsacas, A. Yassin, The Historical Discovery of the Nine Species in the Drosophila melanogaster Species Subgroup. *Genetics* **177**, 1969–1973 (2007).

53. S. Leigh, M. G. Ritchie, A history of studies of reproductive isolation between Drosophila pseudoobscura and D. persimilis. *Fly* **19**, 2439111 (2025).

54. T. O. Auer, M. P. Shahandeh, R. Benton, Drosophila sechellia: A Genetic Model for Behavioral Evolution and Neuroecology. *Annu Rev Genet* **55**, 1–28 (2021).

55. M. Kabra, A. A. Robie, M. Rivera-Alba, S. Branson, K. Branson, JAABA: interactive machine learning for automatic annotation of animal behavior. *Nat Methods* **10**, 64–67 (2013).

56. E. Eyjolfsdottir, S. Branson, X. P. Burgos-Artizzu, E. D. Hoopfer, J. Schor, D. J. Anderson, P. Perona, Detecting Social Actions of Fruit Flies. *ECCV*, 772–787 (2014).

57. E. D. Hoopfer, Y. Jung, H. K. Inagaki, G. M. Rubin, D. J. Anderson, P1 interneurons promote a persistent internal state that enhances inter-male aggression in Drosophila. *eLife* **4**, e11346 (2015).

58. J. Linz, A. Baschwitz, A. Strutz, H. K. M. Dweck, S. Sachse, B. S. Hansson, M. C. Stensmyr, Host plant-driven sensory specialization in Drosophila erecta. *Proc Royal Soc B* **280**, 20130626 (2013).

59. S. J. Certel, M. G. Savella, D. C. F. Schlegel, E. A. Kravitz, Modulation of Drosophila male behavioral choice. *PNAS* **104**, 4706–4711 (2007).

60. S. Sawtelle, L. Narayan, Y. Ding, E. Kim, E. L. Behrman, J. L. Lillvis, T. Kawase, D. L. Stern, Song Torrent: A modular, open-source 96-chamber audio and video recording apparatus with optogenetic activation and inactivation capabilities for Drosophila. *bioRxiv*, doi: 10.1101/2024.01.09.574712 (2024).

61. E. T. Watson, E. Rodewald, J. A. Coyne, The courtship song of Drosophila santomea and a comparison to its sister species D. yakuba (Diptera: Drosophilidae). *Eur J Entomol* **104**, 145–148 (2007).

62. J. E. Blyth, D. Lachaise, M. G. Ritchie, Divergence in Multiple Courtship Song Traits between Drosophila santomea and D. yakuba. *Ethology* **114**, 728–736 (2008).

63. Y. Ding, J. L. Lillvis, J. Cande, G. J. Berman, B. J. Arthur, X. Long, M. Xu, B. J. Dickson, D. L. Stern, Neural Evolution of Context-Dependent Fly Song. *Curr Biol* **29**, 1089-1099.e7 (2019).

64. N. W. Bailey, M. Zuk, Same-sex sexual behavior and evolution. *Trends Ecol Evol* **24**, 439–446 (2009).

65. J. Jallon, J. R. David, Variations in Cuticular Hydrocarbons Among the Eight Species of the Drosophila melanogaster Subgroup. *Evolution* **41**, 294–302 (1987).

66. F. Mas, J.-M. Jallon, Sexual Isolation and Cuticular Hydrocarbon Differences between Drosophila santomea and Drosophila yakuba. *J Chem Ecol* **31**, 2747–2752 (2005).

67. M. A. Khallaf, R. Cui, J. Weißflog, M. Erdogmus, A. Svatoš, H. K. M. Dweck, D. R. Valenzano, B. S. Hansson, M. Knaden, Large-scale characterization of sex pheromone communication systems in Drosophila. *Nat Commun* **12**, 4165 (2021).

68. F. Lacaille, M. Hiroi, R. Twele, T. Inoshita, D. Umemoto, G. Manière, F. Marion-Poll, M. Ozaki, W. Francke, M. Cobb, C. Everaerts, T. Tanimura, J.-F. Ferveur, An Inhibitory Sex Pheromone Tastes Bitter for Drosophila Males. *PLOS One* **2**, e661 (2007).

1542 69. T. Miyamoto, H. Amrein, Suppression of male courtship by a Drosophila pheromone receptor. *Nat Neurosci* **11**,
1543 874–876 (2008).

1544 70. A. Llopart, S. Elwyn, D. Lachaise, J. A. Coyne, Genetics of a Difference in Pigmentation between Drosophila
1545 yakuba and Drosophila santomea. *Evolution* **56**, 2262–2277 (2002).

1546 71. J.-C. Billeter, J. Atallah, J. J. Krupp, J. G. Millar, J. D. Levine, Specialized cells tag sexual and species identity
1547 in Drosophila melanogaster. *Nature* **461**, 987–991 (2009).

1548 72. L. Wang, X. Han, J. Mehren, M. Hiroi, J.-C. Billeter, T. Miyamoto, H. Amrein, J. D. Levine, D. J. Anderson,
1549 Hierarchical chemosensory regulation of male-male social interactions in Drosophila. *Nat Neurosci* **14**, 757–762
1550 (2011).

1551 73. R. Thistle, P. Cameron, A. Ghorayshi, L. Dennison, K. Scott, Contact Chemoreceptors Mediate Male-Male
1552 Repulsion and Male-Female Attraction during Drosophila Courtship. *Cell* **149**, 1140–1151 (2012).

1553 74. P. Fan, D. S. Manoli, O. M. Ahmed, Y. Chen, N. Agarwal, S. Kwong, A. G. Cai, J. Neitz, A. Renslo, B. S.
1554 Baker, N. M. Shah, Genetic and Neural Mechanisms that Inhibit Drosophila from Mating with Other Species. *Cell*
1555 **154**, 89–102 (2013).

1556 75. D. A. Turissini, D. R. Matute, Fine scale mapping of genomic introgressions within the Drosophila yakuba
1557 clade. *PLOS Genet* **13**, e1006971 (2017).

1558 76. M. Cobb, J.-M. Jallon, Pheromones, mate recognition and courtship stimulation in the Drosophila melanogaster
1559 species sub-group. *Anim Behav* **39**, 1058–1067 (1990).

1560 77. F. M. Butterworth, Lipids of Drosophila: A Newly Detected Lipid in the Male. *Science* **163**, 1356–1357 (1969).

1561 78. G. Brieger, F. M. Butterworth, Drosophila melanogaster: Identity of Male Lipid in Reproductive System.
1562 *Science* **167**, 1262–1262 (1970).

1563 79. R. J. Bartelt, A. M. Schaner, L. L. Jackson, cis-Vaccenyl acetate as an aggregation pheromone in Drosophila
1564 melanogaster. *J Chem Ecol* **11**, 1747–1756 (1985).

1565 80. P. Xu, R. Atkinson, D. N. M. Jones, D. P. Smith, Drosophila OBP LUSH Is Required for Activity of
1566 Pheromone-Sensitive Neurons. *Neuron* **45**, 193–200 (2005).

1567 81. S. Lebreton, V. Grabe, A. B. Omondi, R. Ignell, P. G. Becher, B. S. Hansson, S. Sachse, P. Witzgall, Love
1568 makes smell blind: mating suppresses pheromone attraction in Drosophila females via Or65a olfactory neurons. *Sci*
1569 *Rep* **4**, 7119 (2014).

1570 82. L. Wang, D. J. Anderson, Identification of an aggression-promoting pheromone and its receptor neurons in
1571 Drosophila. *Nature* **463**, 227–231 (2010).

1572 83. W. Liu, X. Liang, J. Gong, Z. Yang, Y.-H. Zhang, J.-X. Zhang, Y. Rao, Social regulation of aggression by
1573 pheromonal activation of Or65a olfactory neurons in Drosophila. *Nat Neurosci* **14**, 896–902 (2011).

1574 84. I. Taisz, E. Donà, D. Münch, S. N. Bailey, B. J. Morris, K. I. Meechan, K. M. Stevens, I. Varela-Martínez, M.
1575 Gkantia, P. Schlegel, C. Ribeiro, G. S. X. E. Jefferis, D. S. Galili, Generating parallel representations of position and
1576 identity in the olfactory system. *Cell* **186**, 2556-2573.e22 (2023).

1577 85. C. Gao, M. Ma, J. Chen, X. Ji, Q. Peng, Y. Pan, Social experience shapes fighting strategies in Drosophila. *eLife*
1578 **13**, RP104212 (2025).

1579 86. J.-M. Jallon, C. Antony, O. Benamar, Un anti-aphrodisiaque produit par les mâles Drosophila melanogaster et
1580 transféré aux femelles lors de la copulation. *C R Acad Sc Paris* **292**, 1147–1149 (1981).

1581 87. S. D. Mane, L. Tompkins, R. C. Richmond, Male Esterase 6 Catalyzes the Synthesis of a Sex Pheromone in
1582 Drosophila melanogaster Females. *Science* **222**, 419–421 (1983).

1583 88. S. Zawistowski, R. C. Richmond, Inhibition of courtship and mating of Drosophila melanogaster by the male-
1584 produced lipid, cis-vaccenyl acetate. *J Insect Physiol* **32**, 189–192 (1986).

1585 89. A. Kurtovic, A. Widmer, B. J. Dickson, A single class of olfactory neurons mediates behavioural responses to a
1586 Drosophila sex pheromone. *Nature* **446**, 542–546 (2007).

1587 90. A. Ejima, B. P. C. Smith, C. Lucas, W. van der G. van Naters, C. J. Miller, J. R. Carlson, J. D. Levine, L. C.
1588 Griffith, Generalization of Courtship Learning in Drosophila Is Mediated by cis-Vaccenyl Acetate. *Curr Biol* **17**,
1589 599–605 (2007).

1590 91. T. S. Ha, D. P. Smith, A Pheromone Receptor Mediates 11-cis-Vaccenyl Acetate-Induced Responses in
1591 Drosophila. *J Neurosci* **26**, 8727–8733 (2006).

1592 92. R. Benton, K. S. Vannice, L. B. Vosshall, An essential role for a CD36-related receptor in pheromone detection
1593 in Drosophila. *Nature* **450**, 289–293 (2007).

1594 93. W. van der G. van Naters, J. R. Carlson, Receptors and Neurons for Fly Odors in Drosophila. *Curr Biol* **17**, 606–
1595 612 (2007).

1596 94. M. L. Schlief, R. I. Wilson, Olfactory processing and behavior downstream from highly selective receptor
1597 neurons. *Nat Neurosci* **10**, 623–630 (2007).

1598 95. S. R. Datta, M. L. Vasconcelos, V. Ruta, S. Luo, A. Wong, E. Demir, J. Flores, K. Balonze, B. J. Dickson, R.
1599 Axel, The Drosophila pheromone cVA activates a sexually dimorphic neural circuit. *Nature* **452**, 473–477 (2008).

1600 96. T. H. Sten, R. Li, F. Hollunder, S. Eleazer, V. Ruta, Male-male interactions shape mate selection in Drosophila.
1601 *Cell* **188**, 1486-1503.e25 (2025).

1602 97. D. J. Anderson, Circuit modules linking internal states and social behaviour in flies and mice. *Nat Rev Neurosci*
1603 **17**, 692–704 (2016).

1604 98. E. D. Hoopfer, Neural control of aggression in Drosophila. *Curr Opin Neurobiol* **38**, 109–118 (2016).

1605 99. M. Koganezawa, K. Kimura, D. Yamamoto, The Neural Circuitry that Functions as a Switch for Courtship
1606 versus Aggression in Drosophila Males. *Curr Biol* **26**, 1395–1403 (2016).

1607 100. Y. Jung, A. Kennedy, H. Chiu, F. Mohammad, A. Claridge-Chang, D. J. Anderson, Neurons that Function
1608 within an Integrator to Promote a Persistent Behavioral State in Drosophila. *Neuron* **105**, 322-333.e5 (2020).

1609 101. K. Ishii, M. Wohl, A. DeSouza, K. Asahina, Sex-determining genes distinctly regulate courtship capability and
1610 target preference via sexually dimorphic neurons. *eLife* **9**, e52701 (2020).

1611 102. M. Wohl, K. Ishii, K. Asahina, Layered roles of fruitless isoforms in specification and function of male
1612 aggression-promoting neurons in Drosophila. *eLife* **9**, e52702 (2020).

1613 103. H. Chiu, E. D. Hoopfer, M. L. Coughlan, H. J. Pavlou, S. F. Goodwin, D. J. Anderson, A circuit logic for
1614 sexually shared and dimorphic aggressive behaviors in Drosophila. *Cell* **184**, 507-520.e16 (2021).

1615 104. C. Han, Q. Peng, M. Sun, X. Jiang, X. Su, J. Chen, M. Ma, H. Zhu, X. Ji, Y. Pan, The doublesex gene regulates
1616 dimorphic sexual and aggressive behaviors in Drosophila. *PNAS* **119**, e2201513119 (2022).

1617 105. G. M. Rubin, C. Managan, M. Dreher, E. Kim, S. Miller, K. Boone, A. Robie, A. L. Taylor, K. Branson, C. E.
1618 Schretter, A. G. Otopalik, Networks of sexually dimorphic neurons that regulate social behaviors in Drosophila.
1619 *bioRxiv*, doi: 10.1101/2025.10.21.683766 (2025).

1620 106. B. J. Duistermars, B. D. Pfeiffer, E. D. Hoopfer, D. J. Anderson, A Brain Module for Scalable Control of
1621 Complex, Multi-motor Threat Displays. *Neuron* **100**, 1474-1490.e4 (2018).

1622 107. L. Tao, D. Ayambem, V. J. Barranca, V. Bhandawat, Neurons Underlying Aggression-Like Actions That Are
1623 Shared by Both Males and Females in Drosophila. *J Neurosci* **44**, e0142242024 (2024).

1624 108. S. Cao, D. J. Anderson, Neural control of coordinated wing and leg movements during a terrestrial threat
1625 display. *bioRxiv*, 2025.10.25.684556 (2025).

1626 109. F. Port, H.-M. Chen, T. Lee, S. L. Bullock, Optimized CRISPR/Cas tools for efficient germline and somatic
1627 genome engineering in Drosophila. *PNAS* **111**, E2967–E2976 (2014).

1628 110. D. Ye, J. T. Walsh, I. P. Junker, Y. Ding, Changes in the cellular makeup of motor patterning circuits drive
1629 courtship song evolution in Drosophila. *Curr Biol* **34**, 2319-2329.e6 (2024).

1630 111. A. C. Groth, M. Fish, R. Nusse, M. P. Calos, Construction of Transgenic Drosophila by Using the Site-Specific
1631 Integrase From Phage φC31. *Genetics* **166**, 1775–1782 (2004).

1632 112. D. L. Stern, J. Crocker, Y. Ding, N. Frankel, G. Kappes, E. Kim, R. Kuzmickas, A. Lemire, J. D. Mast, S.
1633 Picard, Genetic and Transgenic Reagents for Drosophila simulans, D. mauritiana, D. yakuba, D. santomea, and D.
1634 virilis. *G3* **7**, 1339–1347 (2017).

1635 113. N. C. Klapoetke, Y. Murata, S. S. Kim, S. R. Pulver, A. Birdsey-Benson, Y. K. Cho, T. K. Morimoto, A. S.
1636 Chuong, E. J. Carpenter, Z. Tian, J. Wang, Y. Xie, Z. Yan, Y. Zhang, B. Y. Chow, B. Surek, M. Melkonian, V.
1637 Jayaraman, M. Constantine-Paton, G. K.-S. Wong, E. S. Boyden, Independent optical excitation of distinct neural
1638 populations. *Nat Methods* **11**, 338–346 (2014).

1639 114. Y. Pan, G. W. Meissner, B. S. Baker, Joint control of Drosophila male courtship behavior by motion cues and
1640 activation of male-specific P1 neurons. *PNAS* **109**, 10065–10070 (2012).

1641 115. C. Rezával, S. Pattnaik, H. J. Pavlou, T. Nojima, B. Brüggemeier, L. A. D. D'Souza, H. K. M. Dweck, S. F.
1642 Goodwin, Activation of Latent Courtship Circuitry in the Brain of Drosophila Females Induces Male-like Behaviors.
1643 *Curr Biol* **26**, 2508–2515 (2016).

1644 116. D. Lachaise, M. Harry, M. Solignac, F. Lemeunier, V. Bnassi, M.-L. Cariou, Evolutionary novelties in islands:
1645 Drosophila santomea, a new melanogaster sister species from São Tomé. *Proc Royal Soc B* **267**, 1487–1495 (2000).

1646 117. M. -L. Cariou, J. -F. Silvain, V. Daubin, J. -L. D. Lage, D. Lachaise, Divergence between Drosophila santomea
1647 and allopatric or sympatric populations of D. yakuba using paralogous amylase genes and migration scenarios along
1648 the Cameroon volcanic line. *Mol Ecol* **10**, 649–660 (2001).

1649 118. A. Llopart, D. Lachaise, J. A. Coyne, An anomalous hybrid zone in Drosophila. *Evolution* **59**, 2602–2607
1650 (2005).

1651 119. J. B. S. Haldane, Sex ratio and unisexual sterility in hybrid animals. *J Genet* **12**, 101–109 (1922).

1652 120. J. A. Coyne, S. Y. Kim, A. S. Chang, D. Lachaise, S. Elwyn, Sexual isolation between two sibling species with
1653 overlapping ranges: Drosophila santomea and Drosophila yakuba. *Evolution* **56**, 2424–2434 (2002).

1654 121. J. A. Coyne, S. Elwyn, E. Rolán-Alvarez, Impact of experimental design on Drosophila sexual isolation
1655 studies: Direct effects and comparison to field hybridization data. *Evolution* **59**, 2588–2601 (2005).

1656 122. J. A. Coyne, H. A. Orr, *Speciation* (Sinauer Associates, Inc., 2004).

1657 123. C. A. Baker, J. Clemens, M. Murthy, Acoustic Pattern Recognition and Courtship Songs: Insights from Insects.
1658 *Annu Rev Neurosci* **42**, 1–19 (2019).

1659 124. K. Connolly, R. Cook, Rejection Responses By Female Drosophila Melanogaster : Their Ontogeny, Causality
1660 and Effects Upon the Behaviour of the Courting Male. *Behaviour* **44**, 142–165 (1973).

1661 125. K. Kimura, C. Sato, M. Koganezawa, D. Yamamoto, Drosophila Ovipositor Extension in Mating Behavior and
1662 Egg Deposition Involves Distinct Sets of Brain Interneurons. *PLOS One* **10**, e0126445 (2015).

1663 126. C. Mezzera, M. Brotas, M. Gaspar, H. J. Pavlou, S. F. Goodwin, M. L. Vasconcelos, Ovipositor Extrusion
1664 Promotes the Transition from Courtship to Copulation and Signals Female Acceptance in Drosophila melanogaster.
1665 *Curr Biol* **30**, 3736-3748.e5 (2020).

1666 127. F. Wang, K. Wang, N. Forknall, R. Parekh, B. J. Dickson, Circuit and Behavioral Mechanisms of Sexual
1667 Rejection by Drosophila Females. *Curr Biol* **30**, 3749-3760.e3 (2020).

1668 128. M. Li, D. S. Chen, I. P. Junker, F. I. Szorenyi, G. H. Chen, A. J. Berger, A. A. Comeault, D. R. Matute, Y.
1669 Ding, Ancestral neural circuits potentiate the origin of a female sexual behavior in Drosophila. *Nat Commun* **15**,
1670 9210 (2024).

1671 129. R. A. Baines, J. P. Uhler, A. Thompson, S. T. Sweeney, M. Bate, Altered electrical properties in Drosophila
1672 neurons developing without synaptic transmission. *J Neurosci* **21**, 1523–31 (2001).

1673 130. D. S. Ronderos, D. P. Smith, Activation of the T1 Neuronal Circuit is Necessary and Sufficient to Induce
1674 Sexually Dimorphic Mating Behavior in Drosophila melanogaster. *J Neurosci* **30**, 2595–2599 (2010).

1675 131. R. Weng, J. S. Chin, J. Y. Yew, N. Bushati, S. M. Cohen, miR-124 controls male reproductive success in
1676 Drosophila. *eLife* **2**, e00640 (2013).

132. A. Yurkovic, O. Wang, A. C. Basu, E. A. Kravitz, Learning and memory associated with aggression in Drosophila melanogaster. *PNAS* **103**, 17519–17524 (2006).

133. D. E. Lancefield, A genetic study of crosses of two races or physiological species of Drosophila obscura. *Z für Indukt Abstamm- Vererbungslehre* **52**, 287–317 (1929).

134. E. Mayr, Th. Dobzhansky, Experiments on Sexual Isolation in Drosophila IV. Modification of the Degree of Isolation Between Drosophila Pseudoobscura and Drosophila Persimilis and Sexual Preferences in Drosophila Prosoltans. *PNAS* **31**, 75–82 (1945).

135. M. A. Noor, Speciation driven by natural selection in Drosophila. *Nature* **375**, 674–675 (1995).

136. L. Partridge, A. Hoffmann, J. S. Jones, Male size and mating success in Drosophila melanogaster and D. pseudoobscura under field conditions. *Anim Behav* **35**, 468–476 (1987).

137. M. A. F. Noor, J. A. Coyne, Genetics of a difference in cuticular hydrocarbons between Drosophila pseudoobscura and D. persimilis. *Genet Res* **68**, 117–123 (1996).

138. R. J. V. Roberts, S. Pop, L. L. Prieto-Godino, Evolution of central neural circuits: state of the art and perspectives. *Nat Rev Neurosci* **23**, 725–743 (2022).

139. J. A. Jezovit, J. D. Levine, J. Schneider, Phylogeny, environment and sexual communication across the Drosophila genus. *J Exp Biol* **220**, 42–52 (2017).

140. M. E. N. Majerus, The genetics and evolution of female choice. *Trends Ecol Evol* **1**, 1–7 (1986).

141. B. R. Grant, P. R. Grant, Songs of Darwin's finches diverge when a new species enters the community. *PNAS* **107**, 20156–20163 (2010).

142. S. Enge, C. Mérot, R. Mozūraitis, V. Apšegaitė, L. Bernatchez, G. A. Martens, S. Radžiutė, H. Pavia, E. L. Berdan, A supergene in seaweed flies modulates male traits and female perception. *Proc Royal Soc B* **290**, 20231494 (2023).

143. O. Rota-Stabelli, M. Blaxter, G. Anfora, Drosophila suzukii. *Curr Biol* **23**, R8–R9 (2013).

144. T. Dekker, S. Revadi, S. Mansourian, S. Ramasamy, S. Lebreton, P. G. Becher, S. Angeli, O. Rota-Stabelli, G. Anfora, Loss of Drosophila pheromone reverses its role in sexual communication in Drosophila suzukii. *Proc Royal Soc B* **282**, 20143018 (2015).

145. A. Depetris-Chauvin, D. Galagovsky, I. W. Keesey, B. S. Hansson, S. Sachse, M. Knaden, Evolution at multiple processing levels underlies odor-guided behavior in the genus Drosophila. *Curr Biol* **33**, 4771-4785.e7 (2023).

146. C. Zhou, Y. Pan, C. C. Robinett, G. W. Meissner, B. S. Baker, Central Brain Neurons Expressing doublesex Regulate Female Receptivity in Drosophila. *Neuron* **83**, 149–163 (2014).

147. G. Guiraudie-Capraz, D. B. Pho, J. Jallon, Role of the ejaculatory bulb in biosynthesis of the male pheromone cis-vaccenyl acetate in Drosophila melanogaster. *Integr Zool* **2**, 89–99 (2007).

148. T. Chertemps, L. Duportets, C. Labeur, C. Wicker-Thomas, A new elongase selectively expressed in Drosophila male reproductive system. *Biochem Biophys Res Commun* **333**, 1066–1072 (2005).

149. J. M. Gómez, A. Gónzalez-Megías, M. Verdú, The evolution of same-sex sexual behaviour in mammals. *Nat Commun* **14**, 5719 (2023).

150. T. Karigo, A. Kennedy, B. Yang, M. Liu, D. Tai, I. A. Wahle, D. J. Anderson, Distinct hypothalamic control of same- and opposite-sex mounting behaviour in mice. *Nature* **589**, 258–263 (2021).

151. F. A. Issa, D. H. Edwards, Ritualized Submission and the Reduction of Aggression in an Invertebrate. *Curr Biol* **16**, 2217–2221 (2006).

152. S. M. Lane, A. E. Haughan, D. Evans, T. Tregenza, C. M. House, Same-sex sexual behaviour as a dominance display. *Anim Behav* **114**, 113–118 (2016).

153. J. M. Smith, G. R. Price, The Logic of Animal Conflict. *Nature* **246**, 15–18 (1973).

1721 154. T. Gregg, M. Hahn, Drosophila 25 species phylogeny, *figshare* (2017).
1722 https://doi.org/10.6084/m9.figshare.5450602.v1.

1723 155. D. E. Miller, C. Staber, J. Zeitlinger, R. S. Hawley, Highly Contiguous Genome Assemblies of 15 Drosophila
1724 Species Generated Using Nanopore Sequencing. *G3* **8**, 3131–3141 (2018).

1725 156. D. Runfola, A. Anderson, H. Baier, M. Crittenden, E. Dowker, S. Fuhrig, S. Goodman, G. Grimsley, R. Layko,
1726 G. Melville, M. Mulder, R. Oberman, J. Panganiban, A. Peck, L. Seitz, S. Shea, H. Slevin, R. Youngerman, L.
1727 Hobbs, geoBoundaries: A global database of political administrative boundaries. *PLOS One* **15**, e0231866 (2020).

1728 157. S. P. Nilsen, Y.-B. Chan, R. Huber, E. A. Kravitz, Gender-selective patterns of aggressive behavior in
1729 Drosophila melanogaster. *PNAS* **101**, 12342–12347 (2004).

1730 158. D. L. Stern, E. Kim, E. L. Behrman, The Janelia Atalanta plasmids provide a simple and efficient
1731 CRISPR/Cas9-mediated homology directed repair platform for Drosophila. *bioRxiv*, 2023.06.17.545412 (2024).

1732 159. B. D. Pfeiffer, A. Jenett, A. S. Hammonds, T.-T. B. Ngo, S. Misra, C. Murphy, A. Scully, J. W. Carlson, K. H.
1733 Wan, T. R. Laverty, C. Mungall, R. Svirskas, J. T. Kadonaga, C. Q. Doe, M. B. Eisen, S. E. Celniker, G. M. Rubin,
1734 Tools for neuroanatomy and neurogenetics in Drosophila. *PNAS* **105**, 9715–9720 (2008).

1735 160. B. D. Pfeiffer, T.-T. B. Ngo, K. L. Hibbard, C. Murphy, A. Jenett, J. W. Truman, G. M. Rubin, Refinement of
1736 Tools for Targeted Gene Expression in Drosophila. *Genetics* **186**, 735–755 (2010).

1737 161. H. K. Inagaki, Y. Jung, E. D. Hoopfer, A. M. Wong, N. Mishra, J. Y. Lin, R. Y. Tsien, D. J. Anderson,
1738 Optogenetic control of Drosophila using a red-shifted channelrhodopsin reveals experience-dependent influences on
1739 courtship. *Nat Methods* **11**, 325–332 (2014).

1740 162. J. Y. Yew, K. Dreisewerd, H. Luftmann, J. Müthing, G. Pohlentz, E. A. Kravitz, A New Male Sex Pheromone
1741 and Novel Cuticular Cues for Chemical Communication in Drosophila. *Curr Biol* **19**, 1245–1254 (2009).

1742 163. L. M. Dembeck, K. Böröczky, W. Huang, C. Schal, R. R. H. Anholt, T. F. C. Mackay, Genetic architecture of
1743 natural variation in cuticular hydrocarbon composition in Drosophila melanogaster. *eLife* **4**, e09861 (2015).

1744

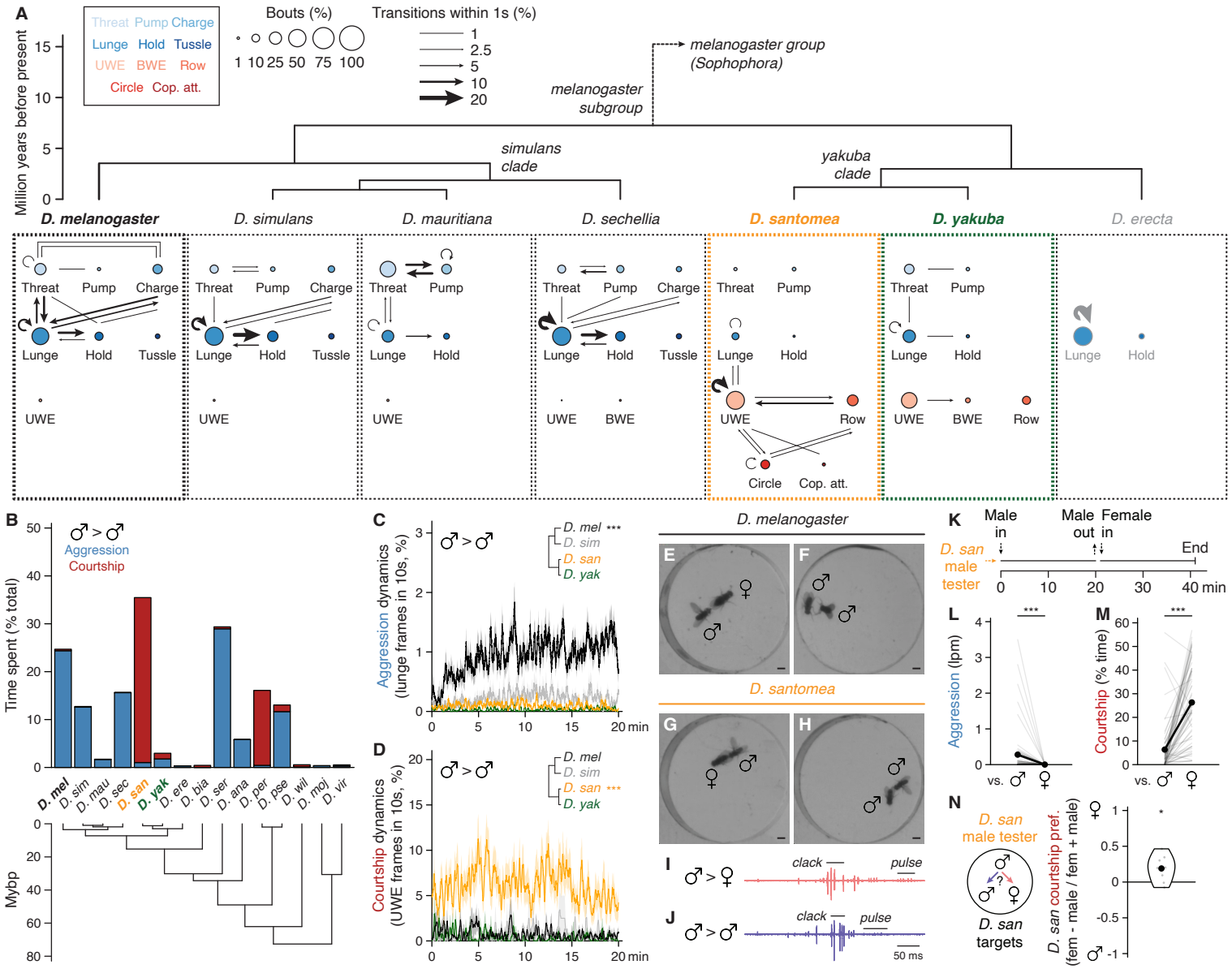
A
Threat Pump Charge
Lunge Hold Tussle
UWE BWE Row
Circle Cop. att.
Bouts (%)
1 10 25 50 75 100
Transitions within 1s (%)
1
2.5
5
10
20
Million years before present
15
10
5
0
melanogaster group
(Sophophora)
melanogaster
subgroup
simulans
clade
yakuba
clade
D. melanogaster
D. simulans
D. mauritiana
D. sechellia
D. santomea
D. yakuba
D. erecta
B
♂ > ♂
Aggression
Courtship
Time spent (% total)
D. mel
D. sim
D. mau
D. sec
D. san
D. yak
D. ere
D. bia
D. ser
D. ana
D. per
D. pse
D. wil
D. moj
D. vir
Mybp
C
Aggression dynamics
(lunge frames in 10s, %)
D. mel ***
D. sim
D. san
D. yak
20 min
D
Courtship dynamics
(UWE frames in 10s, %)
D. mel
D. sim
D. san ***
D. yak
20 min
D. melanogaster
E
F
D. santomea
G
H
I
♂ > ♀
clack
pulse
J
♂ > ♂
clack
pulse
50 ms
K
Male in
Male out
Female in
D. san male tester
End
0 10 20 30 40 min
L
Aggression (lpm)
***
vs. ♂ ♀
M
Courtship (% time)
***
vs. ♂ ♀
N
D. san male tester
D. san targets
D. san courtship pref.
(fem - male / fem + male)
*

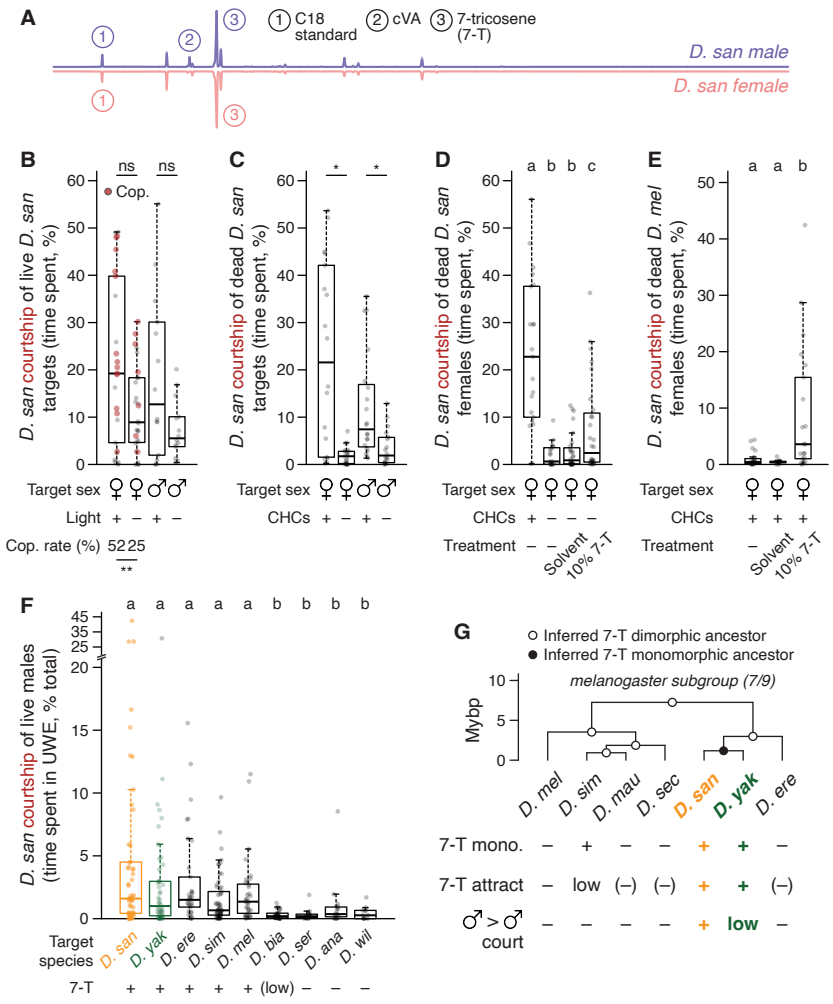
A
1 C18 standard
2 cVA
3 7-tricosene (7-T)
D. san male
D. san female
B
D. san courtship of live D. san targets (time spent, %)
Cop.
ns
Target sex
Light
Cop. rate (%) 52 25
**
C
D. san courtship of dead D. san targets (time spent, %)
CHCs
D
D. san courtship of dead D. san females (time spent, %)
Treatment
Solvent
10% 7-T
E
D. san courtship of dead D. mel females (time spent, %)
F
D. san courtship of live males (time spent in UWE, % total)
Target species
D. san
D. yak
D. ere
D. sim
D. mel
D. bia
D. ser
D. ana
D. wil
7-T
G
Inferred 7-T dimorphic ancestor
Inferred 7-T monomorphic ancestor
melanogaster subgroup (7/9)
Mybp
D. mel
D. sim
D. mau
D. sec
D. san
D. yak
D. ere
7-T mono.
7-T attract
♂>♂ court

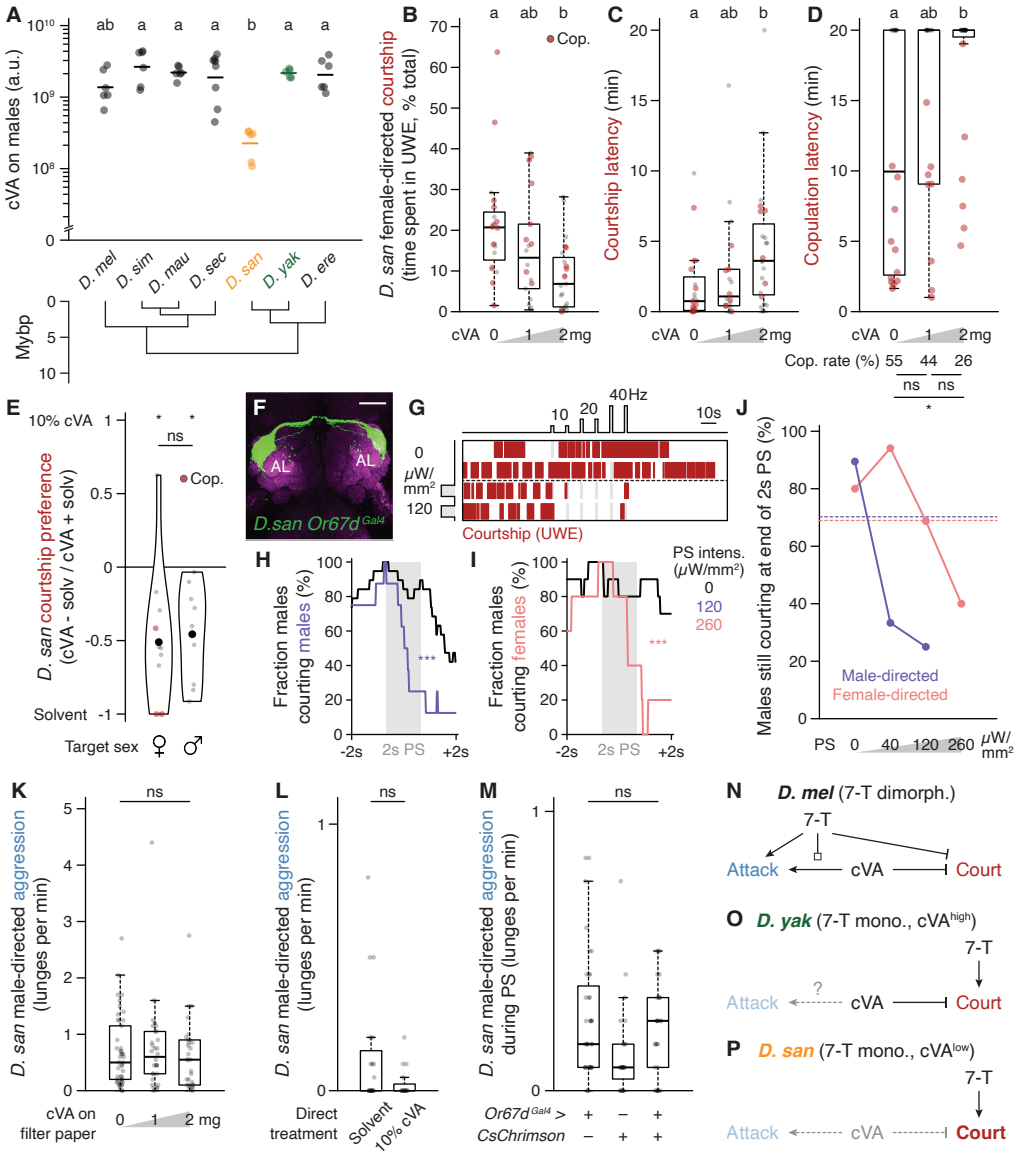
A
cVA on males (a.u.)
D. mel
D. sim
D. mau
D. sec
D. san
D. yak
D. ere
Mybp
B
D. san female-directed courtship (time spent in UWE, % total)
Cop.
cVA 0 1 2mg
C
Courtship latency (min)
D
Copulation latency (min)
Cop. rate (%) 55 44 26
ns ns
E
10% cVA
Solvent
D. san courtship preference (cVA - solv / cVA + solv)
Target sex ♀ ♂
F
AL
D.san Or67d Gal4
G
40Hz
10s
μW/mm²
Courtship (UWE)
H
Fraction males courting males (%)
-2s 2s PS +2s
I
Fraction males courting females (%)
PS intens. (μW/mm²)
0
120
260
J
Males still courting at end of 2s PS (%)
Male-directed
Female-directed
PS 0 40 120 260 μW/mm²
K
D. san male-directed aggression (lunges per min)
cVA on filter paper 0 1 2 mg
L
Direct treatment Solvent 10% cVA
M
D. san male-directed aggression during PS (lunges per min)
Or67d Gal4 >
CsChrimson
N
D. mel (7-T dimorph.)
7-T
Attack
cVA
Court
O
D. yak (7-T mono., cVA high)
P
D. san (7-T mono., cVA low)

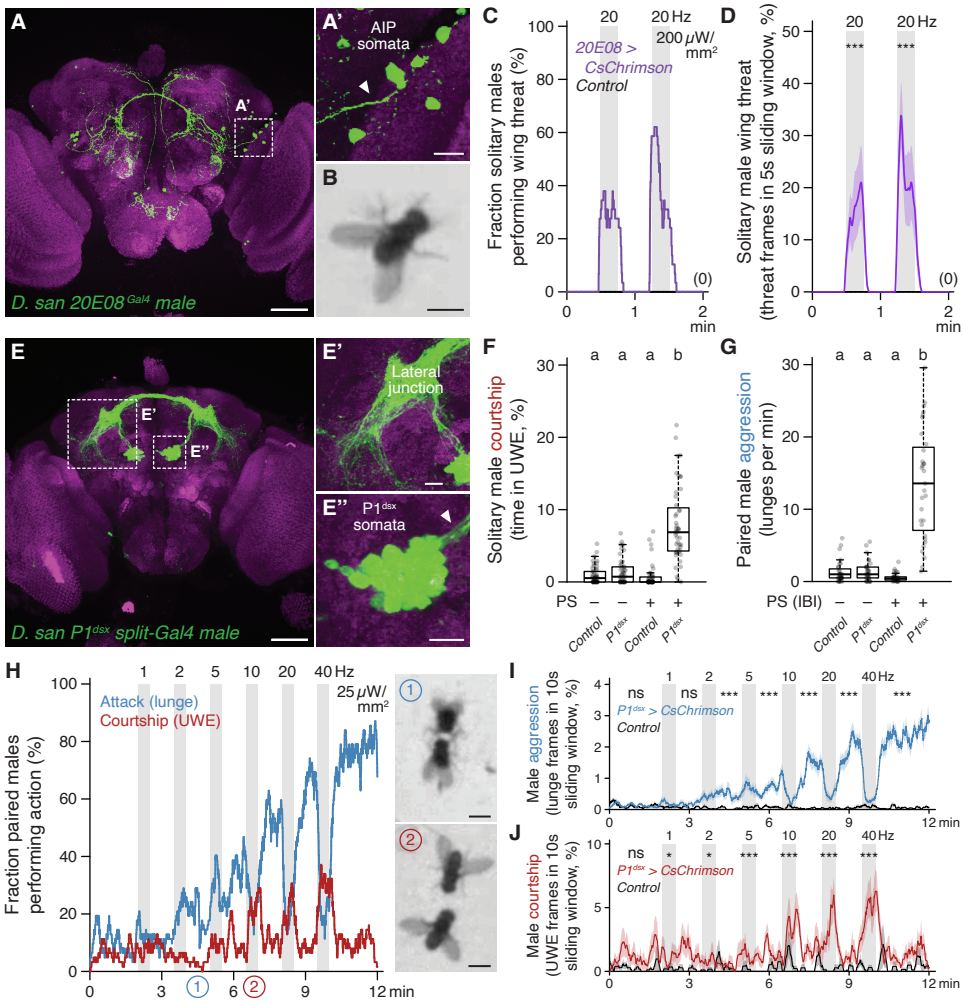
A
A'
AIP somata
B
D. san 20E08 Gal4 male
C
20
20 Hz
200 μW/mm²
20E08 > CsChrimson
Control
Fraction solitary males performing wing threat (%)
(0)
min
D
Solitary male wing threat (threat frames in 5s sliding window, %)
E
E'
E''
Lateral junction
P1dsx somata
D. san P1dsx split-Gal4 male
F
Solitary male courtship (time in UWE, %)
PS
Control
P1dsx
G
Paired male aggression (lunges per min)
PS (IBI)
H
1 2 5 10 20 40 Hz
25 μW/mm²
Attack (lunge)
Courtship (UWE)
Fraction paired males performing action (%)
12 min
I
Male aggression (lunge frames in 10s sliding window, %)
ns
P1dsx > CsChrimson
Control
J
Male courtship (UWE frames in 10s sliding window, %)

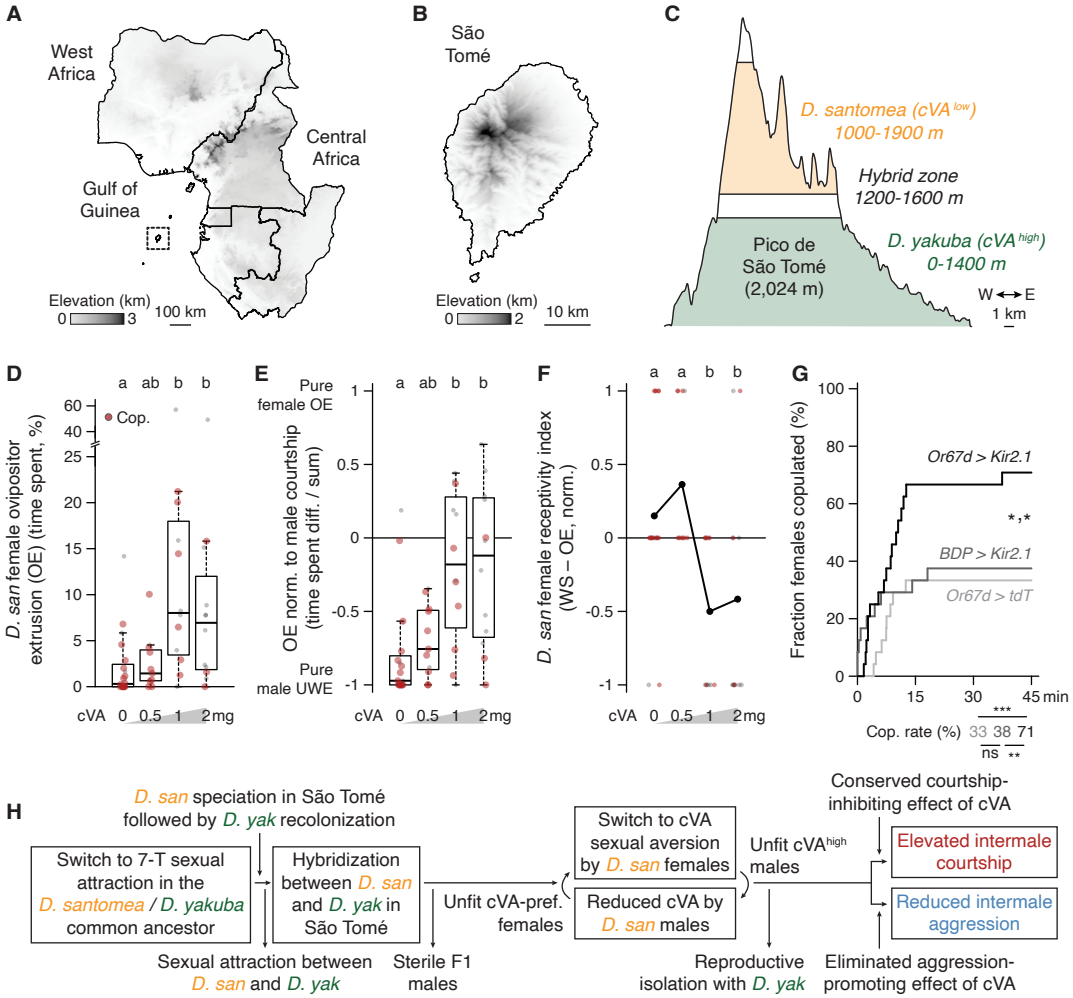
A
West Africa
Central Africa
Gulf of Guinea
Elevation (km)
0 3
100 km
B
São Tomé
Elevation (km)
0 2
10 km
C
D. santomea (cVA low)
1000-1900 m
Hybrid zone
1200-1600 m
Pico de São Tomé (2,024 m)
D. yakuba (cVA high)
0-1400 m
W E
1 km
D
D. san female ovipositor extrusion (OE) (time spent, %)
Cop.
a ab b b
cVA 0 0.5 1 2 mg
E
Pure female OE
Pure male UWE
OE norm. to male courtship (time spent diff. / sum)
a ab b b
cVA 0 0.5 1 2 mg
F
D. san female receptivity index (WS – OE, norm.)
a a b b
cVA 0 0.5 1 2 mg
G
Fraction females copulated (%)
Or67d > Kir2.1
,
BDP > Kir2.1
Or67d > tdT
0 15 30 45 min
***
Cop. rate (%) 33 38 71
ns **
H
D. san speciation in São Tomé followed by D. yak recolonization
Switch to 7-T sexual attraction in the D. santomea / D. yakuba common ancestor
Hybridization between D. san and D. yak in São Tomé
Sexual attraction between D. san and D. yak
Sterile F1 males
Unfit cVA-pref. females
Switch to cVA sexual aversion by D. san females
Reduced cVA by D. san males
Unfit cVA high males
Reproductive isolation with D. yak
Conserved courtship-inhibiting effect of cVA
Elevated intermale courtship
Reduced intermale aggression
Eliminated aggression-promoting effect of cVA

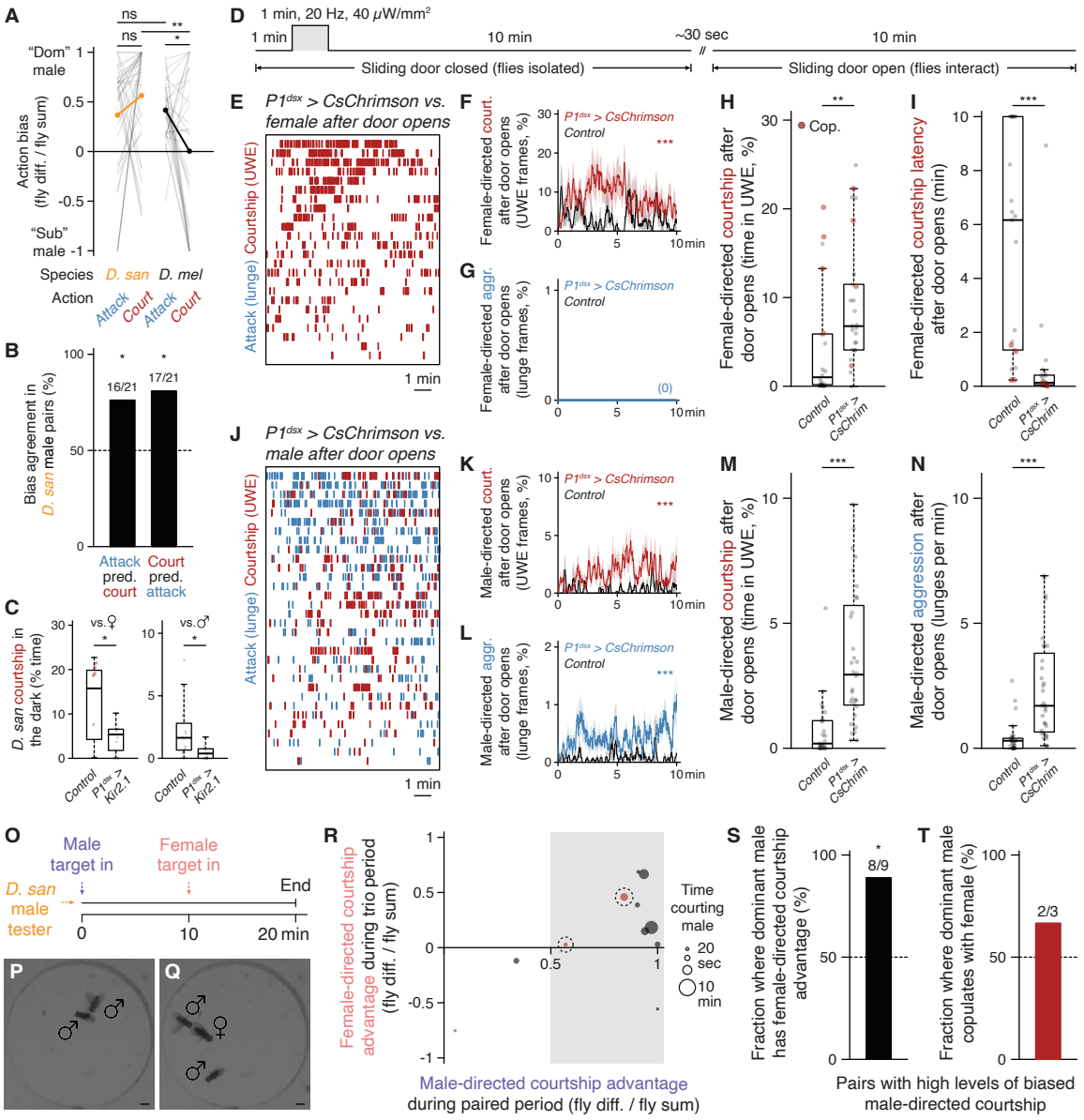
A
ns
ns
**
*
"Dom" male
"Sub" male
Action bias (fly diff. / fly sum)
Species D. san D. mel
Action Attack Court Attack Court
B
Bias agreement in D. san male pairs (%)
16/21
17/21
Attack pred. court
Court pred. attack
C
D. san courtship in the dark (% time)
vs.♀
vs.♂
Control
P1dsx > Kir2.1
D
1 min, 20 Hz, 40 μW/mm²
1 min
10 min
~30 sec
10 min
Sliding door closed (flies isolated)
Sliding door open (flies interact)
E
P1dsx > CsChrimson vs. female after door opens
Courtship (UWE)
Attack (lunge)
1 min
F
Female-directed court. after door opens (UWE frames, %)
P1dsx > CsChrimson
Control
G
Female-directed aggr. after door opens (lunge frames, %)
(0)
H
Female-directed courtship after door opens (time in UWE, %)
Cop.
I
Female-directed courtship latency after door opens (min)
J
P1dsx > CsChrimson vs. male after door opens
K
Male-directed court. after door opens (UWE frames, %)
L
Male-directed aggr. after door opens (lunge frames, %)
M
Male-directed courtship after door opens (time in UWE, %)
N
Male-directed aggression after door opens (lunges per min)
O
Male target in
Female target in
D. san male tester
End
0
10
20 min
P
Q
R
Female-directed courtship advantage during trio period (fly diff. / fly sum)
Time courting male
20 sec
10 min
Male-directed courtship advantage during paired period (fly diff. / fly sum)
S
Fraction where dominant male has female-directed courtship advantage (%)
8/9
T
Fraction where dominant male copulates with female (%)
2/3
Pairs with high levels of biased male-directed courtship

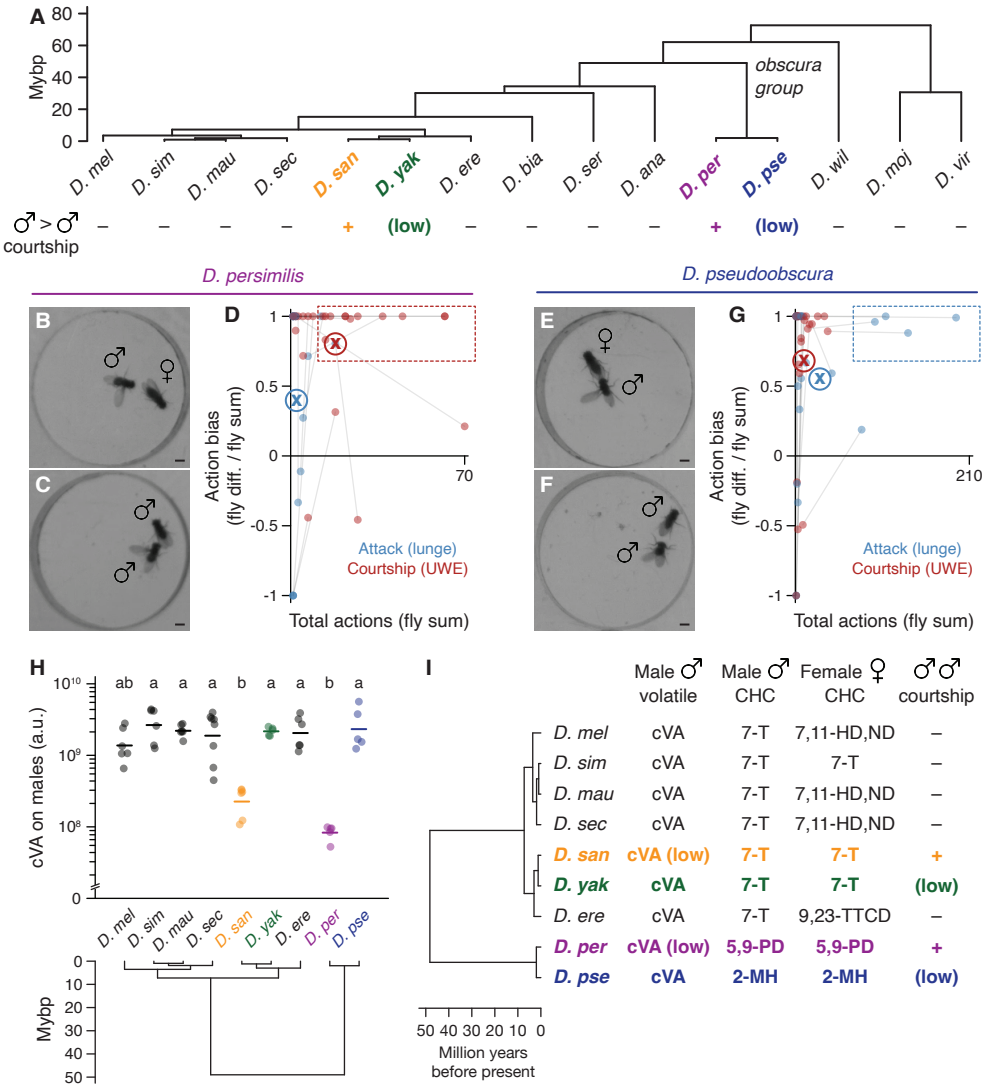
A
Mybp
80
60
40
20
0
obscura group
D. mel
D. sim
D. mau
D. sec
D. san
D. yak
D. ere
D. bia
D. ser
D. ana
D. per
D. pse
D. wil
D. moj
D. vir
♂ > ♂ courtship
– – – – + (low) – – – – + (low) – – –
D. persimilis
D. pseudoobscura
B
C
D
E
F
G
Action bias (fly diff. / fly sum)
Total actions (fly sum)
Attack (lunge)
Courtship (UWE)
70
210
H
cVA on males (a.u.)
ab a a a b a a b a
D. mel
D. sim
D. mau
D. sec
D. san
D. yak
D. ere
D. per
D. pse
Mybp
I
Male ♂ volatile
Male ♂ CHC
Female ♀ CHC
♂♂ courtship
D. mel cVA 7-T 7,11-HD,ND –
D. sim cVA 7-T 7-T –
D. mau cVA 7-T 7,11-HD,ND –
D. sec cVA 7-T 7,11-HD,ND –
D. san cVA (low) 7-T 7-T +
D. yak cVA 7-T 7-T (low)
D. ere cVA 7-T 9,23-TTCD –
D. per cVA (low) 5,9-PD 5,9-PD +
D. pse cVA 2-MH 2-MH (low)
50 40 30 20 10 0
Million years before present

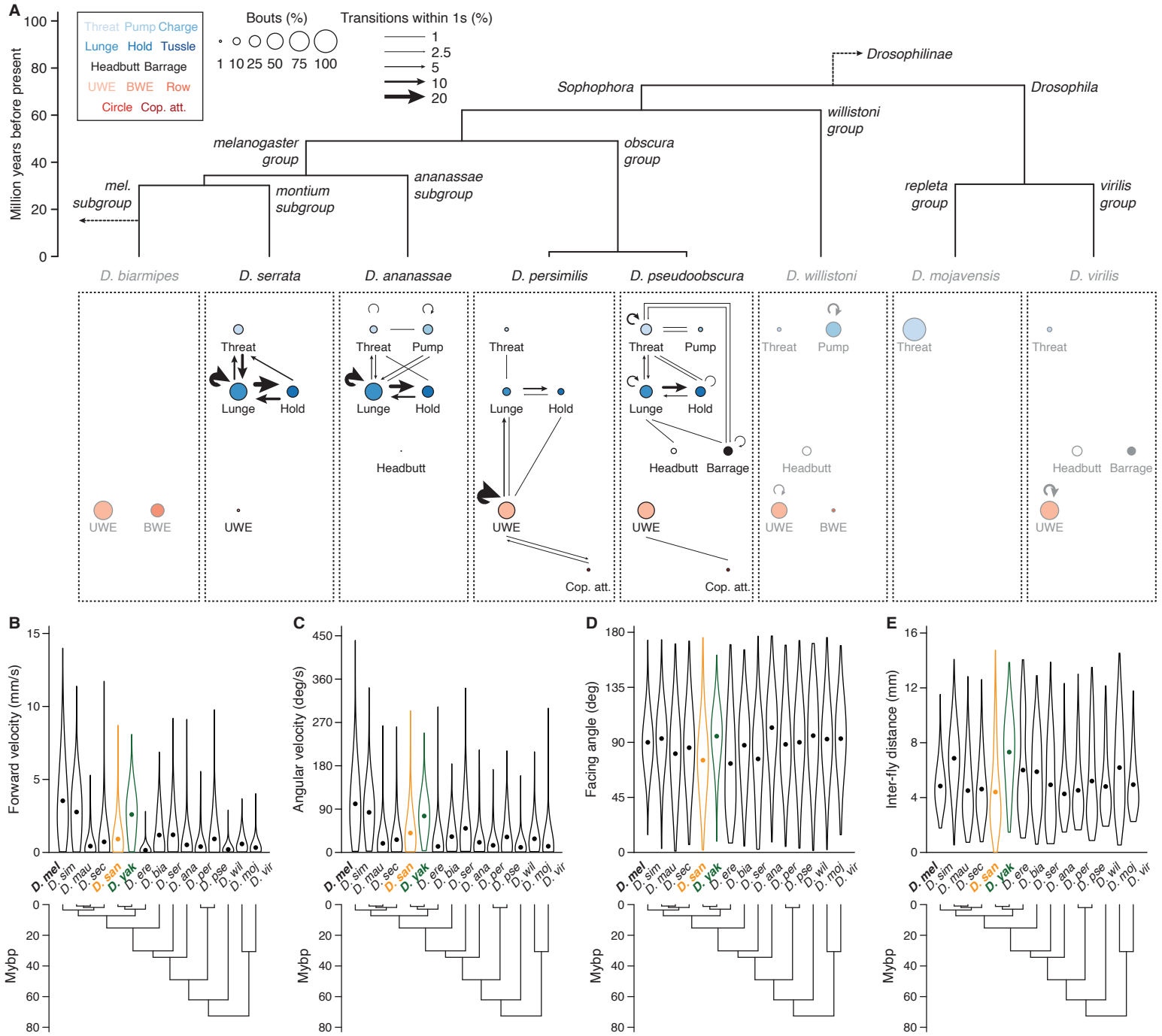
A
Million years before present
Threat Pump Charge
Lunge Hold Tussle
Headbutt Barrage
UWE BWE Row
Circle Cop. att.
Bouts (%)
1 10 25 50 75 100
Transitions within 1s (%)
1
2.5
5
10
20
Drosophilinae
Sophophora
Drosophila
willistoni group
melanogaster group
obscura group
mel. subgroup
montium subgroup
ananassae subgroup
repleta group
virilis group
D. biarmipes
D. serrata
D. ananassae
D. persimilis
D. pseudoobscura
D. willistoni
D. mojavensis
D. virilis
B
Forward velocity (mm/s)
C
Angular velocity (deg/s)
D
Facing angle (deg)
E
Inter-fly distance (mm)
Mybp
D. mel
D. sim
D. mau
D. sec
D. san
D. yak
D. ere
D. bia
D. ser
D. ana
D. per
D. pse
D. wil
D. moj
D. vir

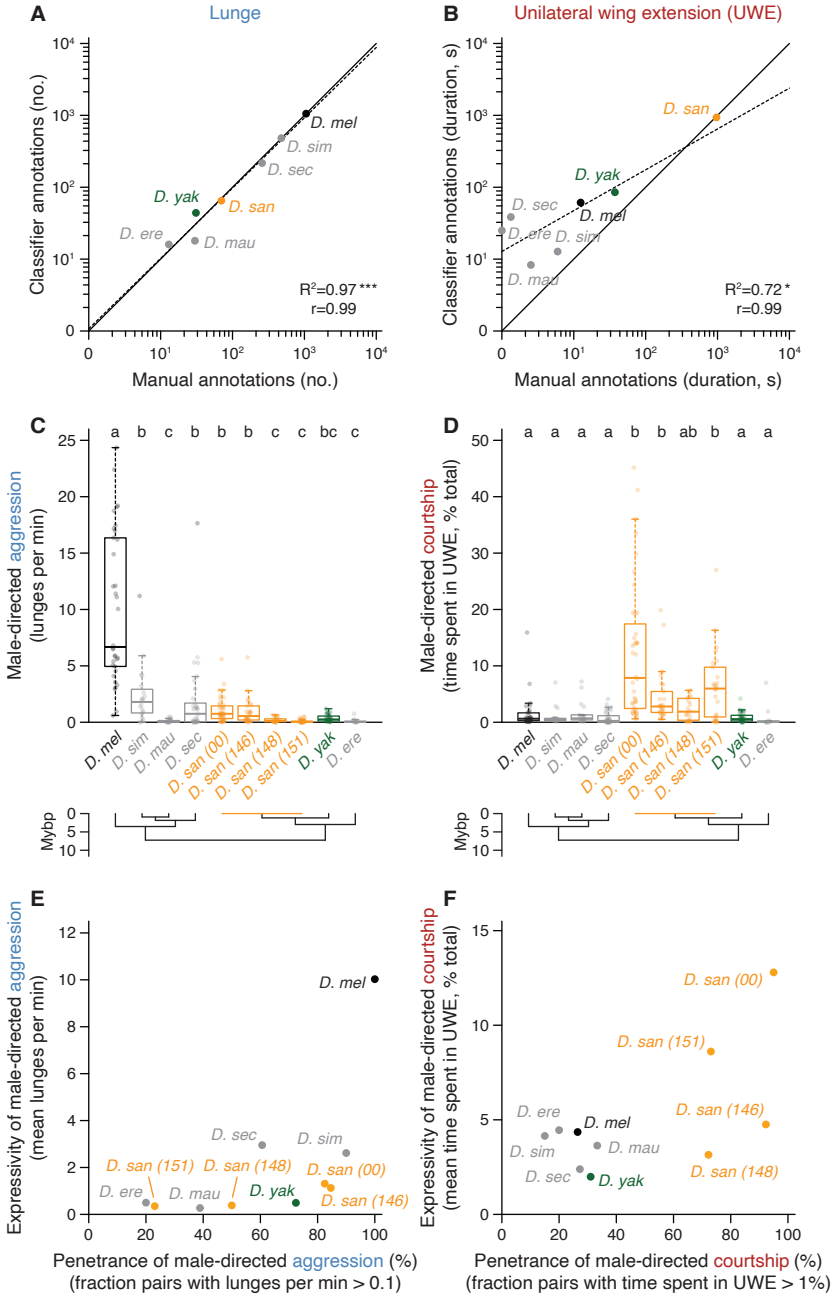
A
Lunge
Classifier annotations (no.)
Manual annotations (no.)
D. mel
D. sim
D. sec
D. yak
D. san
D. ere
D. mau
R²=0.97 ***
r=0.99
B
Unilateral wing extension (UWE)
Classifier annotations (duration, s)
Manual annotations (duration, s)
D. san
D. yak
D. sec
D. mel
D. ere
D. sim
D. mau
R²=0.72 *
r=0.99
C
Male-directed aggression (lunges per min)
a b c b b b c c bc c
D. mel
D. sim
D. mau
D. sec
D. san (00)
D. san (146)
D. san (148)
D. san (151)
D. yak
D. ere
Mybp
D
Male-directed courtship (time spent in UWE, % total)
a a a a b b ab b a a
E
Expressivity of male-directed aggression (mean lunges per min)
Penetrance of male-directed aggression (%) (fraction pairs with lunges per min > 0.1)
F
Expressivity of male-directed courtship (mean time spent in UWE, % total)
Penetrance of male-directed courtship (%) (fraction pairs with time spent in UWE > 1%)

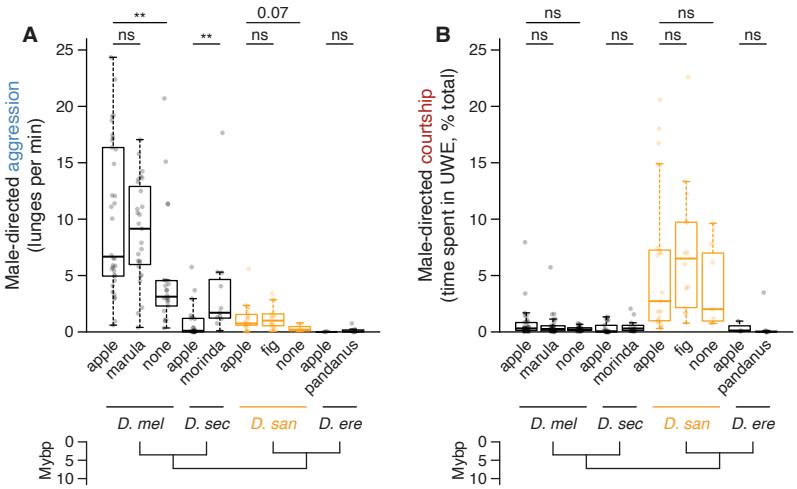
A
B
Male-directed aggression
(lunges per min)
Male-directed courtship
(time spent in UWE, % total)
**
0.07
ns
apple
marula
none
apple
morinda
apple
fig
none
apple
pandanus
D. mel
D. sec
D. san
D. ere
Mybp

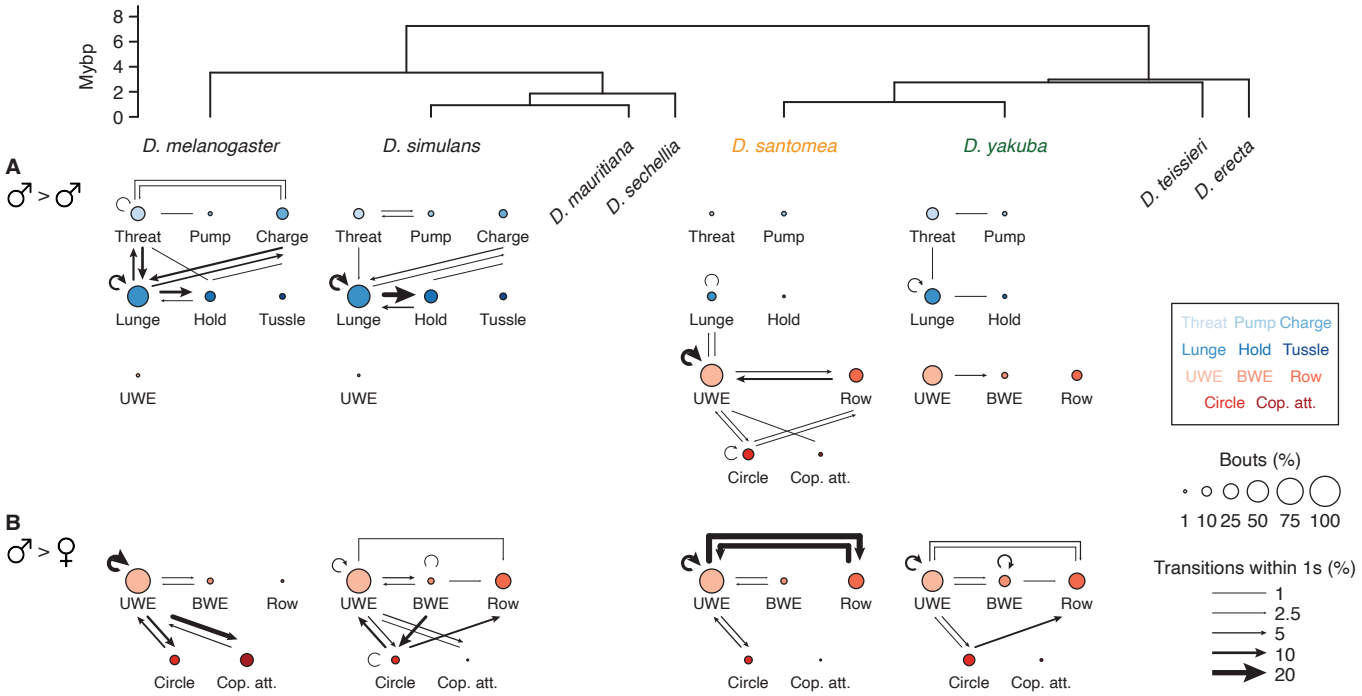
Mybp
8
6
4
2
0
D. melanogaster
D. simulans
D. mauritiana
D. sechellia
D. santomea
D. yakuba
D. teissieri
D. erecta
A
♂ > ♂
Threat
Pump
Charge
Lunge
Hold
Tussle
UWE
BWE
Row
Circle
Cop. att.
Threat Pump Charge
Lunge Hold Tussle
UWE BWE Row
Circle Cop. att.
Bouts (%)
1 10 25 50 75 100
B
♂ > ♀
Transitions within 1s (%)
1
2.5
5
10
20

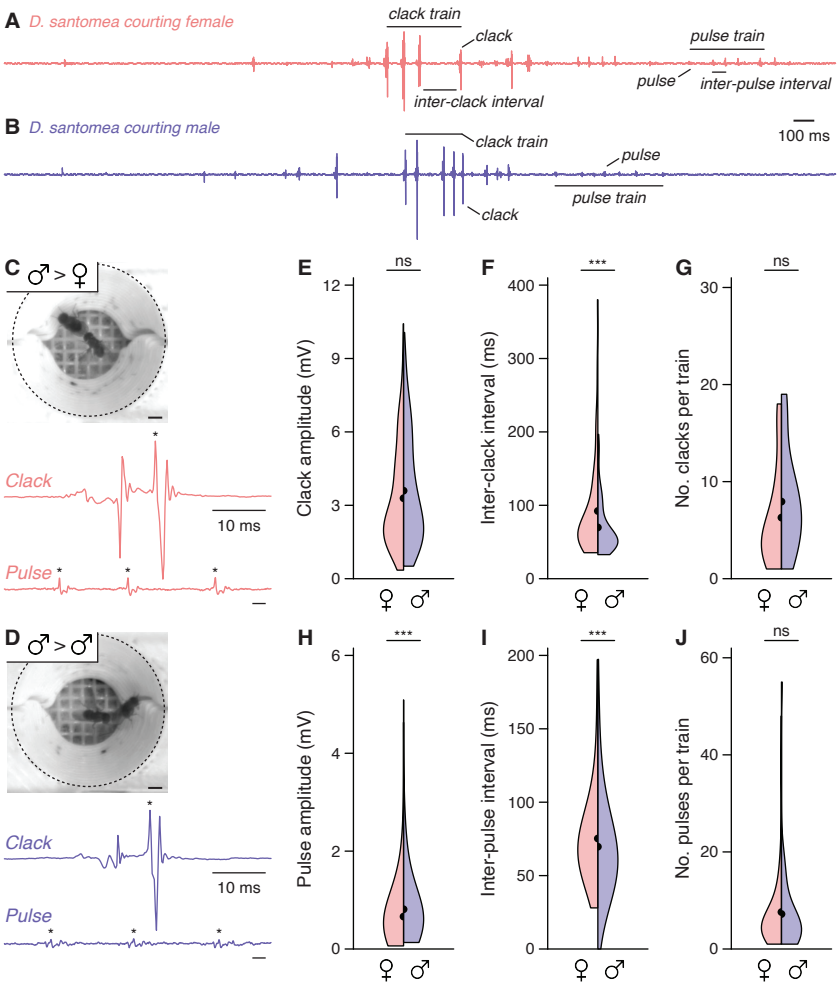
A D. santomea courting female
clack train
clack
pulse train
pulse
inter-pulse interval
inter-clack interval
B D. santomea courting male
clack train
pulse
pulse train
clack
100 ms
C ♂ > ♀
Clack
Pulse
10 ms
D ♂ > ♂
Clack
Pulse
10 ms
E
ns
Clack amplitude (mV)
F
***
Inter-clack interval (ms)
G
ns
No. clacks per train
H
***
Pulse amplitude (mV)
I
***
Inter-pulse interval (ms)
J
ns
No. pulses per train
♀ ♂

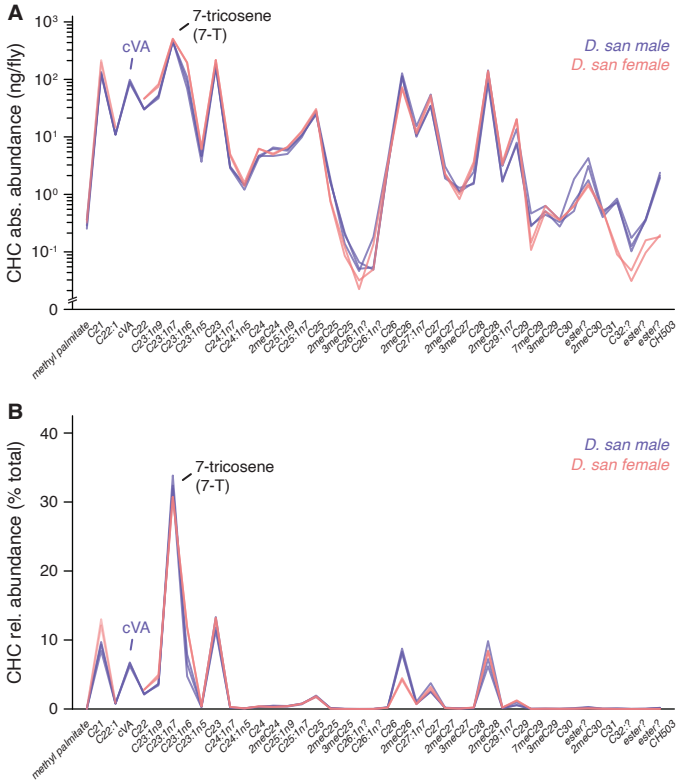
A
CHC abs. abundance (ng/fly)
7-tricosene
(7-T)
cVA
D. san male
D. san female
methyl palmitate
C21
C22:1
cVA
C22
C23:1n9
C23:1n7
C23:1n6
C23:1n5
C23
C24:1n7
C24:1n5
C24
2meC24
C25:1n9
C25:1n7
C25
2meC25
3meC25
C26:1n7
C26:1n7
C26
2meC26
C27:1n7
C27
2meC27
3meC27
C28
2meC28
C29:1n7
C29
7meC29
3meC29
C30
ester?
2meC30
C31
C32:2
ester?
ester?
CHB03
B
CHC rel. abundance (% total)
7-tricosene
(7-T)
cVA
D. san male
D. san female

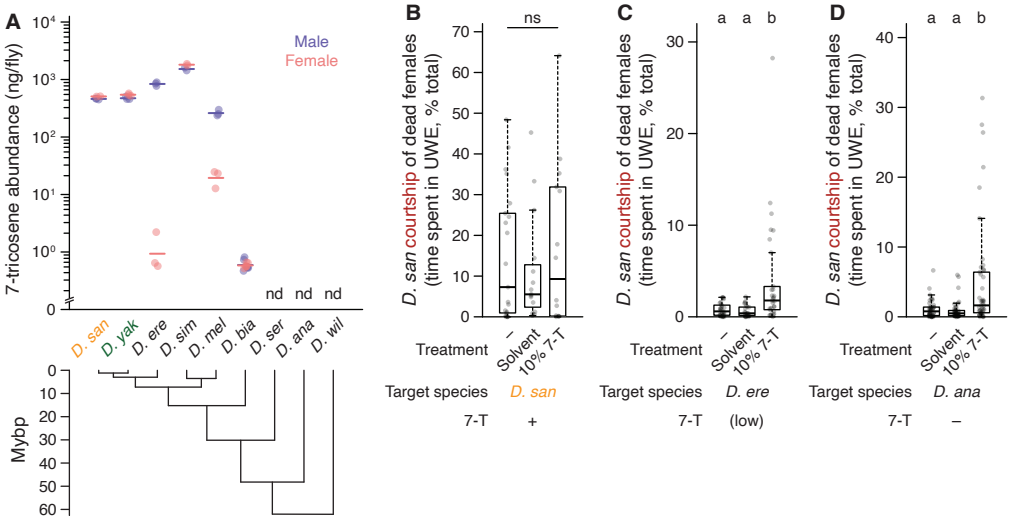
A
7-tricosene abundance (ng/fly)
Male
Female
nd nd nd
D. san
D. yak
D. ere
D. sim
D. mel
D. bia
D. ser
D. ana
D. wil
Mybp
B
D. san courtship of dead females (time spent in UWE, % total)
ns
Treatment
–
Solvent
10% 7-T
Target species
D. san
7-T
+
C
a a b
Target species
D. ere
7-T
(low)
D
a a b
Target species
D. ana
7-T
–

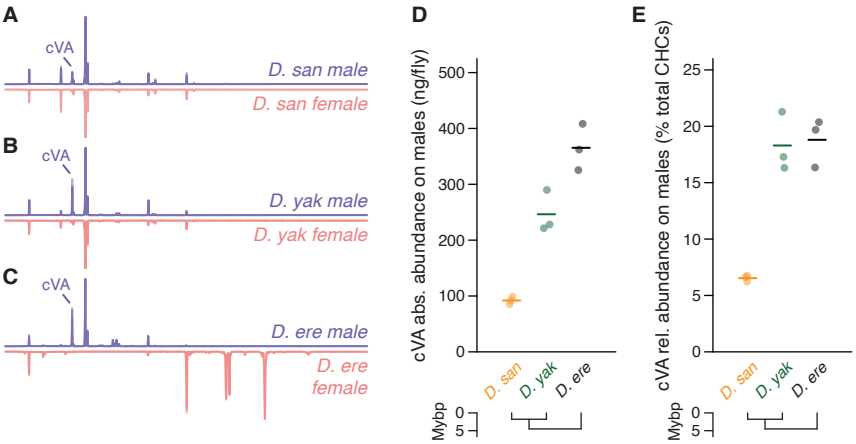
A
cVA
D. san male
D. san female
B
cVA
D. yak male
D. yak female
C
cVA
D. ere male
D. ere female
D
cVA abs. abundance on males (ng/fly)
500
400
300
200
100
0
D. san
D. yak
D. ere
Mybp
0
5
E
cVA rel. abundance on males (% total CHCs)
25
20
15
10
5
0
D. san
D. yak
D. ere
Mybp
0
5

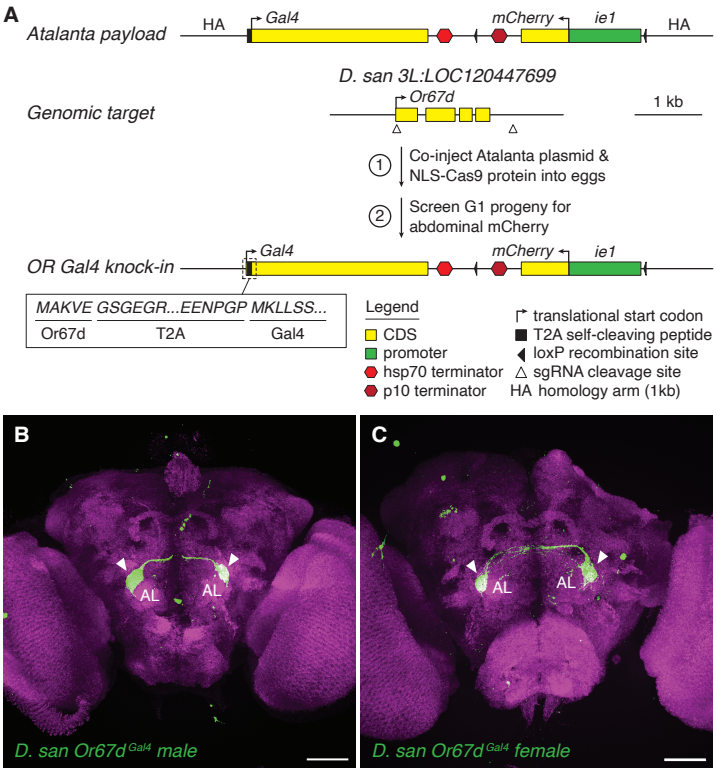
A
Atalanta payload
HA
Gal4
mCherry
ie1
HA
D. san 3L:LOC120447699
Genomic target
Or67d
1 kb
1
Co-inject Atalanta plasmid &
NLS-Cas9 protein into eggs
2
Screen G1 progeny for
abdominal mCherry
OR Gal4 knock-in
Gal4
mCherry
ie1
MAKVE GSGEGR...EENPGP MKLLSS...
Or67d
T2A
Gal4
Legend
CDS
promoter
hsp70 terminator
p10 terminator
translational start codon
T2A self-cleaving peptide
loxP recombination site
sgRNA cleavage site
HA homology arm (1kb)
B
AL
AL
D. san Or67d Gal4 male
C
AL
AL
D. san Or67d Gal4 female

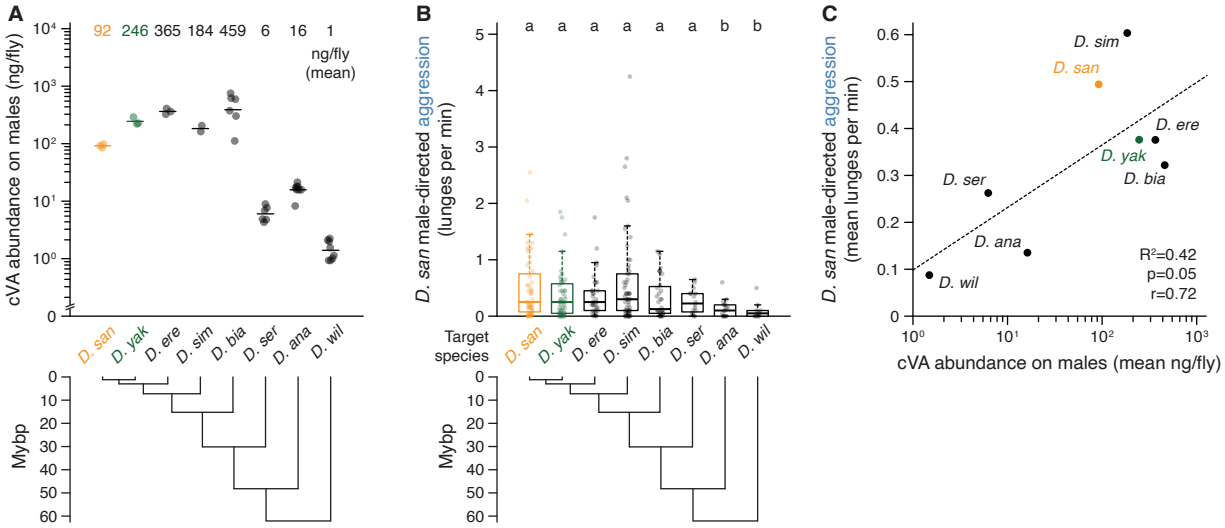
A
cVA abundance on males (ng/fly)
92 246 365 184 459 6 16 1
ng/fly (mean)
D. san
D. yak
D. ere
D. sim
D. bia
D. ser
D. ana
D. wil
Mybp
B
D. san male-directed aggression (lunges per min)
a a a a a a b b
Target species
C
D. san male-directed aggression (mean lunges per min)
cVA abundance on males (mean ng/fly)
R²=0.42
p=0.05
r=0.72

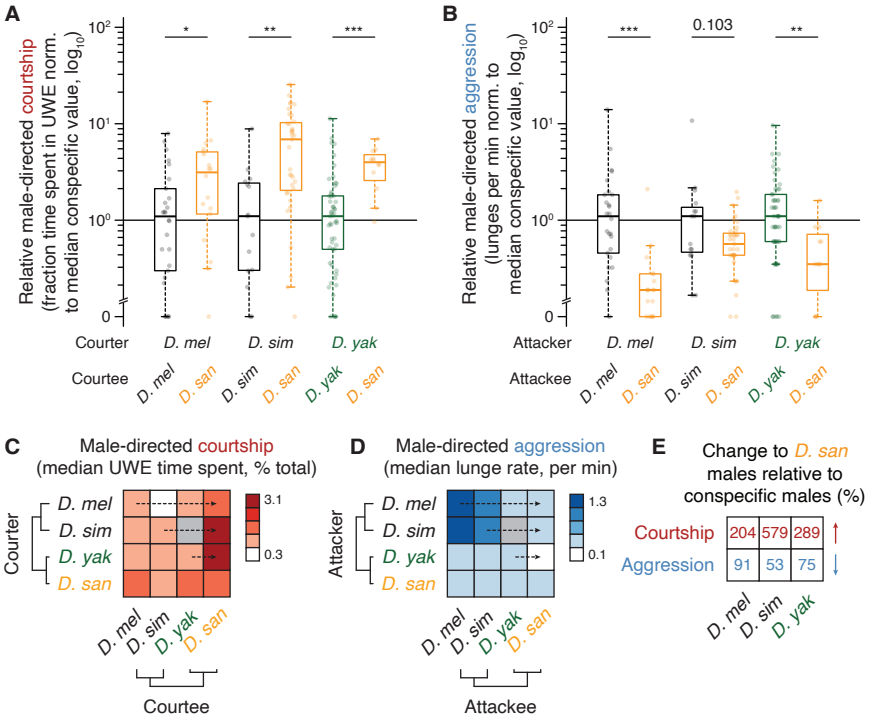
A
Relative male-directed courtship (fraction time spent in UWE norm. to median conspecific value, log10)
Courter
Courtee
D. mel
D. sim
D. yak
D. san
B
Relative male-directed aggression (lunges per min norm. to median conspecific value, log10)
Attacker
Attackee
0.103
C
Male-directed courtship (median UWE time spent, % total)
3.1
0.3
D
Male-directed aggression (median lunge rate, per min)
1.3
0.1
E
Change to D. san males relative to conspecific males (%)
Courtship 204 579 289
Aggression 91 53 75

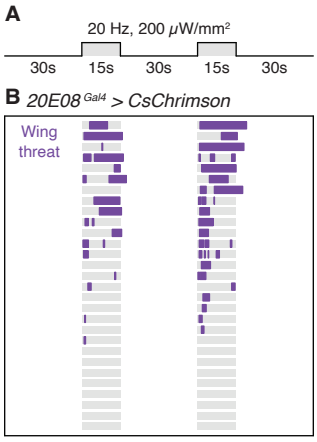
A
20 Hz, 200 μW/mm²
30s
15s
30s
15s
30s
B 20E08 Gal4 > CsChrimson
Wing threat

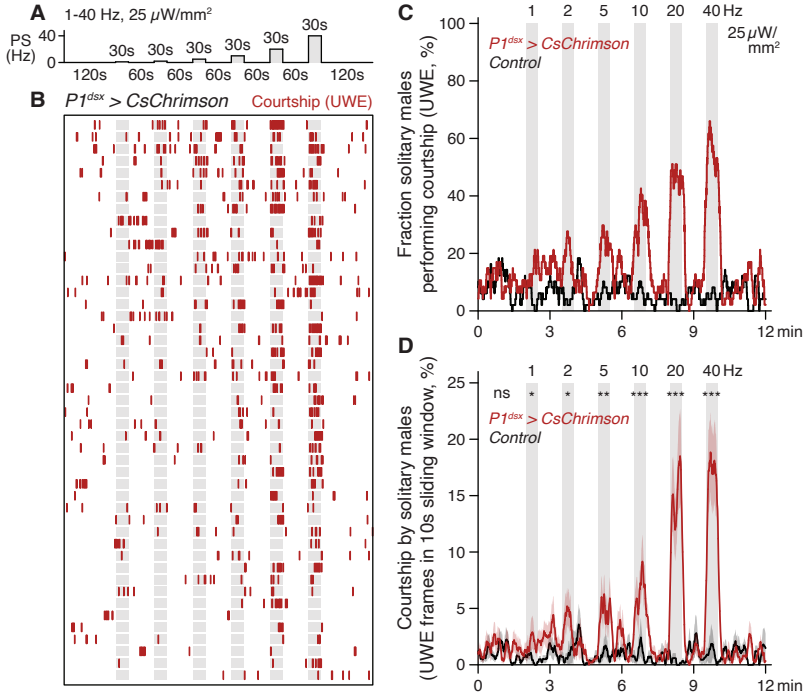
A
1-40 Hz, 25 μW/mm²
PS (Hz)
40
0
30s
120s
60s
B
P1dsx > CsChrimson
Courtship (UWE)
C
1 2 5 10 20 40 Hz
25 μW/mm²
P1dsx > CsChrimson
Control
Fraction solitary males performing courtship (UWE, %)
100
80
60
40
20
0
3
6
9
12 min
D
ns * * ** *** *** ***
Courtship by solitary males (UWE frames in 10s sliding window, %)
25
20
15
10
5

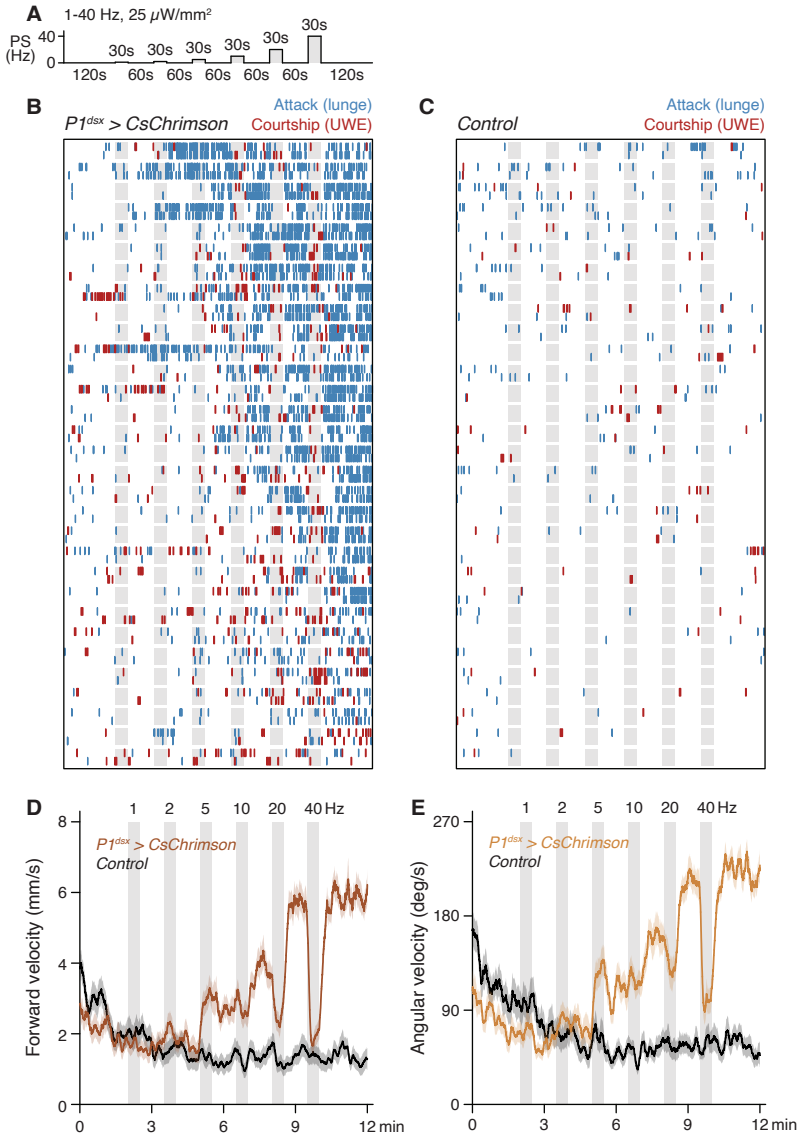
A
1-40 Hz, 25 μW/mm²
PS (Hz)
40
0
30s
120s
60s
B
P1dsx > CsChrimson
Attack (lunge)
Courtship (UWE)
C
Control
D
1 2 5 10 20 40 Hz
P1dsx > CsChrimson
Control
Forward velocity (mm/s)
12 min
E
Angular velocity (deg/s)
270
180
90

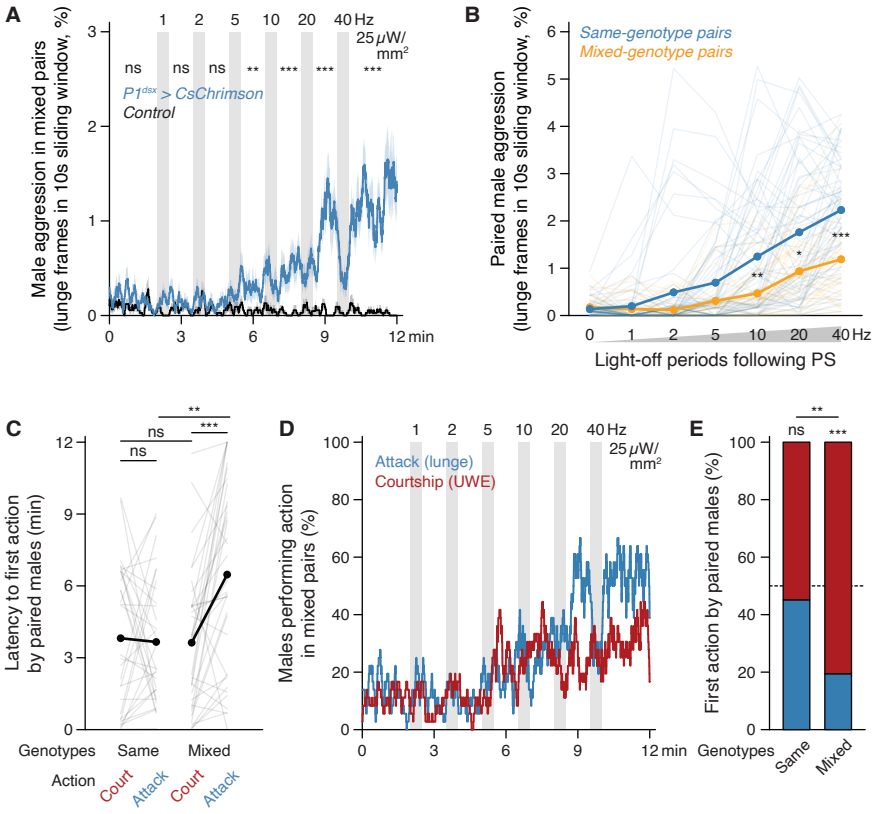
A
Male aggression in mixed pairs (lunge frames in 10s sliding window, %)
1 2 5 10 20 40 Hz
25 μW/mm²
ns ns ns ** *** *** ***
P1dsx > CsChrimson
Control
0 3 6 9 12 min
B
Paired male aggression (lunge frames in 10s sliding window, %)
Same-genotype pairs
Mixed-genotype pairs
Light-off periods following PS
C
Latency to first action by paired males (min)
Genotypes Same Mixed
Action Court Attack Court Attack
D
Males performing action in mixed pairs (%)
Attack (lunge)
Courtship (UWE)
E
First action by paired males (%)
Genotypes Same Mixed

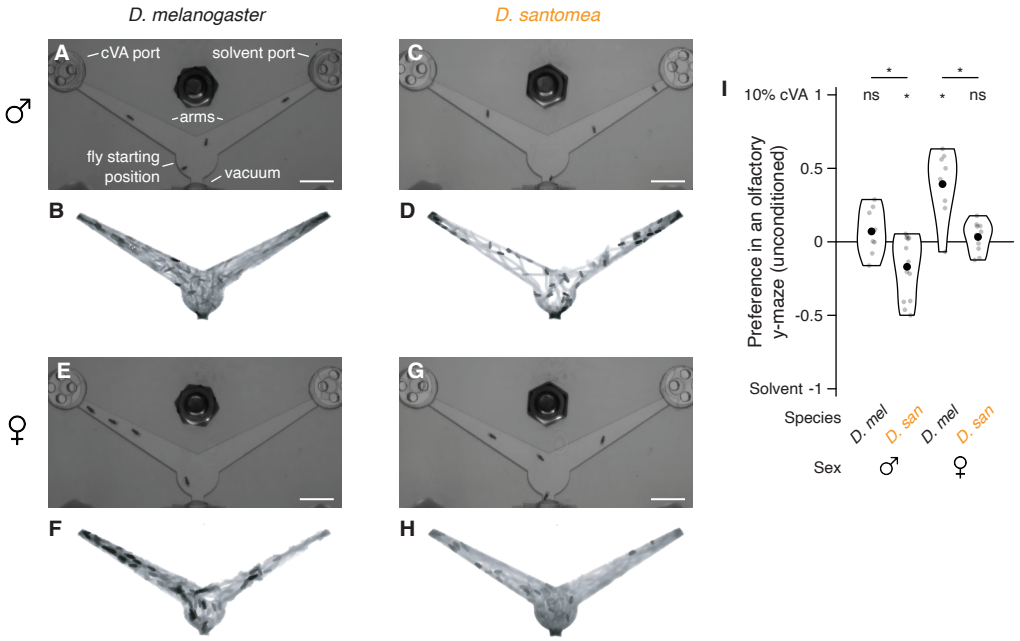
D. melanogaster
D. santomea
A
cVA port
solvent port
arms
fly starting position
vacuum
B
C
D
E
F
G
H
♂
♀
I
10% cVA 1
Solvent -1
0.5
0
-0.5
Preference in an olfactory y-maze (unconditioned)
ns
*
*
*
ns
Species
D. mel
D. san
D. mel
D. san
Sex
♂
♀

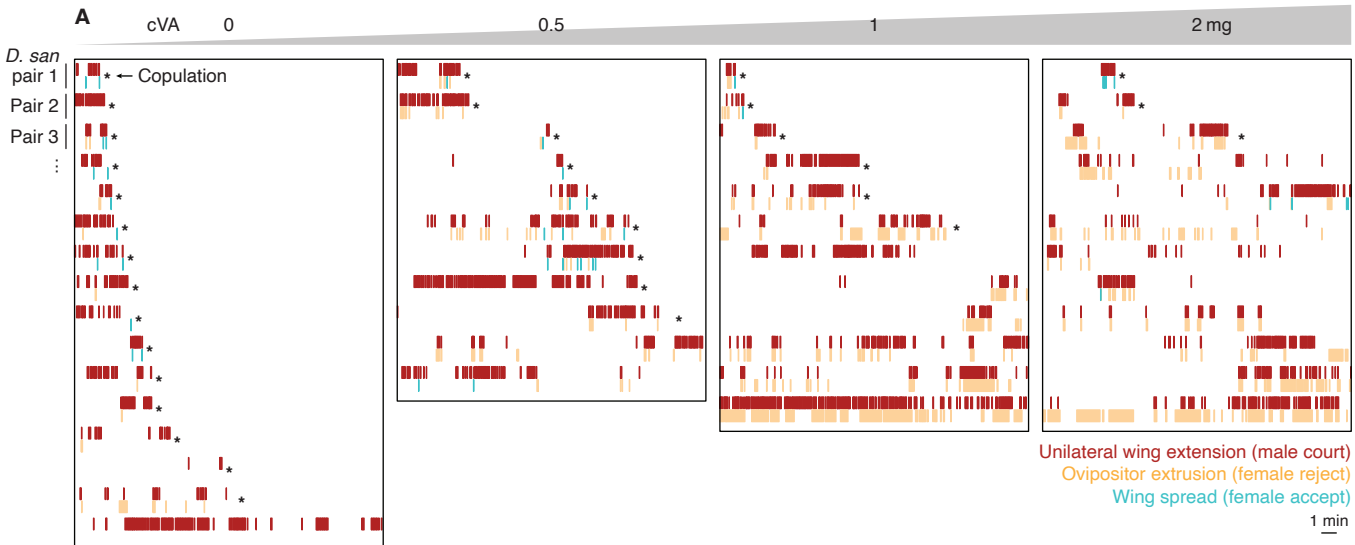
A
cVA
0
0.5
1
2 mg
D. san
pair 1
Pair 2
Pair 3
← Copulation
Unilateral wing extension (male court)
Ovipositor extrusion (female reject)
Wing spread (female accept)
1 min

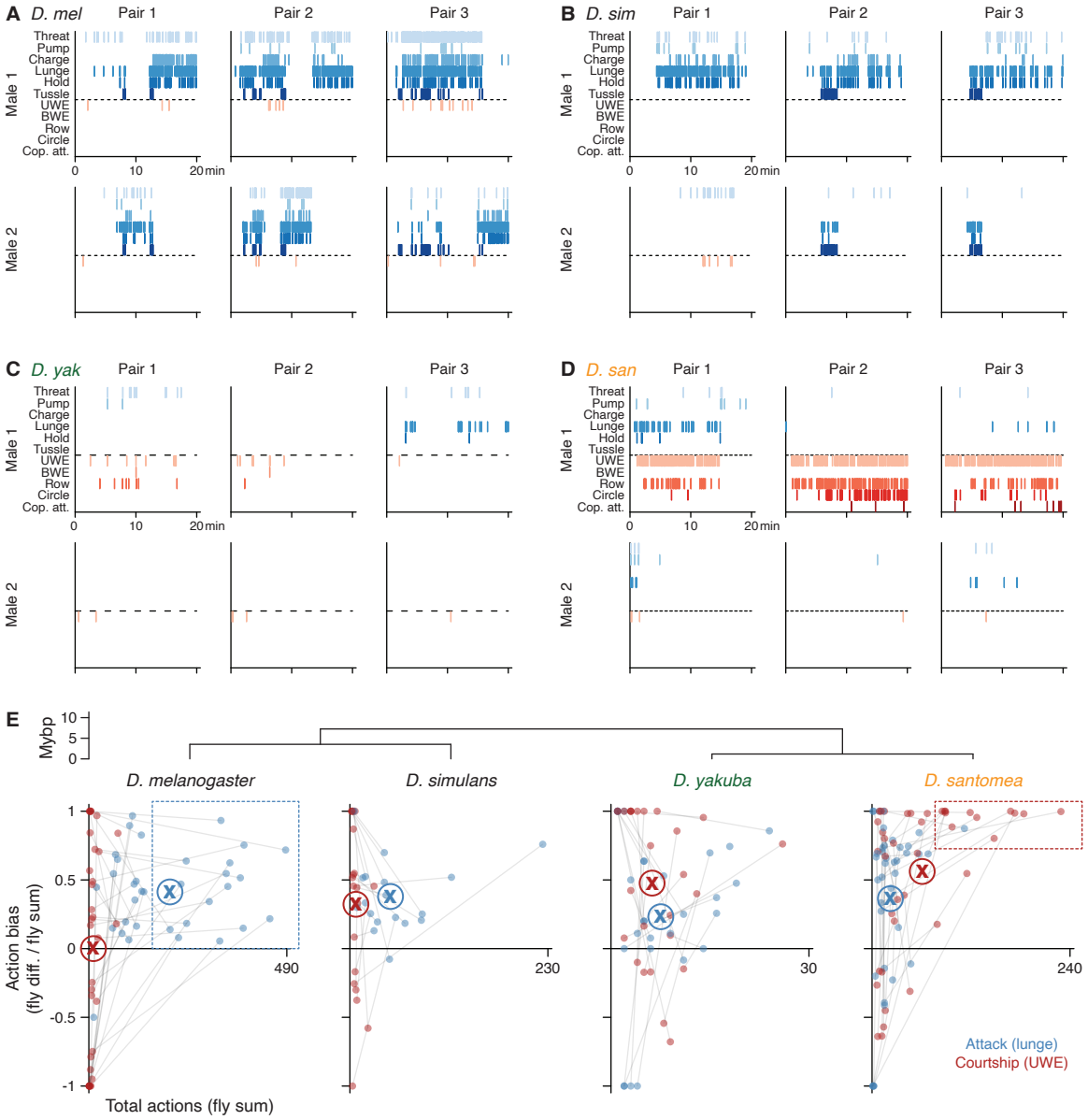
A D. mel
B D. sim
C D. yak
D D. san
Pair 1
Pair 2
Pair 3
Threat
Pump
Charge
Lunge
Hold
Tussle
UWE
BWE
Row
Circle
Cop. att.
Male 1
Male 2
0
10
20 min
E
Mybp
10
5
0
D. melanogaster
D. simulans
D. yakuba
D. santomea
Action bias
(fly diff. / fly sum)
1
0.5
0
-0.5
-1
490
230
30
240
Total actions (fly sum)
Attack (lunge)
Courtship (UWE)

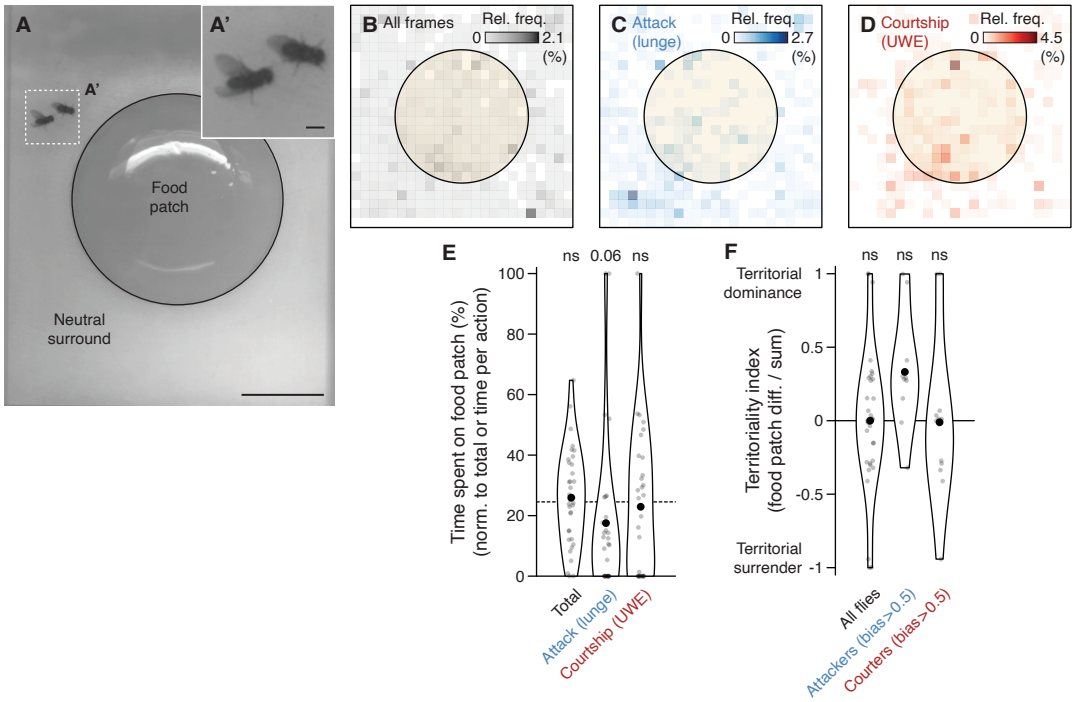
A
A'
A'
Food patch
Neutral surround
B All frames
Rel. freq.
0
2.1
(%)
C Attack (lunge)
Rel. freq.
0
2.7
(%)
D Courtship (UWE)
Rel. freq.
0
4.5
(%)
E
ns
0.06
ns
Time spent on food patch (%) (norm. to total or time per action)
100
80
60
40
20
0
Total
Attack (lunge)
Courtship (UWE)
F
ns
ns
ns
Territorial dominance
Territorial surrender
Territoriality index (food patch diff. / sum)
1
0.5
0
-0.5
-1
All flies
Attackers (bias>0.5)
Courters (bias>0.5)

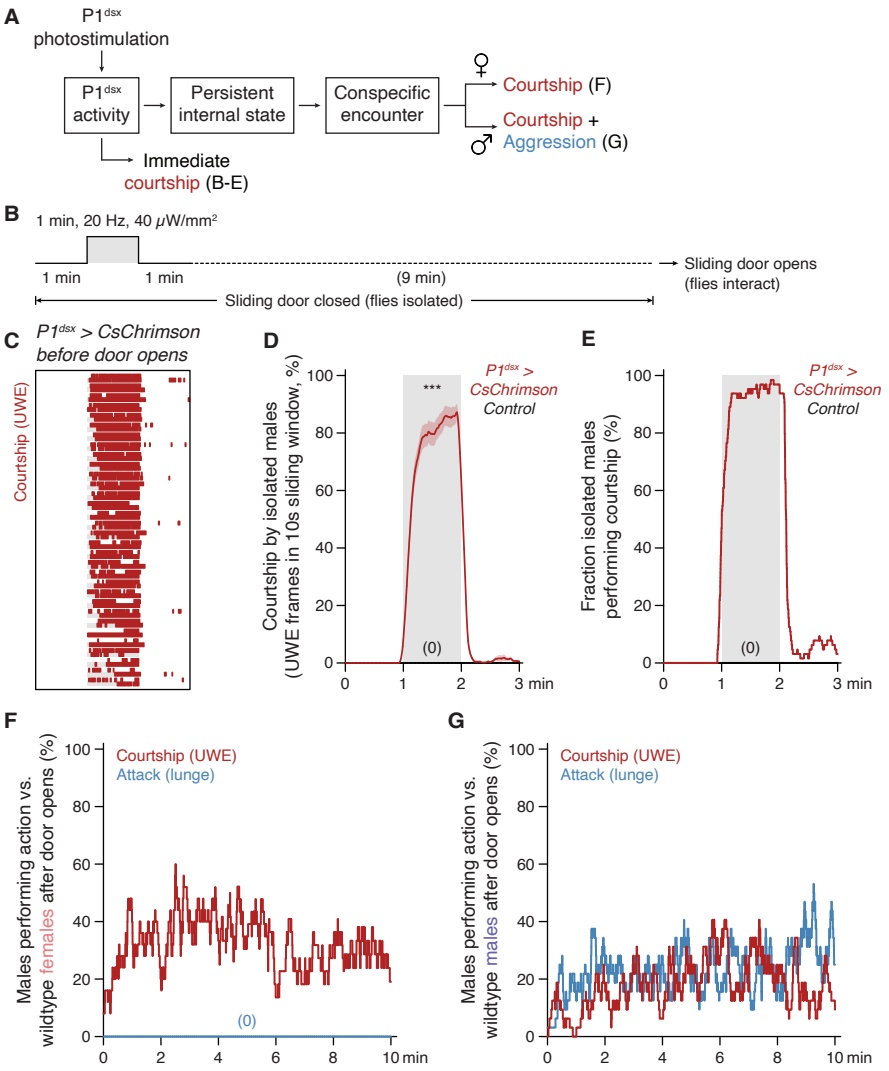
A
P1dsx photostimulation
P1dsx activity
Persistent internal state
Conspecific encounter
Courtship (F)
Courtship + Aggression (G)
Immediate courtship (B-E)
B
1 min, 20 Hz, 40 μW/mm2
1 min
1 min
(9 min)
Sliding door opens (flies interact)
Sliding door closed (flies isolated)
C
P1dsx > CsChrimson before door opens
Courtship (UWE)
D
Courtship by isolated males (UWE frames in 10s sliding window, %)
P1dsx > CsChrimson
Control
***
(0)
3 min
E
Fraction isolated males performing courtship (%)
P1dsx > CsChrimson
Control
(0)
3 min
F
Males performing action vs. wildtype females after door opens (%)
Courtship (UWE)
Attack (lunge)
(0)
10 min
G
Males performing action vs. wildtype males after door opens (%)
Courtship (UWE)
Attack (lunge)
10 min

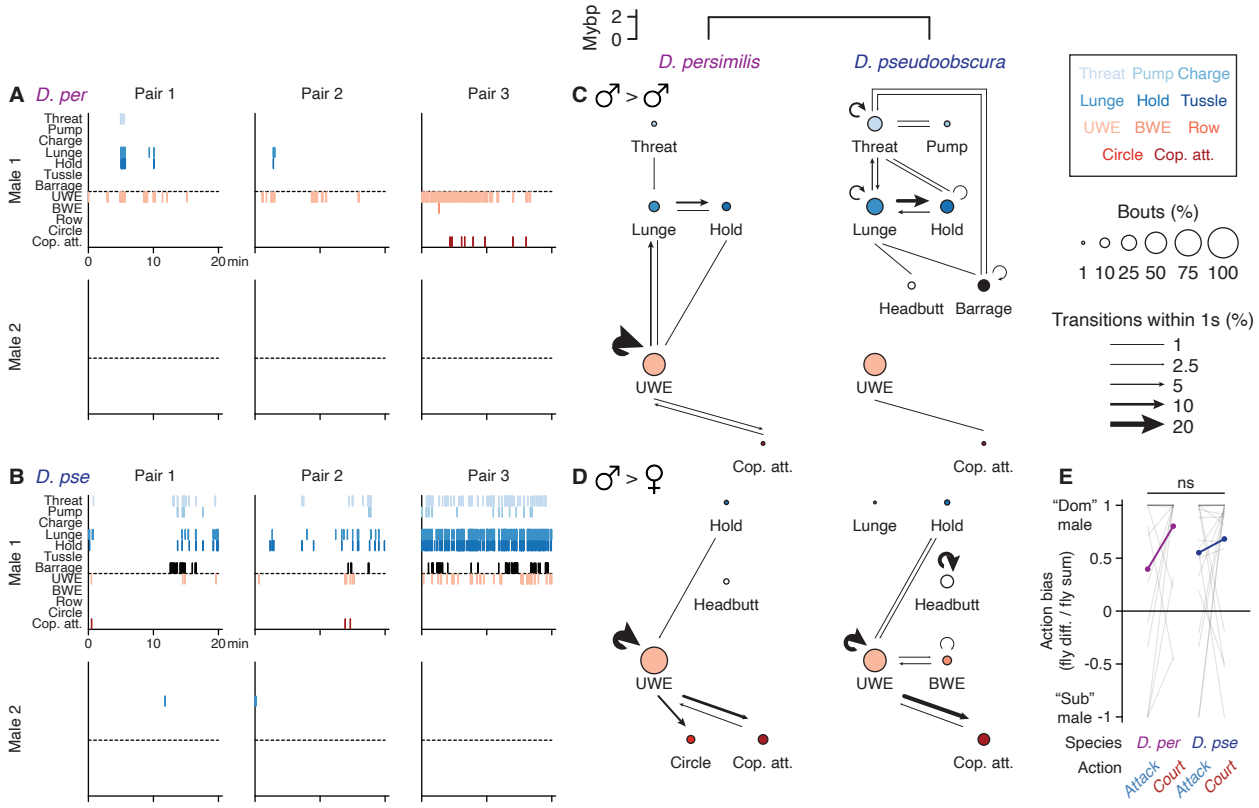
A D. per
Pair 1
Pair 2
Pair 3
Threat
Pump
Charge
Lunge
Hold
Tussle
Barrage
UWE
BWE
Row
Circle
Cop. att.
Male 1
Male 2
0
10
20 min
B D. pse
Mybp
2
0
D. persimilis
D. pseudoobscura
C ♂ > ♂
Threat
Lunge
Hold
UWE
Cop. att.
Pump
Headbutt
Barrage
D ♂ > ♀
Circle
BWE
Threat Pump Charge
Lunge Hold Tussle
UWE BWE Row
Circle Cop. att.
Bouts (%)
1 10 25 50 75 100
Transitions within 1s (%)
1
2.5
5
10
20
E
ns
"Dom" male
"Sub" male
Action bias (fly diff. / fly sum)
1
0.5
0
-0.5
-1
Species
D. per
D. pse
Action
Attack
Court
Attack
Court